

# Neutrinos: DRAFT

<sup>1</sup> Conveners: A. de Gouvêa, K. Pitts, K. Scholberg, G.P. Zeller

<sup>2</sup> Subgroup Conveners: J. Alonso, A. Bernstein, M. Bishai, S. Elliot, K. Heeger, K. Hoffman, P. Huber,  
<sup>3</sup> L. Kaufman, B. Kayser, J. Link, C. Lunardini, B. Monreal, J. Morfin, H. Robertson, R. Tayloe, N. Tolich

## 1.1 Executive Summary

The standard model is the most successful theoretical description of Nature in the history of humankind. Decades of experimental and observational scrutiny have revealed less than a handful of phenomena outside the standard model: the dark energy and dark matter puzzles, and the existence of non-zero neutrino masses. While many experiments continue to look for other new phenomena and deviations from standard model predictions, it is clear that continued detailed study of the neutrino sector is of the utmost importance.

Compared to the other fermions, the elusive nature of the neutrino has made it extremely difficult to study in detail. In spite of the challenges, **neutrino physics has been tremendously successful over the past two decades.** From almost complete lack of knowledge about neutrino mass and mixing twenty years ago, we now have a robust, simple, three-flavor paradigm, describing most of the data. Key questions in the three-flavor sector remain, however – we do not know the mass ordering, nor whether neutrinos violate CP symmetry. On the other hand, we have only just begun to test the three-flavor paradigm. A precision neutrino oscillation program is required for that. Furthermore, some experiments have uncovered intriguing anomalies that merit additional study, and could lead to the discovery of beyond-the-standard-model states or interactions. Advances in detector technology and analytical techniques needed for the next generation of neutrino experiments are well underway. **We have clear experimental paths forward for building on our success,** both for precision testing of the three-flavor paradigm, and for exploration of anomalies.

We are now poised to take the experimental opportunities to answer some of the most fundamental and important questions of our time: are neutrinos Majorana or Dirac particles? Is there CP violation in the lepton sector? Does the small, but non-zero neutrino mass couple to a mass scale that is far beyond what we can hope to reach in colliders? Although these questions have been asked for many years, we will soon be able to answer at least some of them.

The next generation of 100 kg-class neutrinoless double-beta-decay search experiments should reach effective masses in the 100 meV range; beyond that, there are opportunities for multi-ton-class experiments that will reach sub 10 meV effective mass sensitivity, pushing below the inverted hierarchy region. The next generation of tritium-beta-decay experiments will directly probe neutrino masses a factor of 10 smaller than the best current bounds; innovative new ideas may help to go beyond.

The neutrino mass hierarchy can be unambiguously resolved using accelerator neutrino oscillation experiments with baselines around 1000 km (or larger) and detector masses of order tens of kilotons. The discovery of a non-zero  $\theta_{13}$  enables long-baseline neutrino experiments to search for leptonic CP violation in appearance experiments. The search for CP violation in the neutrino sector is a top priority for particle physics efforts worldwide. Regardless of the experimental approach, high-power proton beams (greater than 1 MW) coupled with massive detectors (order 100 kton), are needed to study CP violation in neutrino oscillations. The US, with the Long-Baseline Neutrino Experiment (LBNE) and a future multi-megawatt beam from Project X, is uniquely positioned to lead an international campaign to test the three-flavor paradigm, measure CP violation and go beyond. Given the challenges associated with precision measurements in the neutrino sector, complementary baselines, sources and detector techniques will be required to piece together a sharp picture. Smaller experiments will also play a key role in addressing some of the remaining anomalies and hints for physics beyond the three-neutrino paradigm, and study neutrino-matter interactions in detail.

The diversity of physics topics that can be probed through the neutrino sector is very significant, and the interplay between neutrino physics and other fields is rich. Neutrinos can and will provide important information on structure formation in the early universe, Earth, solar and supernova physics, nuclear properties, and rare decays of charged leptons and hadrons. In other words, the neutrino sector sits at the nexus of the worldwide effort in energy, intensity and cosmic frontier physics.

48 Finally, the unique physics potential and technological advancements have conspired to produce a fertile  
49 environment for new ideas for improved measurements and new techniques, as well as both direct and  
50 spin-off applications. This provides an important training ground for the next generation of scientists and  
51 engineers, and exciting ideas to share with the public.

## 1.2 Introduction

Neutrinos are the most elusive of the known fundamental particles. They are color-neutral and charge-neutral spin one-half fermions, and, to the best of our knowledge, only interact with charged fermions and massive gauge bosons, through the weak interactions. For this reason, neutrinos can only be observed and studied because there are very intense neutrino sources (natural and artificial) and only if one is willing to work with large detectors.

The existence of neutrinos was postulated in the early 1930s, but they were only first observed in the 1950s. The third neutrino flavor eigenstate, the tau-type neutrino  $\nu_\tau$ , was the last of the fundamental matter particles to be observed [1], eluding direct observation six years longer than the top quark [2, 3]. More relevant to this chapter, in the late 1990s the discovery of non-zero neutrino masses moved the study of neutrino properties to the forefront of experimental and theoretical particle physics.

Experiments with solar [4, 5, 6, 7, 8, 9], atmospheric [10, 11], reactor [12, 13] and accelerator [14, 15] neutrinos have established, beyond reasonable doubt, that a neutrino produced in a well-defined flavor state (say, a muon-type neutrino  $\nu_\mu$ ) has a non-zero probability of being detected in a different flavor state (say, an electron-type neutrino  $\nu_e$ ). This flavor-changing probability depends on the neutrino energy and the distance traversed between the source and the detector. The simplest and only consistent explanation of all neutrino data collected over the last two decades is a phenomenon referred to as ‘neutrino mass-induced flavor oscillation.’ These neutrino oscillations, which will be discussed in more detail in Sec. 1.3, in turn imply that neutrinos have nonzero masses and neutrino mass eigenstates are different from neutrino weak eigenstates, *i.e.*, leptons mix.

In a nutshell, if the neutrino masses are distinct and leptons mix, a neutrino can be produced, via weak interactions, as a coherent superposition of mass-eigenstates, e.g., a neutrino  $\nu_\alpha$  with a well-defined flavor, and has a non-zero probability to be measured as a neutrino  $\nu_\beta$  of a different flavor ( $\alpha, \beta = e, \mu, \tau$ ). The oscillation probability  $P_{\alpha\beta}$  depends on the neutrino energy  $E$ , the propagation distance  $L$ , and on the neutrino mass-squared differences,  $\Delta m_{ij}^2 \equiv m_i^2 - m_j^2$ ,  $i, j = 1, 2, 3, \dots$ , and the elements of the leptonic mixing matrix,<sup>1</sup>  $U$ , which relates neutrinos with a well-defined flavor ( $\nu_e, \nu_\mu, \nu_\tau$ ) and neutrinos with a well-defined mass ( $\nu_1, \nu_2, \nu_3, \dots$ ). For three neutrino flavors, the elements of  $U$  are defined by

$$\begin{pmatrix} \nu_e \\ \nu_\mu \\ \nu_\tau \end{pmatrix} = \begin{pmatrix} U_{e1} & U_{e2} & U_{e3} \\ U_{\mu1} & U_{\mu2} & U_{\mu3} \\ U_{\tau1} & U_{\tau2} & U_{\tau3} \end{pmatrix} \begin{pmatrix} \nu_1 \\ \nu_2 \\ \nu_3 \end{pmatrix}. \quad (1.1)$$

Almost all neutrino data to date can be explained assuming that neutrinos interact as prescribed by the Standard Model, there are only three neutrino mass eigenstates, and  $U$  is unitary. Under these circumstances, it is customary to parameterize  $U$  in Eq. (1.1) with three mixing angles  $\theta_{12}, \theta_{13}, \theta_{23}$  and three complex phases,  $\delta, \xi, \zeta$ , defined by

$$\frac{|U_{e2}|^2}{|U_{e1}|^2} \equiv \tan^2 \theta_{12}; \quad \frac{|U_{\mu3}|^2}{|U_{\tau3}|^2} \equiv \tan^2 \theta_{23}; \quad U_{e3} \equiv \sin \theta_{13} e^{-i\delta}, \quad (1.2)$$

with the exception of  $\xi$  and  $\zeta$ , the so-called Majorana  $CP$ -odd phases. These are only physical if the neutrinos are Majorana fermions, and have essentially no effect in flavor-changing phenomena.

In order to relate the mixing elements to experimental observables, it is necessary to properly define the neutrino mass eigenstates, *i.e.*, to ‘order’ the neutrino masses. This is done in the following way:  $m_2^2 > m_1^2$  and  $\Delta m_{21}^2 < |\Delta m_{31}^2|$ . In this case, there are three mass-related oscillation observables:  $\Delta m_{21}^2$  (positive-definite),  $|\Delta m_{31}^2|$ , and the sign of  $\Delta m_{31}^2$ . A positive (negative) sign for  $\Delta m_{31}^2$  implies  $m_3^2 > m_2^2$  ( $m_3^2 < m_1^2$ )

<sup>1</sup>Often referred to as the Maki-Nakagawa-Sakata (MNS) Matrix, or the Pontecorvo-Maki-Nakagawa-Sakata (PMNS) Matrix.

89 and characterizes a so-called normal (inverted) neutrino mass hierarchy. The two mass hierarchies are depicted in Fig. 1-1.

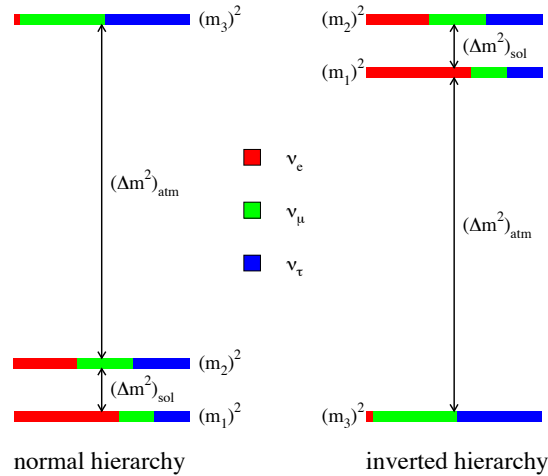


**Figure 1-1.** Cartoon of the two distinct neutrino mass hierarchies that fit all of the current neutrino data, for fixed values of all mixing angles and mass-squared differences. The color coding (shading) indicates the fraction  $|U_{\alpha i}|^2$  of each distinct flavor  $\nu_\alpha$ ,  $\alpha = e, \mu, \tau$  contained in each mass eigenstate  $\nu_i$ ,  $i = 1, 2, 3$ . For example,  $|U_{e2}|^2$  is equal to the fraction of the  $(m_2)^2$  “bar” that is painted red (shading labeled as “ $\nu_e$ ”).

90

91 Our knowledge of neutrino oscillation parameters has evolved dramatically over the past two decades. As  
 92 summarized in Sec. 1.5, all three mixing angles have been measured relatively well, along with (the magnitude  
 93 of) the mass-squared difference. On the other hand, we have virtually no information concerning  $\delta$  (and,  
 94 for that matter,  $\xi$  and  $\zeta$ ) or the sign of  $\Delta m_{31}^2$ . We also don’t know the value of the neutrino masses  
 95 themselves – only differences of the masses-squared. We can’t rule out the possibility that the lightest  
 96 neutrino is virtually massless ( $m_{\text{lightest}} \ll 10^{-3}$  eV) or that all neutrino masses are virtually the same (e.g.  
 97  $m_1 \sim m_2 \sim m_3 \sim 0.1$  eV). Probes outside the realm of neutrino oscillations are required to investigate the  
 98 values of the neutrino masses. These are described in Sec. 1.7.

99 One of the main goals of next-generation experiments is to test whether the scenario outlined above, the  
 100 standard three-massive-neutrinos paradigm, is correct and complete. This can be achieved by next-generation  
 101 experiments sensitive to neutrino oscillations via not simply determining all of the parameters above, but  
 102 by “over-constraining” the parameter space in order to identify potential inconsistencies. This is far from a  
 103 simple task, and the data collected thus far, albeit invaluable, allow for only the simplest consistency checks.  
 104 Precision measurements, as will be discussed in Sec. 1.5, will be required.

105 In more detail, given all we know about the different neutrino oscillation lengths, it is useful to step back and  
 106 appreciate what oscillation experiments have been able to measure. Solar data, and data from KamLAND,  
 107 are, broadly speaking, sensitive to  $|U_{e2}|$ ,  $|U_{\mu 2}|^2 + |U_{\tau 2}|^2$ , and  $|U_{e2}U_{e1}|$ . Data from atmospheric neutrinos and  
 108 long-baseline, accelerator-based experiments are sensitive to  $|U_{\mu 3}|$  and, to a much lesser extent,  $|U_{\mu 3}U_{\tau 3}|$   
 109 and  $|U_{\mu 3}U_{e3}|$ . Finally, km scale reactor experiments are sensitive to  $|U_{e3}|$ . Out of the nine (known) complex  
 110 entries of  $U$ , we have information, usually very limited, regarding the magnitude of around six of them.  
 111 Clearly, we have a long way to go before concluding that the three-flavor paradigm is the whole story.

112 Life may, indeed, already be much more interesting. There are several, none too significant, hints in the  
 113 world neutrino data that point to a neutrino sector that is more complex than the one outlined above. These

114 will be discussed in Sec. 1.9. Possible surprises include new, gauge singlet fermion states that manifest  
 115 themselves only by mixing with the known neutrinos, and new weaker-than-weak interactions.

116 Another issue of fundamental importance is the investigation of the status of CP-invariance in leptonic  
 117 processes. Currently, all observed CP-invariance violating phenomena are governed by the single physical  
 118 CP-odd phase parameter in the quark mixing matrix. Searches for other sources of CP-invariance violation,  
 119 including the so-called strong CP-phase  $\theta_{QCD}$ , have, so far, failed. The picture currently emerging from  
 120 neutrino oscillation data allow for a completely new, independent source of CP-invariance violation. The  
 121 CP-odd parameter  $\delta$ , if different from zero or  $\pi$ , implies that neutrino oscillating probabilities violate  
 122 CP-invariance, i.e., the values of the probabilities for neutrinos to oscillate are different from those of  
 123 antineutrinos! We describe this phenomenon in more detail in Secs. 1.3, 1.5.

124 It should be noted that, if neutrinos are Majorana fermions, the CP-odd phases  $\xi$  and  $\zeta$  also mediate CP-  
 125 invariant violating phenomena [16] (alas, we don't yet really know how to study these in practice). In  
 126 summary, if neutrinos are Majorana fermions, the majority of CP-odd parameters in particle physics —  
 127 even in the absence of other new physics — belong to the lepton sector. These are completely unknown  
 128 and can “only” be studied in neutrino experiments. Neutrino oscillations provide a unique opportunity  
 129 to revolutionize our understanding of CP-invariance violation, with potentially deep ramifications for both  
 130 particle physics and cosmology.

131 In the Standard Model, neutrinos were predicted to be exactly massless. The discovery of neutrino masses  
 132 hence qualifies as the first instance where the Standard Model failed. This is true even if the three-massive-  
 133 neutrino paradigm described above turns out to be the whole story. More important is the fact that all  
 134 modifications to the Standard Model that lead to massive neutrinos change it qualitatively. For a more  
 135 detailed discussion of this point see, for example, [17].

136 Neutrino masses, while non-zero, are tiny when compared to all other known fundamental fermion masses  
 137 in the Standard Model, as depicted in Fig. 1-2. Two features readily stand out: (i) neutrino masses are at  
 138 least six orders of magnitude smaller than the electron mass, and (ii) there is, to the best of our knowledge,  
 139 a “gap” between the largest allowed neutrino mass and the electron mass. We don't know why neutrino  
 140 masses are so small or why there is such a large gap between the neutrino and the charged fermion masses.

We suspect, however, that this may be Nature's way of telling us that neutrino masses are “different.”

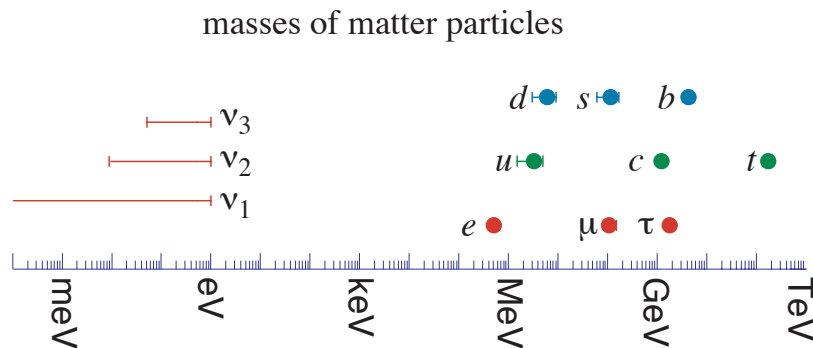


**Figure 1-2.** Standard Model fermion masses. For the neutrino masses, the normal mass hierarchy was assumed, and a loose upper bound  $m_i < 1$  eV, for all  $i = 1, 2, 3$  was imposed.

141

142 This suspicion is only magnified by the possibility that massive neutrinos, unlike all other fermions in the  
 143 Standard Model, may be Majorana fermions. The reason is simple: neutrinos are the only electrically neutral  
 144 fundamental fermions and hence need not be distinct from their antiparticles. Determining the nature of  
 145 the neutrino – Majorana or Dirac – would not only help guide theoretical work related to uncovering the

146 origin of neutrino masses, but could also reveal that the conservation of lepton number is not a fundamental  
 147 law of Nature. The most promising avenue for learning the fate of lepton number, as will be discussed  
 148 in Sec. 1.6, is to look for neutrinoless double-beta decay, a lepton-number violating nuclear process. The  
 149 observation of a non-zero rate for this hypothetical process would easily rival, as far as its implications for our  
 150 understanding of nature are concerned, the first observations of parity violation and  $CP$ -invariance violation  
 151 in the mid-twentieth century.

152 It is natural to ask what augmented, “new” Standard Model ( $\nu$ SM) leads to non-zero neutrino masses. The  
 153 answer is that we are not sure. There are many different ways to modify the Standard Model in order to  
 154 accommodate neutrino masses. While these can differ greatly from one another, all succeed – by design – in  
 155 explaining small neutrino masses and all are allowed by the current particle physics experimental data. The  
 156 most appropriate question, therefore, is not what are the candidate  $\nu$ SM’s, but how can one identify the  
 157 “correct”  $\nu$ SM? The answers potentially lie in next-generation neutrino experiments, which are described  
 158 throughout this chapter.

159 Before discussing concrete examples, it is important to highlight the potential theoretical significance of  
 160 nonzero neutrino masses. In the standard model, the masses of all fundamental particles are tied to the  
 161 phenomenon of electroweak symmetry breaking and a single mass scale – the vacuum expectation value of  
 162 the Higgs field. Nonzero neutrino masses may prove to be the first direct evidence of either a new mass scale,  
 163 completely unrelated to electroweak symmetry breaking, or evidence that electroweak symmetry breaking is  
 164 more complex than dictated by the standard model.

165 Here we discuss one generic mechanism in more detail. The effect of heavy new degrees of freedom in low-  
 166 energy phenomena can often be captured by adding to the Standard Model higher-dimensional operators.  
 167 As first pointed out in [18], given the Standard Model particle content and gauge symmetries, one is allowed  
 168 to write only one type of dimension-five operator – all others are dimension-six or higher:

$$\frac{1}{\Lambda} (LH)(LH) + h.c. \quad \Rightarrow \quad \frac{v^2}{\Lambda} \nu\nu + h.c., \quad (1.3)$$

169 where  $L$  and  $H$  are the lepton and Higgs boson  $SU(2)_L$  doublets, and the arrow indicates one of the  
 170 components of the operator after electroweak symmetry is broken.  $v$  is the vacuum expectation value of the  
 171 neutral component of  $H$ , and  $\Lambda$  is the effective new physics scale. If this operator is indeed generated by  
 172 some new physics, neutrinos obtain Majorana masses  $m_\nu \sim v^2/\Lambda$ . For  $\Lambda \sim 10^{15}$  GeV,  $m_\nu \sim 10^{-1}$  eV, in  
 173 agreement with the current neutrino data. This formalism explains the small neutrino masses via a seesaw  
 174 mechanism:  $m_\nu \ll v$  because  $\Lambda \gg v$ .

175  $\Lambda$  is an upper bound for the masses of the new particles that lead to Eq. (1.3). If the new physics is  
 176 strongly coupled and Eq. (1.3) is generated at the tree-level, the new degrees of freedom are super-heavy:  
 177  $M_{\text{new}} \sim 10^{15}$  GeV. If that turns out to be the case, we will only be able to access the new physics indirectly  
 178 through neutrino experiments and the study of relics in the cosmic frontier. If, however, the new physics is  
 179 weakly coupled or Eq. (1.3) is generated at the loop level, virtually any value for  $M_{\text{new}} \gtrsim 1$  eV is allowed.  
 180 There are many scenarios where the new physics responsible for nonzero neutrino masses can be probed at  
 181 the energy frontier or elsewhere in the intensity frontier [19]. In summary, if Eq. (1.3) is correct, we expect  
 182 new physics to show up at a new mass scale  $M_{\text{new}}$  which lies somewhere between  $10^{-9}$  GeV and  $10^{15}$  GeV.  
 183 Clearly, more experimental information is required!

184 Neutrino data also provide a new piece to the flavor puzzle: the pattern of neutrino mixing. The absolute  
185 value of the entries of the CKM quark mixing matrix are, qualitatively, given by

$$|V_{\text{CKM}}| \sim \begin{pmatrix} 1 & 0.2 & 0.004 \\ 0.2 & 1 & 0.04 \\ 0.008 & 0.04 & 1 \end{pmatrix}, \quad (1.4)$$

186 while those of the entries of the PMNS matrix are given by

$$|U_{\text{PMNS}}| \sim \begin{pmatrix} 0.8 & 0.5 & 0.2 \\ 0.4 & 0.6 & 0.7 \\ 0.4 & 0.6 & 0.7 \end{pmatrix}. \quad (1.5)$$

187 It is clear that the two matrices look very different. While the CKM matrix is almost proportional to the  
188 identity matrix plus hierarchically ordered off-diagonal elements, the PMNS matrix is far from diagonal  
189 and, with the possible exception of the  $U_{e3}$  element, all elements are  $\mathcal{O}(1)$ . Significant research efforts are  
190 concentrated on understanding what, if any, is the relationship between the quark and lepton mixing matrices  
191 and what, if any, is the “organizing principle” responsible for the observed pattern of neutrino masses and  
192 lepton mixing. There are several different theoretical ideas in the market (for summaries, overviews and  
193 more references see, for example, [20, 21]). Typical results include predictions for the currently unknown  
194 neutrino mass and mixing parameters ( $\sin^2 \theta_{13}$ ,  $\cos 2\theta_{23}$ , the mass hierarchy, *etc.*) and the establishment of  
195 sum rules involving different parameters. Some of the challenges are discussed in Sec. 1.5

196 Precision neutrino oscillation measurements are required to address the flavor questions above. That can  
197 only be achieved as the result of significant investments in intense, well-characterized neutrino sources and  
198 massive high-precision detectors. Some of these are summarized in Sec. 1.4 and spelled out in more detail  
199 throughout this Chapter. Excellent understanding of neutrino interactions – beyond the current state of the  
200 art – is also mandatory. This will require a comprehensive experimental program on neutrino scattering, as  
201 summarized in Sec. 1.8. These, of course, are not only ancillary to neutrino oscillation experiments, but are  
202 also interesting in their own right. Neutrinos, since they interact only weakly, serve as a unique probes of  
203 nucleon and nuclear properties, and may reveal new physics phenomena at the electroweak scale, including  
204 some that are virtually invisible to the Tevatron and the LHC.

205 (Massive) neutrinos also serve as unique messengers in astrophysics and cosmology, as discussed in Sec. 1.10.  
206 Astrophysical neutrino searches may uncover indirect evidence for dark matter annihilation in the Earth,  
207 the Sun, or the center of galaxy. Neutrinos produced in supernova explosions contain information from  
208 deep within the innards of the exploding stars and their studies may also help reveal unique information  
209 regarding neutrino properties. Big Bang neutrinos play a definitive role in the thermal history of the universe.  
210 Precision cosmology measurements also may reveal neutrino properties, including the absolute values of the  
211 neutrino masses. Finally, the unique character of the neutrinos and the experiments used to study them  
212 provide unique opportunities outside the realm of particle physics research. More details along these lines  
213 are discussed in Sec. 1.11.

## 214 1.3 Overview of Neutrino Oscillations

215 Physical effects of non-zero neutrino masses, to date, have been observed only in neutrino oscillation  
216 experiments. Those are expected to remain, for the foreseeable future, the most powerful tools available  
217 for exploring the new physics revealed by solar and atmospheric neutrino experiments at the end of the  
218 twentieth century.

219 The standard setup of a neutrino oscillation experiment is as follows. A detector is located a distance  $L$   
 220 away from a source, which emits ultra-relativistic neutrinos or antineutrinos with, most often, a continuous  
 221 spectrum of energies  $E$ , and flavor  $\alpha = e, \mu$ , or  $\tau$ . According to the Standard Model, the neutrinos interact  
 222 with matter either via  $W$ -boson exchange charged-current interactions where a neutrino with a well-defined  
 223 flavor  $\nu_\alpha$  gets converted into a charged lepton of the same flavor ( $\nu_\alpha X \rightarrow eX'$ , *etc.*) or via  $Z$ -boson  
 224 exchange neutral-current interactions, which preserve the neutrino flavor ( $\nu_\mu X \rightarrow \nu_\mu X'$ ). The occurrence  
 225 of a neutral-current process is tagged by observing the system against which the neutrinos are recoiling.  
 226 The detector hence is capable of measuring the flux of neutrinos or antineutrinos with flavor  $\beta = e, \mu$ , or  
 227  $\tau$ , or combinations thereof, often as a function of the neutrino energy. By comparing measurements in the  
 228 detector with expectations from the source, one can infer  $P_{\alpha\beta}(L, E)$  or  $\bar{P}_{\alpha\beta}(L, E)$ , the probability that a(n)  
 229 (anti)neutrino with energy  $E$  produced in a flavor eigenstate  $\nu_\alpha$  is measured in a flavor  $\nu_\beta$  after it propagates  
 230 a distance  $L$ . In practice, it is often preferable to make multiple measurements of neutrinos at different  
 231 distances from the source, which can be helpful for both the cancellation of systematic uncertainties and for  
 232 teasing out effects beyond the standard three-flavor paradigm.

233 In the standard three-flavor paradigm,  $P_{\alpha\beta}$  is a function of the mixing angles  $\theta_{12,13,23}$ , the Dirac  $CP$ -odd  
 234 phase  $\delta$ , and the two independent neutrino mass-squared differences  $\Delta m_{21,31}^2$ , defined in the Introduction.  
 235 Assuming the neutrinos propagate in vacuum, and making explicit use of the unitarity of  $U$ , one can express  
 236  $P_{\alpha\beta}(L, E) = |A_{\alpha\beta}|^2$ , where

$$A_{\alpha\beta} = \delta_{\alpha\beta} + U_{\alpha 2} U_{\beta 2}^* \left( \exp \left( -i \frac{\Delta m_{21}^2 L}{2E} \right) - 1 \right) + U_{\alpha 3} U_{\beta 3}^* \left( \exp \left( -i \frac{\Delta m_{31}^2 L}{2E} \right) - 1 \right), \quad (1.6)$$

$$\bar{A}_{\alpha\beta} = \delta_{\alpha\beta} + U_{\alpha 2}^* U_{\beta 2} \left( \exp \left( -i \frac{\Delta m_{21}^2 L}{2E} \right) - 1 \right) + U_{\alpha 3}^* U_{\beta 3} \left( \exp \left( -i \frac{\Delta m_{31}^2 L}{2E} \right) - 1 \right), \quad (1.7)$$

237 up to an unphysical overall phase.  $A$  ( $\bar{A}$ ) is the amplitude for (anti)neutrino oscillations. It is easy to see  
 238 that  $P_{\alpha\beta}$  are oscillatory functions of  $L/E$  with, in general, three distinct, two independent oscillation lengths  
 239 proportional to  $\Delta m_{21}^2$ ,  $\Delta m_{31}^2$  and  $\Delta m_{32}^2 \equiv \Delta m_{31}^2 - \Delta m_{21}^2$ , as depicted in Figure 1-3. Ideally, measurements  
 240 of some  $P_{\alpha\beta}$  as a function of  $L/E$  would suffice to determine all neutrino oscillation parameters. These would  
 241 also allow one to determine whether the standard paradigm is correct, *i.e.*, whether Eqs. (1.6,1.7) properly  
 242 describe neutrino flavor-changing phenomena.

243 For example, if one could measure both  $P_{ee}$  and  $P_{\mu\mu}$  as a function of  $L/E$ , one should be able to determine  
 244 not only  $\Delta m_{21}^2$  and  $|\Delta m_{31}^2|$ , but also  $|U_{e2}|^2$ ,  $|U_{e3}|^2$ ,  $|U_{\mu 2}|^2$  and  $|U_{\mu 3}|^2$ , and the sign of  $\Delta m_{31}^2$ . This in turn  
 245 would translate into measurements of all mixing parameters, including the  $CP$ -odd phase  $\delta$ . One would also  
 246 be able to determine, for example, whether there are other oscillation lengths, which would indicate there  
 247 are new, yet-to-be-observed, neutrino states, or whether  $P_{ee, \mu\mu} \neq 1$  in the limit  $L \rightarrow 0$ , which would indicate,  
 248 for example, the existence of new, weaker-than-weak, charged-current type interactions.

249 In the real world, such measurements are, to say the least, very hard to perform, for several reasons.  $\Delta m_{21}^2$  is  
 250 much smaller than the magnitude of  $\Delta m_{31,32}^2$ , which in turn makes it challenging to observe two independent  
 251 oscillation frequencies in the same experimental setup. For this reason all measurements of  $P_{\mu\mu}$  performed to  
 252 date are, effectively, only sensitive to  $|\Delta m_{31}^2|$  and  $|U_{\mu 3}|$  – the  $L/E$  factors probed are too small to “see” the  
 253  $\Delta m_{21}^2$ -driven oscillations or distinguish  $\Delta m_{31}^2$  from  $\Delta m_{32}^2$ . On the other hand, the magnitude of  $|U_{e3}|$  is much  
 254 smaller than that of the other entries of  $U$ . For this reason, measurements of  $P_{ee}$  for solar neutrinos have  
 255 only been precise enough to definitively observe  $\Delta m_{21}^2$ -driven oscillations and hence determine its magnitude,  
 256 along with that of  $U_{e2}$ .

257 Another real-world issue is that, for any setup, it is not possible to measure any  $P_{\alpha\beta}$  with perfect  $L/E$   
 258 resolution. Furthermore, the available  $L/E$  ranges are, in most cases, narrow. More realistically, one expects

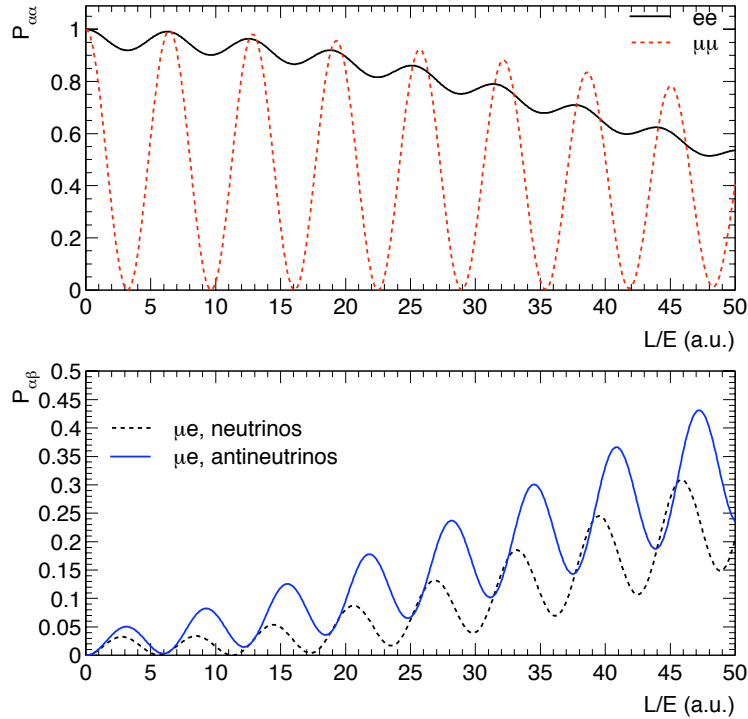


**Figure 1-3.** Top:  $P_{ee}$  and  $P_{\mu\mu}$  in vacuum as a function of  $L/E$  (in arbitrary units), for representative values of the neutrino oscillation parameters, including a non-zero value of  $\delta$ . Bottom:  $P_{\mu e}$  and  $\bar{P}_{\mu e}$  in vacuum as a function of  $L/E$ , for representative values of the neutrino oscillation parameters.

259 to measure, with decent statistics and small systematic errors,  $P_{\alpha\beta}$  integrated over a few finite-sized  $L/E$   
 260 bins. This discreteness of the data leads to ambiguities when it comes to measuring the different mixing  
 261 parameters. For example, different pairs of  $\theta_{13}, \delta$  values lead to identical values for  $P_{\alpha\beta}$  integrated over a  
 262 fixed  $L/E$ . The same is true for pairs of  $\theta_{13}, \theta_{23}$ , and so on. A so-called eight-fold degeneracy has been  
 263 identified and studied in great detail in the neutrino literature (see, for example, [22, 23, 24]). The solution  
 264 to this challenge is to perform several measurements of different  $P_{\alpha\beta}$  at different values of  $L$  and  $E$  (and  
 265  $L/E$ ). This is especially true if one is interested in not only measuring the three-flavor neutrino mixing  
 266 parameters but also, much more importantly, over-constraining the standard paradigm and hence testing its  
 267 validity. For example, one would like to precisely measure  $\theta_{13}$  in different channels, for different values of  $L$   
 268 and  $E$ , to find out if all of them agree.

269 Measurements of vacuum survival probabilities,  $P_{\alpha\alpha}$  or  $\bar{P}_{\alpha\alpha}$  do not violate  $CP$  invariance:  $P_{\alpha\alpha} = \bar{P}_{\alpha\alpha}$  is  
 270 guaranteed by  $CPT$ -invariance. In order to directly observe  $CP$ -invariance violation, one needs to measure  
 271 an appearance probability, say  $P_{\mu e}$ .  $P_{\mu e}$  is different from  $\bar{P}_{\mu e}$ ,<sup>2</sup> as depicted in Fig. 1-3 (bottom), if the  
 272 following conditions are met, as one can readily confirm by studying Eqs. (1.6,1.7): (i) all  $U_{\alpha i}$  have non-zero  
 273 magnitude, (ii)  $U_{\alpha 2}U_{\beta 2}^*$  and  $U_{\alpha 3}U_{\beta 3}^*$  are relatively complex, (iii)  $L/E$  is large enough that both  $\Delta m_{21,31}^2 \times L/E$   
 274 are significantly different from zero. Given what is known about the oscillation parameters, condition (iii)  
 275 can be met for any given neutrino source by choosing a large enough value for  $L$ . This, in turn, translates  
 276 into the need for a very intense source and a very large, yet high-precision, detector, given that for all known  
 277 neutrino sources the neutrino flux falls off like  $1/L^2$  for any meaningful value of  $L$ . Whether conditions

<sup>2</sup>Note that T-invariance violation,  $P_{e\mu} \neq P_{\mu e}$ , is also present under the same conditions.

(i) and (ii) are met lies outside the control of the experimental setups. Given our current understanding, including the newly acquired knowledge that  $|U_{e3}| \neq 0$ , condition (i) holds. That being the case, condition (ii) is equivalent to  $\delta \neq 0, \pi$ . In the standard paradigm, the existence of  $CP$ -invariance violation is entirely at the mercy of the value of  $CP$ -odd phase  $\delta$ , currently unconstrained.

All neutrino data accumulated so far provide only hints for non-zero  $P_{\mu\tau}$  [25, 26] and  $P_{\mu e}$  [27, 28].<sup>3</sup> Both results are only sensitive to one mass-square difference ( $|\Delta m_{31}^2|$ ) and to  $|U_{\mu 3}U_{\tau 3}|$  and  $|U_{\mu 3}U_{e 3}|$ , respectively. The goal of the current neutrino oscillation experiments NO $\nu$ A and T2K is to observe and study  $P_{\mu e}$  and  $\bar{P}_{\mu e}$  governed by  $\Delta m_{31}^2$ , aiming at measuring  $U_{e3}$  and, perhaps, determining the sign of  $\Delta m_{31}^2$  through matter effects, as will be discussed promptly.

Eqs. (1.6,1.7) are valid only when the neutrinos propagate in a vacuum. When neutrinos propagate through a medium, the oscillation physics is modified by so-called matter effects [29]. These are due to the coherent forward scattering of neutrinos with the electrons present in the medium, and they create an additional contribution to the phase differences. Notably, this additional contribution distinguishes between neutrinos and antineutrinos, since there are no positrons present in the Earth.<sup>4</sup> Matter effects also depend on whether the electron neutrino is predominantly made out of the heaviest or lightest mass eigenstates, thus allowing one to address the ordering of the neutrino mass eigenstates. For one mass hierarchy, the oscillation of neutrinos for a certain range of  $L/E$  values can be enhanced with respect to that of antineutrinos, while for the other mass hierarchy the effect is reversed. On the flip side, if the mass hierarchy is not known, matter effects lead to ambiguities in determining the oscillation parameters, as discussed briefly earlier. Matter effects have already allowed the determination of one “mass hierarchy,” that of  $\nu_1$  and  $\nu_2$ . Thanks to matter effects in the sun, we know that  $\nu_1$ , which is lighter than  $\nu_2$ , has the larger electron component:  $|U_{e1}|^2 > |U_{e2}|^2$ . A similar phenomenon should be observable in the  $\Delta m_{31}^2$  sector, given the recent discovery that  $|U_{e3}|$  is not zero. Quantitatively, the importance of matter effects will depend on the density of the medium being traversed, which determines the so-called matter potential  $A \equiv \sqrt{2}G_F N_e$ , where  $G_F$  is the Fermi constant and  $N_e$  is the electron number-density of the medium, and on the value of  $\Delta m_{21,31}^2/E$ . Matter effects are irrelevant when  $A \ll \Delta m_{21,31}^2/E$ . For  $\Delta m_{31(21)}^2$  matter effects in the Earth’s crust are significant for  $E \gtrsim 1$  GeV (20 MeV).

## 1.4 Neutrino Experiments: Sources and Detectors

Next-generation experiments have at their disposal a handful of neutrino sources, which we describe qualitatively here, concentrating on their prospects for neutrino oscillation searches. The sources span many orders of magnitude in energy: see Fig. 1-4. Associated with each experiment is an appropriate detector. The natures and the requirements for the detectors depend on the neutrino source.

The Sun is a very intense source of  $\nu_e$  with energies between 100 keV and 10 MeV. Precision measurements of the low-energy component of the solar neutrino flux (the so-called  $pp$ -neutrinos) may provide an unique opportunity to improve on the precision with which  $\sin^2 \theta_{12}$  is known [31]. The detection of very low-energy solar neutrinos is very challenging, but R&D related to building such detectors profits from significant synergy with efforts to look for dark matter and observe neutrinoless double-beta decay. Solar neutrinos in the few-MeV range are very sensitive to solar matter effects, and provide a unique opportunity to test the Standard Model through the Mikheev-Smirnov-Wolfenstein (MSW) matter effect [29, 32]. Indeed, data from the SNO experiment seem to hint at potential deviations from Standard Model expectations [33]. During

<sup>3</sup>Solar data translate into overwhelming evidence for  $P_{e\mu} + P_{e\tau} \neq 0$ . In the standard paradigm, this is indistinguishable from  $1 - P_{ee} \neq 1$  and hence cannot, even in principle, provide more information than a disappearance result.

<sup>4</sup>In fact, the electron background explicitly violates  $CPT$  symmetry. For neutrinos oscillating in matter, it is no longer true, for example, that  $P_{\alpha\alpha} = \bar{P}_{\alpha\alpha}$ .

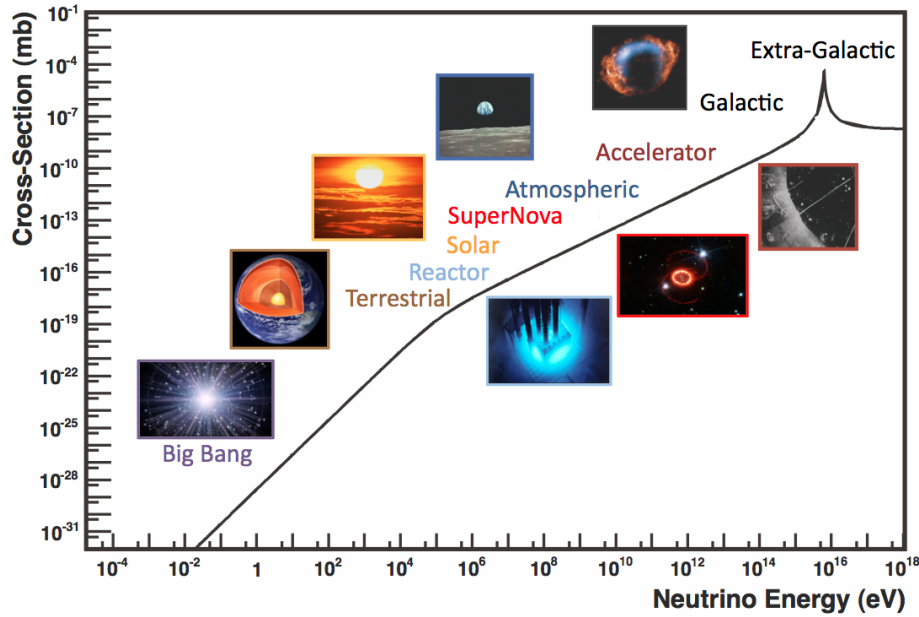


**Figure 1-4.** Neutrino interaction cross section as a function of energy, showing typical energy regimes for different sources. The scattering cross section for  $\bar{\nu}_e e^- \rightarrow e^- \bar{\nu}_e$  on free electrons is shown for comparison. Plot is reproduced from [30].

318 this decade, more (neutrino) light is expected to shine on this potentially very important matter, from the  
 319 Borexino [34] and the SNO+ [35] experiments.

320 Nuclear reactors are an intense, very pure source of  $\bar{\nu}_e$  with energies between a few and several MeV. Due  
 321 to the low neutrino energies, only  $\bar{\nu}_e$  can be detected in the final state, which is done via inverse  $\beta$ -decay,  
 322  $\bar{\nu}_e + p \rightarrow e^+ + n$ . The current generation of reactor experiments aims at percent-level measurements of the  $\bar{\nu}_e$   
 323 spectrum, one or two kilometers away from the source. At these distances and energies one is sensitive only  
 324 to  $\Delta m_{31}^2$ -driven oscillations. The necessary precision is expected to be achieved through the comparison of  
 325 data obtained at near and far detectors. In a nutshell, the near detector measures the neutrino flux before  
 326 oscillations have had time to act, while the far detector measures the effects of the oscillations [36]. Reactor  
 327 neutrino experiments with much longer baselines (say, 50 km) have been considered: see, for example,  
 328 [37, 38]. These would be sensitive to both  $\Delta m_{31}^2$  and  $\Delta m_{21}^2$ -driven oscillations, and, in principle, would allow  
 329 much more precise measurements of  $\Delta m_{21}^2$  and  $|U_{e2}|$ . A detector with exquisite energy resolution may also  
 330 be sensitive to the neutrino mass hierarchy (see, for example, [39]). A concrete proposal for 10 km reactor  
 331 neutrino experiment, Daya Bay II, is currently under serious consideration in China [40].

332 Meson decays are a very good source of  $\nu_\mu$  and  $\nu_\tau$  and their antiparticles. The heavy  $\tau$ -lepton mass, however,  
 333 prevents any realistic means of producing anything that would qualify as a  $\nu_\tau$ -beam, so we will only discuss  
 334  $\nu_\mu$  beams. Pions and, to a lesser extent, kaons are produced in large numbers through proton-nucleus  
 335 interactions. These, in turn, can be sign-selected in a variety of ways to yield a mostly pure  $\nu_\mu$  or  $\bar{\nu}_\mu$  beam.  
 336 The neutrino energy is directly related to the pion energy.

337 The lowest energy  $\nu_\mu$  “beams” (really, isotropic sources) are achieved from pion decay at rest. A large  
 338 sample of mostly  $\pi^+$  at rest yields a very well-characterized flux of mono-energetic  $\nu_\mu$  (from the  $\pi^+$  decay),  
 339 along with  $\bar{\nu}_\mu$  and  $\nu_e$  from the subsequent daughter muon decay. All neutrino energies are below the muon  
 340 production threshold, so only  $\nu_e$  and  $\bar{\nu}_e$  can be detected via charged-current interactions. An interesting

341 experimental strategy is to search for  $\bar{\nu}_e$  via inverse  $\beta$ -decay, a very well understood physics process, and  
 342 hence measure with good precision  $\bar{P}_{\mu e}$  [41]. Matter effects play an insignificant role for the decay-at-rest  
 343 beams, rendering oscillation results less ambiguous. On the other hand, even very precise measurements of  
 344  $\bar{P}_{\mu e}$  from pion decay at rest are insensitive to the neutrino mass hierarchy.

345 Boosted pion-decay beams are the gold standard of readily accessible neutrino oscillation experiments. A  
 346 pion beam is readily produced by shooting protons on a target. These can be charge- and energy-selected,  
 347 yielding a beam of either mostly  $\nu_\mu$  or  $\bar{\nu}_\mu$ . Larger neutrino energies allow one to look for  $\nu_e$ ,  $\nu_\mu$  and,  
 348 for energies above a few GeV,  $\nu_\tau$  in the far detector. Large neutrino energies, in turn, require very long  
 349 baselines<sup>5</sup> and hence very intense neutrino sources and very large detectors. Intense neutrino sources, in  
 350 turn, require very intense proton sources, of the type described in Sec. 1.4. For this reason, these pion-decay-  
 351 in-flight beams are often referred to as superbeams. Larger neutrino energies and longer baselines also imply  
 352 nontrivial matter effects even for  $\Delta m_{31}^2$ -driven oscillations. A neutrino beam with energies around 1 GeV and  
 353 baselines around 1000 km will allow the study of  $P_{\mu\mu}$  and  $P_{\mu e}$  (and, in principle, the equivalent oscillation  
 354 probabilities for antineutrinos) as long as the far detector is sensitive to both  $\nu_\mu$  and  $\nu_e$  charged-current  
 355 interactions. One may choose to observe the neutrino flux a few degrees off the central beam axis, where  
 356 the pion decay kinematics result in a narrowly peaked neutrino spectrum. This is beneficial for optimizing  
 357 sensitivity at the oscillation maximum and for reducing backgrounds outside the energy regime of interest.

358 The constant collision of cosmic rays with the atmosphere produces mesons (mostly pions and kaons) and,  
 359 upon their decays,  $\nu_\mu$ ,  $\bar{\nu}_\mu$ ,  $\nu_e$ ,  $\bar{\nu}_e$ . These atmospheric neutrinos cover a very wide energy range (100 MeV to  
 360 100 GeV and beyond) and many different distances (15 km to 13000 km), some going through the core of  
 361 the Earth and hence probing matter densities not available for Earth-skimming neutrino beams. This is, by  
 362 far, the broadest (in terms of  $L/E$  range) neutrino “beam.” As far as challenges are concerned, uncertainties  
 363 in the atmospheric neutrino flux are not small, and the incoming neutrino energy and direction must be  
 364 reconstructed only with information from the neutrino detector.

365 In the past, atmospheric neutrinos have provided the first concrete evidence for neutrino oscillations, and  
 366 at present they are still a major contributor to the global fits to neutrino oscillation parameters. They will  
 367 continue to be important in the future. They are also ubiquitous and unavoidable. IceCube DeepCore is  
 368 already taking data and will accumulate close to a million events with energies above about 10 GeV over  
 369 the next decade [42]. Any other very large detector associated with the intensity frontier program will also  
 370 collect a large number of atmospheric neutrino events in various energy ranges, through different types of  
 371 signatures. While atmospheric neutrino data suffer from larger systematic uncertainties, some of these can  
 372 be greatly reduced by studying angular and energy distributions of the very high statistics data. Their study  
 373 can complement that of the high precision measurements from fixed baseline experiments. For example, non-  
 374 standard interactions of neutrinos, additional neutrino flavors and other new physics phenomena affecting  
 375 neutrinos could be present, and their effects are likely to be more important at higher energies or in the  
 376 presence of matter, thus making atmospheric neutrinos an ideal testing ground (see, for example, [43]).  
 377 Furthermore, a precise, very high statistics measurement of the atmospheric neutrino flux itself over a very  
 378 large range of energies will also contribute to a better understanding of cosmic ray propagation through the  
 379 atmosphere [44, 45, 46].

380 Muon decays are also excellent sources of neutrinos. The physics and the kinematics of muon decay are  
 381 very well known and yield two well-characterized neutrino beams for the price of one:  $\nu_\mu + \bar{\nu}_e$  in case of  
 382  $\mu^-$  decays,  $\bar{\nu}_\mu + \nu_e$  in the case of  $\mu^+$ . A neutrino factory is a storage ring for muons with a well-defined  
 383 energy. Depending on the muon energy, one can measure, with great precision,  $P_{\mu\mu}$  and  $P_{e\mu}$ , assuming the  
 384 far detector can tell positive from negative muons, potentially along with  $P_{\mu e}$  and  $P_{ee}$ , if the far detector  
 385 is sensitive to electron charged-current events and can deal with the  $\pi^0$  backgrounds, or  $P_{\mu\tau}$  and  $P_{e\tau}$ , if

<sup>5</sup>The oscillation phase scales like  $L/E$ . For a 1 GeV beam, one aims at  $L$  values close to 1000 km.

386 the muon energy is large enough and if the far detector has the ability to identify  $\tau$ -leptons with enough  
387 efficiency. Neutrino factories are widely considered the ultimate sources for neutrino oscillation experiments  
388 [47], and probably allow for the most comprehensive tests of the standard three-neutrino paradigm.

389 Finally, nuclei that undergo  $\beta$ -decay serve as a very well-characterized source of  $\nu_e$  or  $\bar{\nu}_e$ . An intense, highly  
390 boosted beam of  $\beta$ -decaying nuclei would allow for the study of  $P_{e\mu}$ . Such sources are known as “ $\beta$ -beams”  
391 [48].

392 To do neutrino experiments, one must of course detect neutrinos. Neutrino detectors span a huge range of  
393 technologies, some standard for particle physics and others highly specialized. Detectors are typically quite  
394 large, up to multi-kton scale and higher, due to the smallness of neutrino-interaction cross sections. Specific  
395 detector needs depend on neutrino energy and physics goals. In general, good reconstruction capabilities,  
396 *i.e.* ability to reconstruct momenta and particle types of interaction products, are needed. For long-baseline  
397 beams and atmospheric neutrinos, for which energies are high ( $\sim$ GeV), a variety of tracking detector technolo-  
398 gies can be used, each with advantages and disadvantages. Commonly-employed detector technologies include  
399 segmented trackers (*e.g.* Soudan, MINOS, NO $\nu$ A, INO), some with magnetic fields to enable interaction-  
400 product sign selection, water-Cherenkov detectors (Super-K, Hyper-K), and liquid argon time projection  
401 chambers (Icarus, LBNE). At the very highest energies, astrophysical neutrino detectors employ enormous  
402 volumes of water or ice (IceCube, Antares). For low-energy neutrinos (few to tens of MeV neutrinos from the  
403 Sun, reactors, supernovae, stopped-pion sources), homogeneous volumes of liquid scintillator are frequently  
404 employed (Borexino, KamLAND, LENA). For the lowest-energy interaction products, dark-matter WIMP  
405 detector technology sensitive to nuclear recoils can be used (see Secs. 1.8.3.2, 1.11.1.2).

406 Many R&D activities related to neutrino detection are currently underway [?]. For neutrino beam sources  
407 experiments, for which neutrinos can be easily separated from cosmogenic backgrounds because they tend  
408 to arrive in sharp bursts associated with beam pulses, surface detectors are possible. However for physics  
409 involving natural neutrinos or steady-state sources, backgrounds become critical. Siting underground, away  
410 from cosmic rays, then becomes essential [49].

411 Tables 1-1 and 1-2 summarize the capabilities of current and future neutrino-oscillation experiments.

**Table 1-1.** Types of current or proposed neutrino oscillation experiments, with some current and future examples (not exhaustive), along with their accessibility to different oscillation channels.  $\sqrt{\sqrt{\quad}}$  indicates the most important oscillation channel(s) while  $\sqrt{\quad}$  indicates other accessible channels. ‘ $\nu_{e,\mu}$  disapp’ refers to the disappearance of  $\nu_e$  or  $\nu_\mu$ , which are related to  $P_{ee}$  and  $P_{\mu\mu}$ , respectively. ‘ $\nu_\mu \leftrightarrow \nu_e$ ’ refers to the appearance of  $\nu_e$  in a  $\nu_\mu$  beam or vice versa, related to  $P_{e\mu}$  or  $P_{\mu e}$ . ‘ $\nu_\tau$  app’ refers to the appearance of  $\nu_\tau$  from an initial state  $\nu_e$  or  $\nu_\mu$ , related to  $P_{(e,\mu)\tau}$ . ‘Pion DAR/DIF’ refers to neutrinos from pion decay at rest or in flight. ‘ $\mu$  DAR/DIF’ and ‘ $\beta$  Beam’ refer to neutrinos from muon decay and nuclear decay in flight, respectively. In particular Pion DIF stands for a so-called conventional neutrino beam. ‘Coherent  $\nu$ -A’ stands for very low-energy neutrino experiments, using DAR or reactors, aiming at measuring coherent neutrino–nucleus scattering. See text for more details.

Expt. Type	$\nu_e$ disapp	$\nu_\mu$ disapp	$\nu_\mu \leftrightarrow \nu_e$	$\nu_\tau$ app <sup>1</sup>	Examples
Reactor	$\sqrt{\sqrt{\quad}}$	–	–	–	KamLAND, Daya Bay, Double Chooz, RENO
Solar <sup>2</sup>	$\sqrt{\sqrt{\quad}}$	–	$\sqrt{\quad}$	–	Super-K, Borexino, SNO+, LENS (prop), Hyper-K (prop)
Supernova <sup>3</sup>	$\sqrt{\sqrt{\quad}}$	$\sqrt{\quad}$	$\sqrt{\sqrt{\quad}}$	–	Super-K, KamLAND, Borexino, IceCube, LBNE (prop), Hyper-K (prop)
Atmospheric	$\sqrt{\quad}$	$\sqrt{\sqrt{\quad}}$	$\sqrt{\quad}$	$\sqrt{\quad}$	Super-K, LBNE (prop), INO (prop), IceCube, Hyper-K (prop)
Pion DAR	$\sqrt{\quad}$	–	$\sqrt{\sqrt{\quad}}$	–	OscSNS <sup>4</sup> , DAE $\delta$ ALUS (prop)
Pion DIF	–	$\sqrt{\sqrt{\quad}}$	$\sqrt{\sqrt{\quad}}$	$\sqrt{\quad}$	MiniBooNE <sup>4</sup> , MINER $\nu$ A <sup>5</sup> , MINOS(+, prop), T2K, NO $\nu$ A, MicroBooNE <sup>4</sup> , LBNE, Hyper-K (prop)
Coherent $\nu$ -A <sup>6</sup>	–	–	–	–	CENNS (prop), CSISNS (prop), RICOCHET (prop)
$\mu$ DIF <sup>6</sup>	$\sqrt{\quad}$	$\sqrt{\sqrt{\quad}}$	$\sqrt{\sqrt{\quad}}$	$\sqrt{\quad}$	NuStorm (prop), NuFact (prop)
$\beta$ Beam	$\sqrt{\quad}$	–	$\sqrt{\sqrt{\quad}}$	–	

<sup>1</sup>In order to observe  $\nu_\tau$  appearance, a dedicated detector or analysis is required, along with a high-enough neutrino energy. <sup>2</sup>Solar neutrino experiments are sensitive, at most, to the  $\nu_e$  and the  $\nu_e + \nu_\mu + \nu_\tau$  components of the solar neutrino flux. <sup>3</sup>Signatures of neutrino oscillation occurring both in the collapsed star matter and in the Earth will be present in the spectra of observed fluxes of different flavors, and do not strictly fall in these categories; detectors are sensitive to  $\nu_e$  and  $\bar{\nu}_e$  fluxes, and to all other flavors by NC interactions. <sup>4</sup>Not sensitive to oscillations in standard 3-flavor context, but sensitive for sterile oscillation searches. <sup>5</sup>MINER $\nu$ A measures neutrino cross sections with the aim of reducing systematics for oscillation experiments. <sup>6</sup>Coherent elastic neutrino-nucleus scattering is purely NC and not sensitive to oscillation between active flavors. <sup>6</sup>The “standard” high-energy neutrino factory setups are not sensitive to electron appearance or disappearance.

**Table 1-2.** Types of current or proposed neutrino oscillation experiments and their ability to address some of the outstanding issues in neutrino physics. ‘NSI’ stands for non-standard neutrino interactions, while  $\nu_s$  ( $s$  for sterile neutrino) stands for the sensitivity to new neutrino mass eigenstates. ‘\*\*\*’ indicates a very significant contribution from the current or proposed version of these experimental efforts, ‘\*\*’ indicates an interesting contribution from current or proposed experiments, or a significant contribution from a next-next generation type experiment, ‘\*’ indicates a marginal contribution from the current or proposed experiments, or an interesting contribution from a next-next generation type experiment. See Table 1-1 and text for more details.

Expt. Type	$\sin^2 \theta_{13}$	$\text{sign}(\Delta m_{31}^2)$	$\delta$	$\sin^2 \theta_{23}$	$ \Delta m_{31}^2 $	$\sin^2 \theta_{12}$	$\Delta m_{21}^2$	NSI	$\nu_s$
Reactor	***	*	–	–	*	**	**	–	**
Solar	*	–	–	–	–	***	*	**	**
Supernova	*	***	–	–	–	*	*	**	**
Atmospheric	**	**	**	**	**	–	–	***	**
Pion DAR	***	–	***	*	**	*	*	–	**
Pion DIF	***	***	***	**	**	*	*	**	**
Coherent $\nu$ -A	–	–	–	–	–	–	–	***	**
$\mu$ DIF	***	***	***	***	***	*	*	**	**
$\beta$ Beam	***	–	***	**	**	*	*	–	**

## 1.5 The Standard Oscillation Paradigm

The three-flavor oscillation framework is quite successful in accounting for a large number of results obtained in very different contexts: the transformation of  $\nu_e$  into  $\nu_{\mu,\tau}$  from the Sun [33]; the disappearance of  $\nu_\mu$  and  $\bar{\nu}_\mu$  from neutrinos produced by cosmic ray interactions in the atmosphere; the disappearance of  $\nu_\mu$  and  $\bar{\nu}_\mu$  [50, 51] from neutrino beams over distances from 200-740 km [52, 53, 54]; the disappearance of  $\bar{\nu}_e$  from nuclear reactors over a distance of about 160 km [55]; the disappearance of  $\bar{\nu}_e$  from nuclear reactors over a distance of about 2 km [56, 57, 58]; and at somewhat lower significance also the appearance of  $\nu_e$  [28, 27] and, at even lower significance, the appearance of  $\nu_\tau$  [26] has been observed in experiments using man-made neutrino beams over 200-740 km distance. All these experimental results can be succinctly and accurately described by the oscillation of three active neutrinos governed by the following parameters, including their  $1\sigma$  ranges [59]

$$\Delta m_{21}^2 = 7.54_{-0.22}^{+0.26} \times 10^{-5} \text{ eV}^2, (3.2\%) \quad \Delta m_{31}^2 = 2.43_{+0.1}^{-0.06} \times 10^{-3} \text{ eV}^2, (3.3\%) \quad (1.8)$$

$$\sin^2 \theta_{12} = 3.07_{-0.16}^{+0.18} \times 10^{-1}, (16\%) \quad \sin^2 \theta_{23} = 3.86_{-0.21}^{+0.24} \times 10^{-1}, (21\%) \quad (1.9)$$

$$\sin^2 \theta_{13} = 2.41 \pm 0.25 \times 10^{-1}, (10\%) \quad \delta = 1.08_{-0.31}^{+0.28} \text{ rad}, (27\%), \quad (1.10)$$

where for all parameters whose value depends on the mass hierarchy, we have chosen the values for the normal mass ordering. The choice of parametrization is guided by the observation that for those parameters the  $\chi^2$  in the global fit is approximately Gaussian. The percentages given in parenthesis indicate the relative error on each parameter. For the mass splitting we reach errors of a few percent; however, for all of the mixing angles and the CP phase the errors are in the 10-30% range. Therefore, while three-flavor oscillation is able to describe a wide variety of experiments, it would seem premature to claim that we have entered the era of precision neutrino physics or that we have established the three-flavor paradigm at a high level of accuracy. This is also borne out by the fact that there are significant hints at short baselines for a fourth neutrino [60]. Also, more general, so-called non-standard interactions are not well constrained by neutrino data; for a recent review on the topic see Ref. [61]. The issue of what may exist beyond three-flavor oscillations will be discussed in detail in Sec. 1.9 of this report.

Once one realizes that the current error bars are uncomfortably large, the next question is: how well do we want/need to determine the various mixing parameters? The answer can be given at two distinct levels. One is a purely technical one – if I want know  $X$  to a precision of  $x$ , I need to know  $Y$  with a precision of  $y$ ; an example is, where  $Y$  is given by  $\theta_{13}$  and  $X$  could be the mass hierarchy. The answer, at another level, is driven by theory expectations of how large possible phenomenological deviations from the three-flavor framework could be. In order to address the technical part of the question, one first has to define the target precision from a physics point of view. Guidance from other subareas of particle physics reveal that the “target precision” evolves over time. For example, history shows that theoretical estimates of the top quark mass from electroweak precision data and other indirect observable, before its eventual discovery, seem to have been, for the most part (and with very large uncertainties), only several GeV ahead of the experimental reach – at the time, there always was a valid physics argument for why the top quark is “just around the corner.” A similar “evolution” of theoretical expectations can be observed in, for example, searches for new phenomena in quark flavor physics. Thus, any argument based on model-building-inspired target precisions is always of a preliminary nature, as our understanding of models evolves over time. With this caveat in mind, one argument for a target precision can be based on a comparison to the quark sector. Based on a theoretical guidance from Grand Unification, one would expect that the answer to the flavor question should find a concurrent answer for leptons and quarks. Therefore, a test of such a models is most sensitive if the precision in the lepton and quark sector is comparable. For instance, the CKM angle  $\gamma$ , which is a very close analog of  $\delta$  in the neutrino sector, is determined to  $(70.4_{-4.4}^{+4.3})^\circ$  [62] and thus, a precision target for  $\delta$  of roughly  $5^\circ$  would follow.

A different argument for a similar level of precision can be made based on the concept of so-called neutrino sum-rules [63]. Neutrino sum-rules arise, for example, in models where the neutrino mixing matrix has a certain simple form or texture at a high energy scale and the actual low-energy mixing parameters are modified by a non-diagonal charged lepton mass matrix. The simplicity of the neutrino mixing matrix is typically a result of a flavor symmetry, where the overall Lagrangian possesses an overall flavor symmetry  $G$ , which can be separated into two sub-groups  $G_\nu$  and  $G_l$  for the neutrinos and charged leptons; it is the mismatch between  $G_\nu$  and  $G_l$  which will yield the observed mixing pattern, see e.g. [64]. Typical candidates for  $G$  are given by discrete subgroups of  $SU(3)$  which have a three dimensional representation, e.g.,  $A_4$ . In a model-building sense, these symmetries can be implemented using so-called flavon fields which undergo spontaneous symmetry breaking and it is this symmetry breaking which picks the specific realization of  $G$ , for a recent review see [65]. The idea of flavor symmetries is in stark contrast to the idea that neutrino mixing parameters are anarchic, *i.e.* random numbers with no underlying dynamics, for the most recent version of this argument, see Ref. [66]. To find out whether the patterns observed in lepton mixing correspond to an underlying symmetry is one of the prime tasks of neutrino physics. Of course, distinguishing among the many candidate underlying symmetries is also a very high priority.

In practice, flavor symmetries will lead to relations between measurable parameters, whereas anarchy will not. For example, if the neutrino mixing matrix is of tri-bi-maximal form,  $|U_{e3}| = 0$  is naively expected to vanish, which is clearly in contradiction to observations. In this case, a non-diagonal charged lepton mass matrix can be used to generate the right value of  $|U_{e3}|$ , and, for one concrete model, the following sum-rule arises

$$\theta_{12} - \theta_{13} \cos \delta = \arcsin \frac{1}{\sqrt{3}}, \quad (1.11)$$

which can be tested if sufficiently precise measured values for the three parameters  $\theta_{12}, \theta_{13}, \delta$  are available. Depending on the underlying symmetry of the neutrino mixing matrix different sum-rules are found. In Fig. 1-5 several examples are shown and for each case the values of  $\theta_{13}$  and  $\theta_{12}$  or  $\theta_{23}$  are drawn many times from a Gaussian distribution where the mean values and ranges are taken from Eq. 1.8. The resulting predictions of the value of the CP phase  $\delta$  are histogrammed and shown as colored lines. The width of the distribution for each sum-rule arises from the finite experimental errors on  $\theta_{12}$  or  $\theta_{23}$  and  $\theta_{13}$ . Two observations arise from this simple comparison: first, the distance of the means of the distributions is as small as  $15^\circ$ , and second, the width of the distributions is significant compared to their separation and a reduction of input errors is mandated. The thin lines show the results if the errors are reduced to the value given in the plot, which would be achieved by Daya Bay for  $\sin^2 2\theta_{13}$ , by Daya Bay II for  $\sin^2 \theta_{12}$ , and by NOvA for  $\sin^2 \theta_{23}$ . Assuming that the errors on  $\theta_{12}$ ,  $\theta_{23}$  and  $\theta_{13}$  are reduced to this level, the limiting factor is the natural spread between models, which is about  $15^\circ$ . A  $3\sigma$  distinction between models translates into a target precision for  $\delta$  of  $5^\circ$ . A measurement at this precision would allow to obtain valuable information on whether indeed there is an underlying symmetry behind neutrino mixing. Moreover, it is likely to also provide hints regarding which specific class of symmetries is realized. This would constitute a major breakthrough in our understanding of flavor.

For the parameter  $\sin^2 2\theta_{13}$  the *status quo* is determined by the results from the reactor experiments Double Chooz [56], Daya Bay [67] and RENO [57] and their results agree well. It is expected that Double Chooz will improve its systematical error by a significant amount with the planned addition of a near detector by the end of 2013. Daya Bay started running in its full eight detector configuration only in the summer of 2012 and it is expected that a 3 year run with all detectors will eventually reach a 3% error on  $\sin^2 2\theta_{13}$ , compared to currently about 12.5% on this parameter. Of all beam experiments only a neutrino factory will be able to match this precision [68]. A comparison of the values of  $\theta_{13}$  obtained in  $\bar{\nu}_e$  disappearance at reactors with the result of  $\nu_e$  and  $\bar{\nu}_e$  appearance in beams will be a sensitive test of the three-flavor framework, which is particularly sensitive to non-standard matter effects.

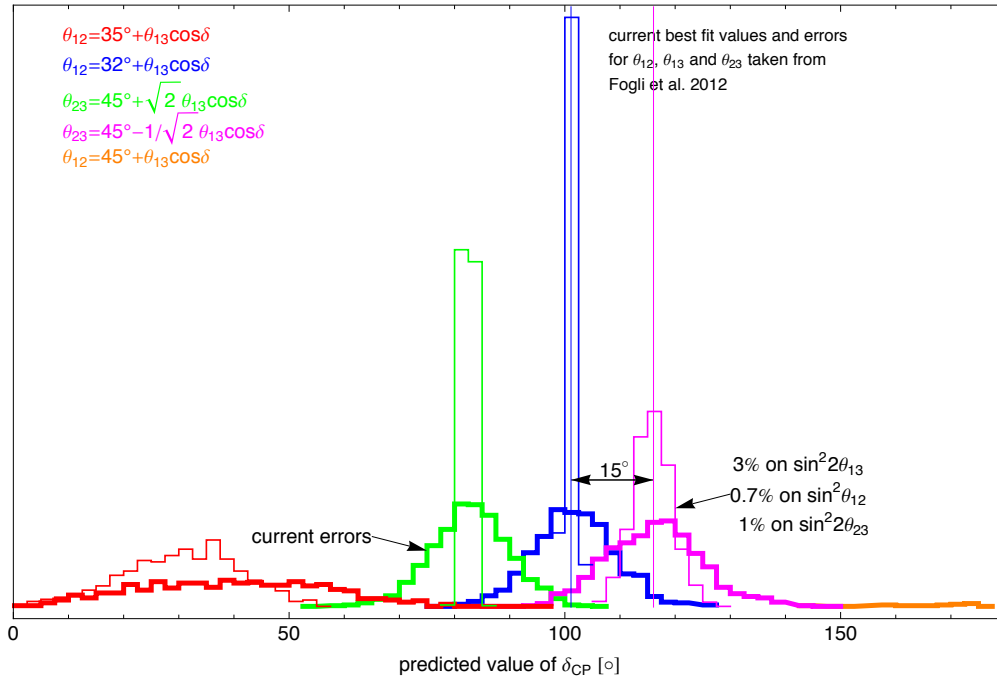


**Figure 1-5.** Shown are the distributions of predicted values from  $\delta$  from various sum-rule as denoted in the legend and explained in the text.

499 For the atmospheric  $\Delta m_{31}^2$ , currently the most precise measurement comes from MINOS [53] with an error  
 500 of 3.2% and MINOS+ [69] will slightly improve on this result. It is expected that both NO $\nu$ A and T2K will  
 501 contribute measurements with errors of  $\sim 3\%$  and  $\sim 4\%$ , respectively. Daya Bay will provide a measurement  
 502 of this parameter in  $\bar{\nu}_e$  disappearance of about 4%. By increasing the size of the event sample and going to  
 503 an off-axis location, CHIPS [70] has the potential to reduce the current error maybe be as much as a factor  
 504 2-3, which is of course subject to sufficient control of systematical errors and needs further study. Daya Bay  
 505 II [40] ultimately may have the potential to bring the error down to below one percent. For  $\theta_{23}$  two related  
 506 but distinct questions arise: what is the precise value of  $\sin^2 2\theta_{23}$  or how close it is to unity; and secondly,  
 507 if  $\sin^2 2\theta_{23} \neq 1$ , is  $\theta_{23}$  smaller or larger than  $\pi/4$ , the so-called octant of  $\theta_{23}$ . An experiment can be very  
 508 good at determining the value of  $\sin^2 2\theta_{23}$  without obtaining any information on the octant question. The  
 509 resolution of the octant question can be either achieved by comparing long-baseline data obtained at different  
 510 baselines, like NO $\nu$ A and T2K or by comparing a precise  $\nu_\mu \rightarrow \nu_e$  long-baseline measurement with a precise  
 511 determination of  $\bar{\nu}_e \rightarrow \bar{\nu}_e$  oscillations from a reactor experiment like Daya Bay. Within the U.S. program,  
 512 the long-baseline pieces of data can come from the NuMI beam and NO $\nu$ A is well positioned, as would be  
 513 potential extensions of the NuMI program in the form of extended NO $\nu$ A running [69], GLADE [71] and  
 514 CHIPS [70]. Eventually, LBNE, with its very long baseline and wide beam spectrum, will provide good  
 515 sensitivity to the octant on its own. NO $\nu$ A and T2K have the potential to reduce the error on  $\sin^2 2\theta_{23}$  to  
 516 1-2% and most likely further improvements in beam experiments will require an improved understanding of  
 517 systematics.

518 For the solar  $\Delta m_{21}^2$  the current errors are determined by KamLAND and a future improvement is necessary  
 519 to measure the mass hierarchy without using matter effects as proposed by Daya Bay II. Daya Bay II is able  
 520 to reduce the error to below 1%. The solar mixing parameter  $\sin^2 \theta_{12}$  is most accurately measured by SNO  
 521 and there are basically two independent ways to further improved this measurement: One is to do a precision

522 measurement of the solar pp-neutrino flux, since this flux can be predicted quite precisely from the solar  
 523 luminosity and the  $\nu - e$  scattering cross section is determined by the Standard Model, an error of 1% maybe  
 524 achievable. The experimental challenge is the required very low threshold and associated low backgrounds  
 525 in a large detector. The other method relies on the observation of  $\bar{\nu}_e$  disappearance at a distance of about  
 526 60 km as proposed in Daya Bay II, with the potential to bring this error to below 1%. The value of  $\theta_{12}$  and  
 527 its associated error play an important role for sum-rules, as explained previously, but also for neutrinoless  
 528 double  $\beta$ -decay.

529 =====

### 530 1.5.1 Towards the Determination of the Neutrino Mass Hierarchy

531 Within the standard oscillation paradigm, the current neutrino data do not allow one to determine whether  
 532  $m_3^2 > m_2^2 > m_1^2$  — a so-called normal neutrino mass hierarchy — or  $m_2^2 > m_1^2 > m_3^2$  — a so-called  
 533 inverted mass hierarchy — keeping in mind that  $m_2^2 > m_1^2$  by definition. The measurement of the mass  
 534 hierarchy may prove fundamental for understanding the mechanism behind neutrino masses and deciphering  
 535 the information potentially encoded in the pattern of lepton mixing. Determination of the mass hierarchy  
 536 will also provide important input for interpretation of next-generation neutrinoless double beta decay ( $0\nu\beta\beta$ )  
 537 experiments and to the search for leptonic CP violation. It will help in the precision determination of  
 538 neutrino oscillation parameters from accelerator experiments and knowing the mass ordering will allow us  
 539 to get better sensitivity to CP violation. When it comes to understanding certain astrophysical phenomena,  
 540 such as supernova explosions, and interpreting observations in cosmology, the fact that we don't know the  
 541 ordering of neutrino masses can no longer be safely ignored. In summary, an unambiguous determination of  
 542 the mass hierarchy provides important understanding of the fundamental nature of neutrinos with profound  
 543 impact in the next decade and beyond. It will also impact other measurements of neutrino properties, the  
 544 extraction of cosmological parameters and studies of the physics of exploding stars.

545 The recently observed “large” value of  $\theta_{13}$  has opened the possibility of determining, mostly using matter  
 546 effects, the mass hierarchy through a variety of different experiments and observations. This includes  
 547 accelerator-based neutrino oscillation experiments, atmospheric neutrino detectors, as well as reactor an-  
 548 tineutrino experiments, and observations of astrophysical neutrinos from supernovae, as well as cosmology.  
 549 A broad suite of experiments has been proposed to study the mass hierarchy using these possibilities and  
 550 R&D is underway to address the viability of these options. It is possible that one or more of these experiments  
 551 will be able to make an unambiguous determination of the mass hierarchy in the next decade. More likely, we  
 552 will obtain a suite of results with indications that may point to the ordering of the neutrino mass eigenstates  
 553 in a joint analysis. Now that we know the size of  $\theta_{13}$ , a measurement of the neutrino mass hierarchy is within  
 554 reach and may well be one of the next big milestones in neutrino physics.

#### 555 1.5.1.1 Mass Hierarchy from Oscillations and Other Observables

556 The neutrino mass hierarchy manifests itself in different types of phenomena, most of which are potentially  
 557 observable in neutrino oscillation experiments. We review them here, before discussing the reach of different  
 558 types of experiments and opportunities for the near and intermediate future.

559 If all mixing angles are nonzero, the neutrino mass hierarchy manifests itself in all oscillation probabilities,  
 560 including those associated to neutrinos propagating in vacuum. This can be quickly understood via a concrete

561 example. The survival probability of, say, electron neutrinos in vacuum is given by

$$P_{ee} = 1 - \left[ A_{21}^e \sin^2 \left( \frac{\Delta m_{21}^2 L}{4E} \right) + A_{31}^e \sin^2 \left( \frac{\Delta m_{31}^2 L}{4E} \right) + A_{32}^e \sin^2 \left( \frac{\Delta m_{32}^2 L}{4E} \right) \right], \quad (1.12)$$

562 where  $A_{ij}^e \equiv 4|U_{ei}|^2|U_{ej}|^2$ . A measurement of  $P_{ee}$  capable of establishing that there are three (related)  
 563 oscillation frequencies can determine the mass hierarchy as long as the three  $A_{ij}^e$  are nonzero and distinct  
 564 (and known). This comes from the fact that under these circumstances one can tell whether  $|\Delta m_{31}^2| > |\Delta m_{32}^2|$   
 565 or vice-versa. For the normal mass hierarchy  $|\Delta m_{31}^2| > |\Delta m_{32}^2|$  as one can readily see from Fig. 1-1, with the  
 566 situation reversed for the inverted mass hierarchy. For a more detailed discussion see, for example, [72]. The  
 567 fact that  $|\Delta m_{31}^2| \gg \Delta m_{21}^2$  and  $\sin^2 \theta_{13} \ll 1$  renders such a measurement, in practice, very hard as, for almost  
 568 all experimental set-ups, observations are very well-described by an effective two-flavor oscillation scheme,  
 569 completely blind to the mass hierarchy. A reactor neutrino experiment with exquisite energy resolution and  
 570 an intermediate baseline (around 50 km) should be able to see the interplay of all oscillation terms with  
 571  $\Delta m_{31}$  and  $\Delta m_{32}$  and would be sensitive to the mass hierarchy.

572 Matter effects allow one to probe the mass hierarchy in a different way, as already discussed in Sec. 1.3.  
 573 Electron-type neutrinos interact with electrons differently from muon-type and tau-type neutrinos. As  
 574 neutrinos propagate inside a medium filled with electrons the neutrino dispersion relation, and hence the  
 575 oscillation probabilities, are modified in a way that can distinguish electron-type neutrinos from muon-type  
 576 or tau-type neutrinos. This translates into a sensitivity to whether the mass eigenstates containing “more”  
 577 electron-type neutrinos –  $\nu_1$  and  $\nu_2$  – are lighter (normal hierarchy) or heavier (inverted hierarchy) than the  
 578 eigenstates containing “less” electron-type neutrinos –  $\nu_3$ . Such a measurement is possible even if  $\Delta m_{12}^2$  had  
 579 turned out to be very small, as long as  $\theta_{13}$  was not vanishingly small and one is probing oscillations of or into  
 580 electron-type neutrinos. In practice, sensitivity to matter effects requires small values of  $|\Delta m_{31}^2|/E$  hence,  
 581 since one requires  $L$  such that  $|\Delta m_{31}^2|L/E$  is large enough, long distances. For neutrino energies around  
 582 1 GeV,  $L$  values of order several hundred kilometers are required.

583 Core collapse supernovae (SN) from massive stars are an abundant source of neutrinos of all flavors: see  
 584 Sec. 1.10.2.1, and matter effects are abundant and qualitatively different from the ones encountered anywhere  
 585 else (except, perhaps, for the very early universe). There are multiple possible signatures sensitive to mass  
 586 hierarchy in the supernova neutrino flux. During neutrino emission from the SN core the MSW effects are  
 587 encountered twice at high and low density, and the resulting flavor conversion depends on the neutrino mass  
 588 hierarchy in addition to the star’s density, neutrino energy, and the oscillation parameters. In addition,  
 589 shock waves in the SN envelope and Earth matter effects can impact the observed neutrino spectra. Shock  
 590 waves change the adiabatic to non-adiabatic conversion and multiple MSW effects take place. They occur  
 591 either in the  $\nu_e$  or  $\bar{\nu}_e$  channel and depend on the mass hierarchy. Turbulences have similar effects as shock  
 592 waves. In addition, neutrino conversion can take place near the neutrino sphere due to  $\nu$ - $\nu$  interactions. The  
 593 conversion probability is energy dependent and may introduce a spectral split. Model-dependent effects in  
 594 the emitted SN spectrum will have to be considered in the use of SN data for a mass hierarchy determination.

595 Finally, observables outside of neutrino oscillations sensitive to the neutrino masses themselves, as opposed  
 596 to only mass-squared differences, are also in principle sensitive to the neutrino mass hierarchy. Some of these  
 597 are discussed in Secs. 1.6, 1.7, 1.10. For example, if the sum of all neutrino masses was constrained to be  
 598 less than around 0.1 eV, the inverted mass hierarchy hypothesis would be ruled out. Such a sensitivity (or  
 599 better) is expected from several next-general probes of the large-scale structure of the universe, as will  
 600 be discussed in more detail in Sec. 1.10.

## 601 1.5.1.2 Experimental Approaches

602 **Accelerator Experiments** Ongoing and future accelerator experiments are a key element in a program  
 603 to determine the neutrino mass hierarchy. Very intense beams of muon neutrinos from pion sources can  
 604 be used to search for electron neutrino appearance. For intermediate and long baselines the appearance  
 605 probability will depend on the ordering of the neutrino mass states. The upcoming NOvA experiment  
 606 together with T2K will have a chance of determining the neutrino mass hierarchy with accelerator neutrinos  
 607 for a range of oscillation parameters. In the long-term, the long-baseline neutrino oscillation experiment  
 608 (LBNE) or experiments at neutrino factories will allow the definitive measurement of the neutrino mass  
 609 hierarchy. See Figure 1-6. The CHIPS and GLADE seek to exploit the NuMI beam from FNAL with new  
 610 detectors at baselines similar to MINOS and NOvA. The experimental advantages of LBNE over current  
 611 experiments such as NOvA and T2K include an optimum baseline from the neutrino source to the detector,  
 612 a large and highly capable far detector, a high-power, broadband, sign-selected muon neutrino beam, an a  
 613 capable near neutrino detector. If placed underground, the LBNE far detector may even allow the possibility  
 614 of atmospheric neutrino studies and oscillation measurements through a channel with different systematics  
 615 than the accelerator-based experiments. Optimization of the LBNE baseline to determine the mass hierarchy  
 616 with no ambiguities depends only on the known oscillation parameters. To achieve mass hierarchy sensitivity  
 over all phase space requires a baseline  $>1000$  km.

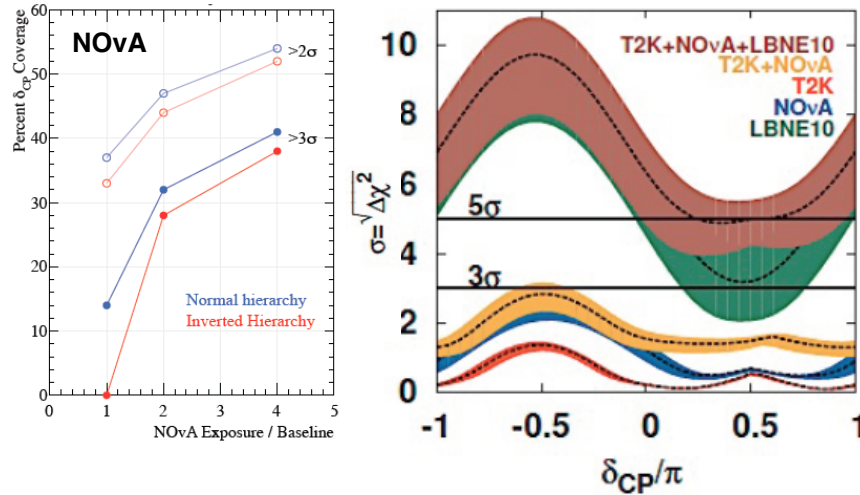
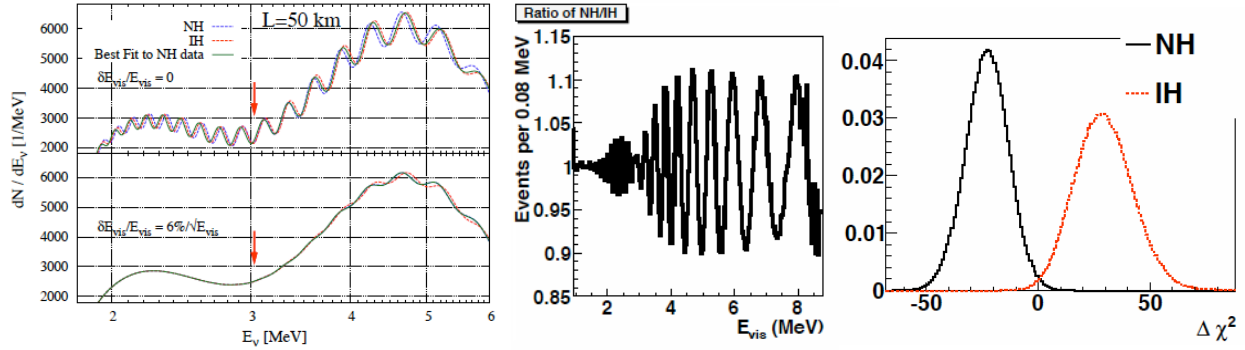


**Figure 1-6.** Left: Percent of  $\delta_{CP}$  values for which NOvA can resolve the neutrino mass hierarchy at 2 and 3  $\sigma$  C.L. NOvA is in construction and has started data taking with a partial detector configuration. Right: Mass hierarchy sensitivity of LBNE10, NOvA, and T2K and combinations thereof. T2K is operational and taking data. NOvA is in the commissioning phase and will finish construction in 2014. LBNE10 is in preliminary design and R&D and preparing for Critical Decision 2. Figures from [73, 74].

617

618 **Reactor Experiments** - The success of recent reactor experiments in the measurement of  $\theta_{13}$  at baselines  
 619 of  $\sim 1$  km has resulted in proposals for the precision study of neutrino oscillation at medium baselines of  
 620 50-60 km. A high-precision, high statistics reactor experiment at 60 km may be able to determine the  
 621 mass hierarchy from the difference in the oscillation effects from  $\Delta m_{31}^2$  and  $\Delta m_{32}^2$ . See Figure 1-7. Such  
 622 a measurement is challenging due to the finite detector resolution, the absolute energy scale calibration, as  
 623 well as degeneracies caused by current experimental uncertainty of  $\Delta m_{32}^2$ . Two experiments are currently  
 624 proposed to make this measurement: Daya Bay II in China and RENO-50 in South Korea, although other  
 625 locations may be suitable. The current design of RENO-50 includes a 10 kton liquid scintillator detector

626  $\sim 47$  km from a 17 GWth power plant. Daya Bay II proposes a 20 kton liquid scintillator detector 700 m  
 627 underground and 60 km from two nuclear power plants with 40 GWth power.



628 **Figure 1-7.** Left: Energy distribution of reactor antineutrinos with baseline length of 50 km. The solid  
 629 line shows the best fit of IH assumption to the NH data. The red arrow points out the energy at which the  
 630 difference due to the mass hierarchy vanishes. The lower panel shows the effect of 6% energy resolution.  
 631 Figure from [75]. Middle: Ratio of reactor antineutrino spectra for NH and IH case for the ideal energy  
 632 spectrum without fluctuation and fixed  $\Delta m_{31}^2$ . Statistical fluctuations, the unknown true value of  $\Delta m_{31}^2$ ,  
 633 as well as experimental effects such as energy scale uncertainty will degrade the observable effect. Right: The  
 634  $\Delta\chi^2$  spectrum from Monte Carlo simulation. The probability of the mass hierarchy being NH is calculated  
 635 as  $P_{NH}/(P_{NH} + P_{IH})$  and found to be 98.9% for 100kT-year exposure. Figures from [76].

627

628 **Atmospheric Neutrino Experiments** – Atmospheric neutrino experiments have played a historic role  
 629 in neutrino physics. From the first observation of the atmospheric neutrino anomaly to the discovery of  
 630 neutrino oscillations in Super-Kamiokande in 1998 precision studies of neutrinos produced in the Earth’s  
 631 atmosphere have been critical to our understanding of neutrino oscillations. Atmospheric neutrinos remain  
 632 an important probe of neutrino oscillations and the large statistics that can be collected by large Cherenkov  
 633 detectors at the Mton-scale such as Hyper-K, PINGU, and ORCA will offer an unprecedented opportunity  
 634 to study them in detail. Atmospheric neutrinos exist in both neutrino and anti-neutrino varieties in both  
 635 muon and electron flavors. Up to  $10^6$  events are expected to be collected in a 10-year period in half megaton  
 636 detectors such as Hyper-K. There are two experimental approaches to the study of the mass hierarchy with  
 637 atmospheric neutrinos. One approach is based on charge discrimination and distinguishes between neutrinos  
 638 and antineutrinos. Large magnetized calorimeters such as INO with good energy and angular resolution and  
 639 thresholds of 1-2 GeV are an example of this type of detector. The second approach uses water Cherenkov  
 640 detectors and makes use of the different cross-sections and different  $\nu$  and  $\bar{\nu}$  fluxes. Examples of future  
 641 water Cherenkov detectors include Hyper-K, a larger version of the successful water-based Super-K detector,  
 642 ORCA, an extension of ANTARES in the Mediterranean Sea, and PINGU, an upgrade of the IceCube Deep  
 643 Core detector at the South Pole. Atmospheric neutrino measurements are also possible in large liquid argon  
 644 TPCs such as that being planned for LBNE. Key to the measurement of the mass hierarchy with these  
 645 experiments will be a large statistical sample collected in a large fiducial volume, good energy and angular  
 646 resolution for the study of the L/E oscillation effects and discrimination of backgrounds. See Figures 1-8  
 647 and 1-9.

648 **Supernova Studies** – A suite of neutrino observatories is currently operational worldwide with a variety of  
 649 target materials including water or ice (Super-K, IceCube), liquid scintillator (KamLAND, Borexino, Daya  
 650 Bay, MiniBooNE, LVD), and lead (HALO). They offer a suite of detection channels through the scattering  
 651 of  $\bar{\nu}_e$  with protons, the  $\nu_e$  scattering with nuclei and  $\nu_x$  interactions with electrons and protons. Together  
 652 they have the ability to measure the SN flux at different thresholds and different flavor sensitivities. The

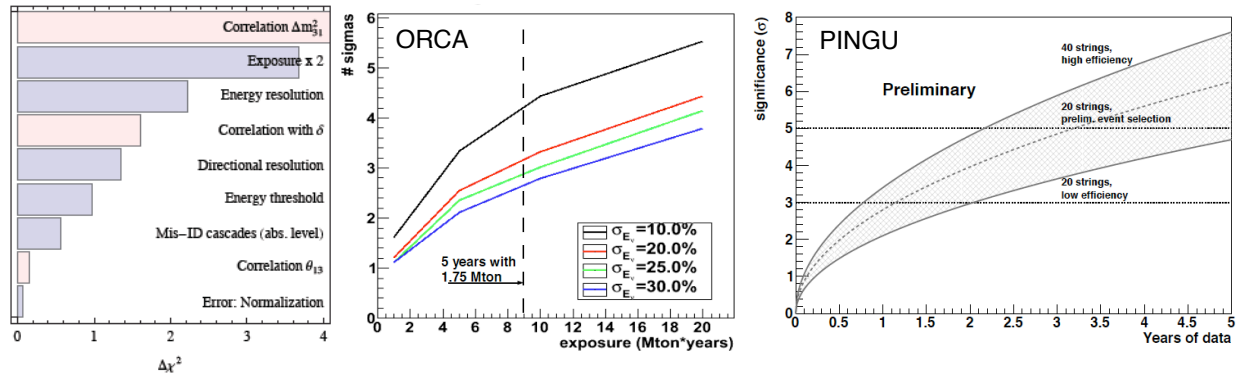


**Figure 1-8.** *Left: Impact of experimental and systematic uncertainties on the determination of the mass hierarchy with atmospheric neutrino experiment such as PINGU and ORCA. The impact is given in form of  $\Delta\chi^2$  for normal hierarchy and  $\delta = 0$  on the default systematics described in [78]. The blue bars indicate experimental systematics. The exposure, energy scale, and directional resolution are most important for the experiment under consideration. Figure from [78]. Right: Sensitivity of the ORCA and PINGU proposals to mass hierarchy. Experimental sensitivities are preliminary. Figures from [79, 77].*

653 observation of SN will offer a rich physics opportunity with discovery potential if we are lucky enough to  
 654 observe during the lifetime of these experiments.

### 655 1.5.1.3 Experimental Status and Opportunities

656 The measurement of large  $\theta_{13}$  has opened a broad range of possibilities for the determination of the neutrino  
 657 mass hierarchy. Several experiments with complementary approaches have been proposed that will allow us to  
 658 determine the neutrino mass hierarchy in oscillation experiments using neutrinos from accelerators, reactors,  
 659 or the atmosphere. NOvA is the only funded oscillation experiment under way to start an experimental  
 660 investigation of the neutrino mass hierarchy in a range of the allowed parameter space. T2K is taking data  
 661 but only has a weak dependence due its short baseline. For some of the recent proposals under consideration  
 662 sometimes significant R&D and design work is still required. A dedicated experiment to measure the neutrino  
 663 mass hierarchy with atmospheric or reactor neutrinos may be feasible by 2018. After 2022, the planned LBNE  
 664 experiment will be able to determine the neutrino mass hierarchy for the entire range of CP values. In the  
 665 mean time double beta decay and direct neutrino mass experiments combined with data from cosmology  
 666 may also tell us about the hierarchy if  $\sum m_\nu$  is measured to be less than 0.1 eV. A supernova event detected  
 667 in one or several of the existing large neutrino observatories would enable a rich physics program and may  
 668 allow the determination of the ordering of the neutrino mass states. Astrophysics and uncertainties in the  
 669 supernova models make this challenging. Table 1-3 summarizes the status of the ongoing and proposed  
 670 experiments.

671 From the early days of neutrino physics the US has hosted and been a leader in several historic neutrino  
 672 experiments. The first solar neutrino experiment, studies of the atmospheric neutrino anomaly, and neutrino  
 673 mass experiments were performed in the US. In recent years US scientists have played major roles in  
 674 experiments overseas including Super-K, SNO, KamLAND, Daya Bay and others. In addition, the US  
 675 has pursued a successful domestic neutrino oscillation program with MINOS, MiniBooNE, and others. With  
 676 NOvA followed by LBNE, the US will lead the experimental determination of the neutrino mass hierarchy  
 677 with accelerator neutrinos for the next decade and beyond. Reactor and atmospheric neutrinos may offer  
 678 the opportunity for alternative, complementary measurements with possibly earlier results. Ongoing R&D

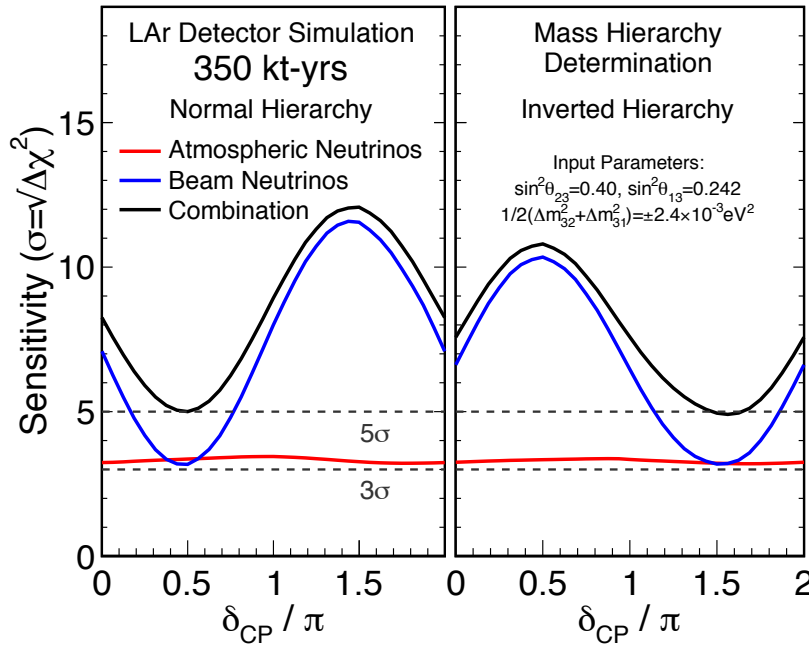


**Figure 1-9.** Mass hierarchy determination possible with atmospheric neutrinos in a 35 kton-year exposure of an underground liquid argon TPC in LBNE shown as a function of possible  $\delta_{CP}$  values for both normal (left) and inverted (right) hierarchies. Atmospheric neutrino information can be combined with beam information in the same detector to improve overall sensitivity. Plot courtesy of A. Blake.

679 will establish the viability of these proposals. US universities and national laboratories have been leaders in  
 680 the study of reactor neutrinos and have pioneered the study of atmospheric neutrino with the largest particle  
 681 physics detector ever built, IceCube. The quest for the neutrino mass hierarchy offers the opportunity for  
 682 US leadership and participation with discovery potential in several international experiments.

### 683 1.5.2 Towards the Determination of CP Violation in Neutrinos

684 The standard approach to measuring CP violation in neutrinos is to use long-baseline beams of both neutrinos  
 685 and antineutrinos. As for the mass hierarchy determination, nature provides beams of atmospheric neutrinos  
 686 and antineutrinos free of charge, over a wide range of energies and baselines— the catch is that one has no  
 687 control over their distribution and so one must measure their properties precisely, and/or gather immense  
 688 statistics in order to extract information on CP violation from these sources. Alternate approaches include  
 689 using well-controlled, well-understood accelerator-based beams of neutrinos or lower-energy neutrinos from  
 690 pion decay-at-rest sources. Here, we will discuss the CP reach of all three possibilities: accelerator-based  
 691 long-baseline neutrinos, atmospheric neutrinos, and pion decay-at-rest sources.

Category	Experiment	Status	Start Date (Proposed)	US Participation/ Leadership	Osc params	References
accelerator	T2K	data taking	ongoing	yes/no	MH/CP/oct.	
accelerator	NO $\nu$ A	commissioning	2014	yes/yes	MH/CP/oct.	
accelerator	GLADE	R&D	2018?	yes/yes	MH/CP/oct.	[71]
accelerator	CHIPS	R&D	2018?	yes/yes	MH/CP/oct.	[70]
accelerator	T2HK	design/ R&D	2020	yes/no	MH/CP/oct.	
accelerator	LBNE	design/ R&D	2022	yes/yes	MH/CP/oct.	[74]
accelerator	DAE $\delta$ ALUS	design/ R&D	2022	yes/yes	CP	[80]
reactor	Daya Bay II	design/R&D	2018	undecided/no	MH	[40]
reactor	RENO-50	design/R&D	2018		MH	
atmospheric	Hyper-K	design/R&D	2020	yes/no	MH/CP/oct.	[81]
atmospheric	INO	design/ R&D	2020		MH/oct.	
atmospheric	PINGU	design/ R&D	2018	yes/yes	MH	[77]
atmospheric	ORCA	design/R&D	2018		MH	[79]
supernova	existing	N/A	N/A	various	MH	

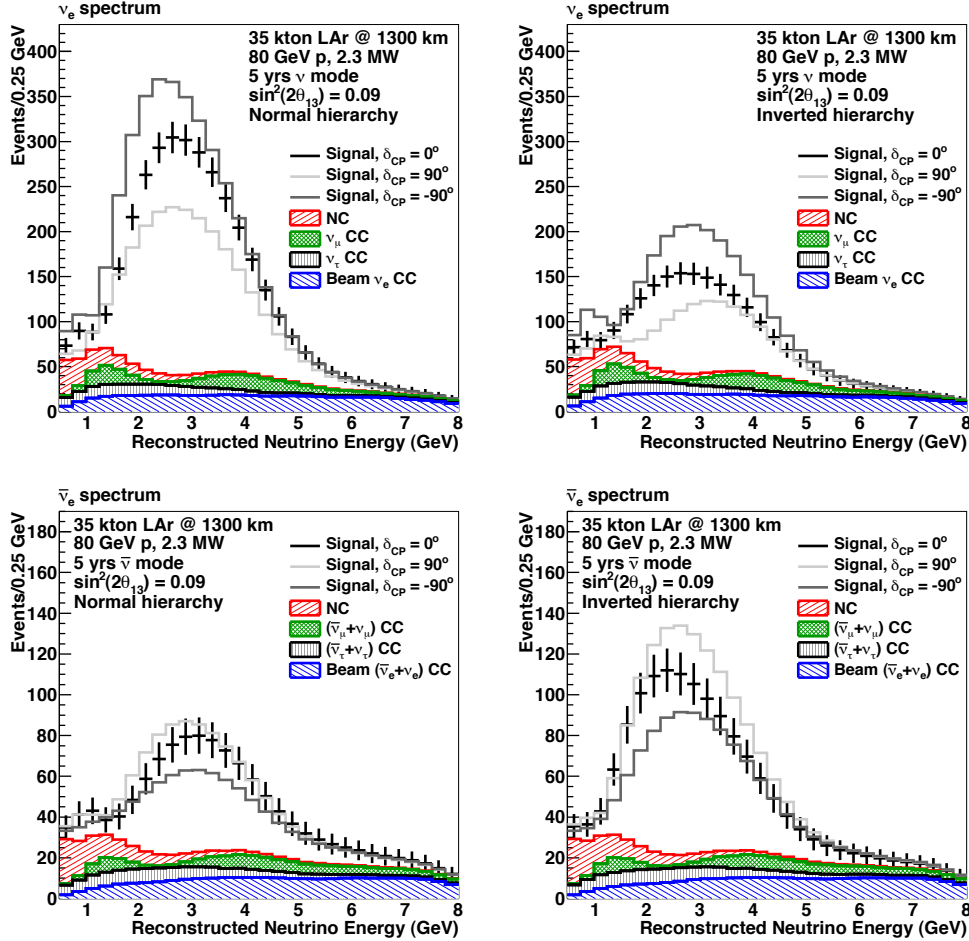
**Table 1-3.** *Ongoing and proposed oscillation experiments for the measurement of neutrino oscillation parameters.*

### 692 1.5.2.1 CP Violation with Accelerator-Based Long-Baseline Neutrinos

693 The study of  $\nu_\mu \rightarrow \nu_e$  and  $\bar{\nu}_\mu \rightarrow \bar{\nu}_e$  transitions using accelerator-based beams is sensitive to CP-violating  
694 phenomena arising from the CP-odd phase  $\delta$  in the neutrino mixing matrix. The evidence for CP-violation  
695 (assuming  $\delta \neq 0, \pi$ ) manifests itself both as an asymmetry in the oscillation of neutrinos and antineutrinos  
696 and as a distortion in the electro-type (anti)neutrino energy spectrum. For experiments that need to tag  
697 the muon-type neutrino flavor at production or detection, baselines longer than 100 km are required. For  
698 long enough baselines, (see Section 1.5.1), the matter effects also induce an asymmetry in the oscillation of  
699 neutrinos and antineutrinos. The matter asymmetry, however, is largest for higher neutrino energies and  
700 hence maximal at the first oscillation maximum, whereas the CP asymmetry induced by  $\delta$  is more significant  
701 at the secondary oscillation nodes and is constant as a function of baseline. An experiment with a wide-band  
702 beam of neutrinos and antineutrinos that can cover at least two oscillation nodes over a long enough baseline  
703 ( $> 1000$  km) can unambiguously determine both the mass hierarchy and the CP phase simultaneously.  
704 This is the philosophy behind the Long-Baseline Neutrino Experiment (LBNE). Additionally, the study of  
705  $\nu_\mu \rightarrow \nu_e$  oscillations can help determine the  $\theta_{23}$  quadrant since the oscillation probability is also proportional  
706 to  $\sin^2 \theta_{23}$  and  $\cos^2 \theta_{23}$ .

707 Figure 1-10 shows examples of observed spectra for a 1300 km baseline and a beam of a few GeV (the  
708 LBNE/Project X configuration with a LAr TPC far detector) for  $\nu_e$  and  $\bar{\nu}_e$  appearance. Different values  
709 of  $\delta_{CP}$  correspond to different spectral shapes for neutrinos versus antineutrinos; also, the  $\nu_e$  signal is  
710 larger in neutrinos for the normal mass hierarchy and in antineutrinos for the inverted hierarchy. Good  
711 event reconstruction and rejection of background are critical for this measurement. In the case of LBNE, a  
712 LAr TPC was chosen as the far detector technology, given its excellent 3D position resolution and superior  
713 particle identification in large volumes. In addition to detailed event topologies and measurements of particle

714 kinematics, such detectors can also unambiguously distinguish electrons from photons over a wide range of  
 715 energies, an important asset in the precision measurement of CP violating effects in  $\nu_\mu \rightarrow \nu_e$  oscillations.



716 **Figure 1-10.** The expected appearance of  $\nu_e$  (top) and  $\bar{\nu}_e$  (bottom) signals for the possible mass  
 717 orderings (left: normal hierarchy, right: inverted hierarchy) and varying values of CP  $\delta$  for the example  
 718 of LBNE/Project X.

719

716 Figure 1-11 illustrates the significance with which measurements of CP violation and the unknown CP phase  
 717 can be made with a staged long-baseline neutrino program in LBNE [82]. Ultimately, a  $5\sigma$  determination  
 718 of CP violation and a  $\leq 10^\circ$  measurement of the CP violating phase are possible with such an experimental  
 719 program.

720 LBNE plays a central role in the future U.S. program, and while being the most advanced of all the proposals  
 721 to measure CP violation in the neutrino sector, there is a large number of alternative proposals in the U.S.  
 722 and abroad. In this short document, we will not be able to provide an in-depth comparison of the scientific  
 723 merit of each of these proposals. Nonetheless, we can give an impression of how their performance for  
 724 specific measurements might look. The most challenging measurement within the framework of oscillation  
 725 of three active neutrinos for long-baseline experiment is the search for leptonic CP violation and a precise

726 measurement of the associated CP phase,  $\delta_{CP}$ . Therefore, apart from the value of a determination of  $\delta_{CP}$ ,  
 727 as outlined in Sec. 1.5, the ability to measure the CP phase with precision is a reasonable proxy for the  
 728 overall potential to have a major scientific impact.

729 The results of this comparison are shown in Fig. 1-12 using the methods and common systematics implemen-  
 730 tation including near detectors as in Ref. [83]. The lines labeled 2020 and 2025 show what can be achieved  
 731 by those dates using a combination of the existing experiments T2K and NO $\nu$ A and Daya Bay, where the  
 732 implementation of all three follows Ref. [84] and the NO $\nu$ A description has been updated for this report [85].  
 733 This is the precision which can be reached without any new experiments. Furthermore, we will compare two  
 734 phases of LBNE: LBNE-1 with a 10 kt detector and a 700 kW beam and LBNE-PX with a 34 kt detector and  
 735 the 2.3 MW beam from Project-X; both phases do include a near detector and the other details can be found  
 736 in the previous section on LBNE. LBNE, coupled with the intense beams from Project X and after sufficient  
 737 exposure, which will require an upgrade of the detector mass, may, in principle, approach a precision for the  
 738 CP-odd phase in the lepton sector comparable to that achieved for the CP-odd phase in the quark sector.  
 739 In order to accomplish this, however, systematic uncertainties on the signal and the background need to be  
 740 controlled at the percent level – almost an order of magnitude improvement. No studies of the feasibility of  
 741 this increase in systematics control have been performed to date.

742 Beyond LBNE, we compare three different superbeam experiments, the European LBNO proposal for two  
 743 different exposures and the Japanese proposal to send a beam to Hyper-Kamiokande. LBNO plans to use  
 744 liquid argon TPC, based on dual-phase readout in contrast to LBNE, and a baseline of 2 300 km. The initial  
 745 detector size will be 20 kt (labeled LBNO<sub>EOI</sub>) as described in detail in Ref. [86] and a later phase using a  
 746 100 kt detector (labeled LBNO<sub>100</sub>); the beam power will be around 700 kW derived from the CERN SPS.  
 747 The T2HK setup [81] in Japan will use a 560 kt water Cherenkov detector and a 1.66 MW beam; however the  
 748 running time will be only 5 years in total, so even if the beam power ultimately were reduced as consequence  
 749 of the tsunami damage, in 10 years of running time, like most experiments in Fig. 1-12, the same overall  
 750 exposure would be reached.

751 Finally, we also show the results obtained from a neutrino factory (NF) – in a neutrino factory an intense  
 752 beam of muons is put in a storage ring with long straight sections and a neutrino beam consisting of equal  
 753 numbers of  $\nu_\mu$  and  $\bar{\nu}_e$  results. The current standard design of a neutrino factory will produce  $10^{21}$  useful  
 754 muon decays (summed over both stored  $\mu^-$  and  $\mu^+$ ) per  $10^7$  s at a muon energy of 10 GeV aimed a 100 kt  
 755 magnetized iron detector (MINOS-like) at a distance of 2 000 km [87]. This facility requires a 4 MW proton  
 756 beam at around 8 GeV, muon phase space cooling and subsequent muon acceleration. This considerable  
 757 technical challenge should be contrasted with the resulting advantages: a neutrino beam with known flux,  
 758 better than 1%, beam spectrum and flavor composition with an easy to identify final state in the far detector.  
 759 The NF offers a unique level of systematics control paired with very high intensity beams, therefore they are  
 760 considered the ultimate tool for precision neutrino physics, see, e.g., [88]. The NF facility would provide the  
 761 most stringent tests of the standard three-flavor paradigm.

762 Several new proposals have been submitted in the form of white papers, notably a series of ideas how to  
 763 use the existing Main Injector neutrino beam line (NuMI) by adding new detectors. GLADE [89] proposes  
 764 to add 5-10 kt of a liquid argon TPC in the NO $\nu$ A far detector hall at a baseline of 810 km. CHIPS [90]  
 765 proposes to build water Cherenkov detectors in shallow, flooded mine pits, which could provide potentially  
 766 large fiducial masses in the range of 100 kt. According to the proponents, in terms of physics reach, this  
 767 would be equivalent to about 20 kt of liquid argon TPC. GLADE and CHIPS, together with NO $\nu$ A, T2K,  
 768 Daya Bay and potential beam power upgrades of the NuMI beamline to about 1 MW have a CP measurement  
 769 potential similar to the phase 1 of LBNE (CP sensitivity of more than  $2\sigma$  over 50% of  $\delta$  values over 10 years.)  
 770 on a comparable time scale. Clearly, for CHIPS considerable R&D is still required and thus, the cost is not  
 771 well understood. For both GLADE and CHIPS the long-term perspective to improve CP precision to  $15^\circ$   
 772 or better for a large fraction of the phase space is unclear and, in particular, systematic effects may limit

773 these approaches well before that. Such efforts probably rely on external information regarding the precise  
 774 value of  $\theta_{13}$  and the resolution of the neutrino mass hierarchy ambiguity in order to unambiguously address  
 775 CP-violation. The long term sensitivities of NuMI based approaches may also be limited by the lifetime of the  
 776 NuMI beamline which cannot operate at powers greater than 1 MW.

777 A staged approach to a neutrino factory is proposed [91], where an initial stage called the low-luminosity  
 778 low-energy neutrino factory is built on the basis of existing accelerator technology and Project X phase 2.  
 779 In this facility, which does not require muon cooling and which starts with a target power of 1 MW,  $10^{20}$   
 780 useful muon decays per polarity and year can be obtained. The muon energy is chosen to be 5 GeV as to  
 781 match the baseline of 1300 km. In combination, this allows to target the LBNE phase 1 detector, maybe  
 782 with the addition of a magnetic field. This approach would allow for a step-wise development from  $\nu$ STORM  
 783 (see Sec. 1.9), via the low-luminosity low-energy neutrino factory to a full neutrino factory, and if desired,  
 784 to a multi-TeV muon collider. This phased muon-based program is well aligned with the development of  
 785 Project X.

786 In summary, a measurement of the leptonic CP phase at levels of precision comparable to those of the  
 787 CP phase in the quark sector is now possible in long baseline oscillation experiments given that  $\theta_{13}$  has  
 788 been measured to be non-zero. To do so will require very high proton beam intensities in excess of 1 MW,  
 789 paired with detectors in the 100kt range or larger, and running times of order one decade – regardless of  
 790 the specifics of the chosen technology or proposal. Experiments with baselines in excess of a 1000km and  
 791 wide-band neutrino beams that cover the first two oscillation maxima have the best sensitivity to leptonic  
 792 CP violation for the minimal required exposure. Wide-band very long baseline experiments such as LBNE  
 793 and LBNO can reach under  $10^\circ$  precision on  $\delta$  with exposures under 1000 kT·MW·years - provided that  
 794 systematic uncertainties can be controlled to the level of a few percent or better. A neutrino factory with  
 795 similar exposure – a next-next generation project – should be able to measure  $\delta$  at  $5^\circ$  level, and provide the  
 796 most stringent constraints on the three-flavor paradigm thanks to its capability to measure several different  
 797 oscillation channels with similar precision.

### 798 1.5.2.2 CP Violation with Atmospheric Neutrinos

799 As noted above, neutrinos and antineutrinos from the atmosphere come with a range of baselines and  
 800 energies, and in principle similar CP-violating observables, are accessible as for beams, for detectors with  
 801 sufficient statistics and resolution. Water Cherenkov detectors have relatively low resolution in energy and  
 802 direction, and have difficulty selecting neutrinos from antineutrinos, although some information is to be had  
 803 via selection of special samples [51] and using statistical differences in kinematic distributions from  $\nu$  and  $\bar{\nu}$ .  
 804 The advantage of water Cherenkov detectors is the potentially vast statistics. Figure 1-13 shows example  
 805 allowed regions for 10 years of Hyper-K running. Large long-string ice and water-based detectors, while  
 806 sensitive to hierarchy if systematics can be reduced, lack resolution for CP studies. LArTPC detectors, in  
 807 contrast, should have significantly improved resolution on both neutrino energy and direction, and even in  
 808 the absence of a magnetic field can achieve better  $\nu$  vs  $\bar{\nu}$  tagging than water Cherenkov. Figure 1-14 shows  
 809 an example sensitivity plot for a liquid argon detector like LBNE. Atmospheric neutrino information can be  
 810 combined with beam information in the same or different detectors to improve overall sensitivity.

### 811 1.5.2.3 CP Violation with Pion Decay-at-Rest Sources

812 A different approach for measuring CP violation is DAE $\delta$ ALUS [41, 92, 93]. The idea is to use muon  
 813 antineutrinos produced by cyclotron stopped-pion decay ( $\pi^- \rightarrow \mu^- \bar{\nu}_\mu$ ) at rest (DAR) neutrino sources, and  
 814 to vary the baseline by having sources at different distances from a detector site. For DAR sources, the

815 neutrino energy is a few tens of MeV. For baselines ranging from 1 to 20 km, both  $L$  and  $E$  are smaller  
816 than for the conventional long baseline beam approach, and the ratio of  $L/E$  is similar. Matter effects are  
817 negligible at short baseline. This means that the CP-violating signal is clean; however there is a degeneracy  
818 in oscillation probability for the two mass hierarchies. This degeneracy can be broken by an independent  
819 measurement of the hierarchy.

820 The electron-type antineutrino appearance signal from the oscillation of muon-type antineutrinos from pion  
821 DAR is detected via inverse beta-decay ( $\bar{\nu}_e p \rightarrow e^+ n$ ). Consequently very large detectors with free protons  
822 are required. The original case was developed for a 300 kt Gd-doped water detector at Homestake, in  
823 coordination with LBNE [94]. Possibilities currently being explored for the detector include LENA [95] or  
824 Super-K/Hyper-K [81].

825 Figure 1-15 shows the projected CP sensitivity.

826 The DAE $\delta$ ALUS collaboration proposes a phased approach [80, 96], with early phases involving IsoDAR [96]  
827 (see Sec. 1.9.1.3) with sterile neutrino sensitivity. The phased program offers also connections to applied  
828 cyclotron research [97] (see Section 1.11.1.4).

829 llllllll .r601

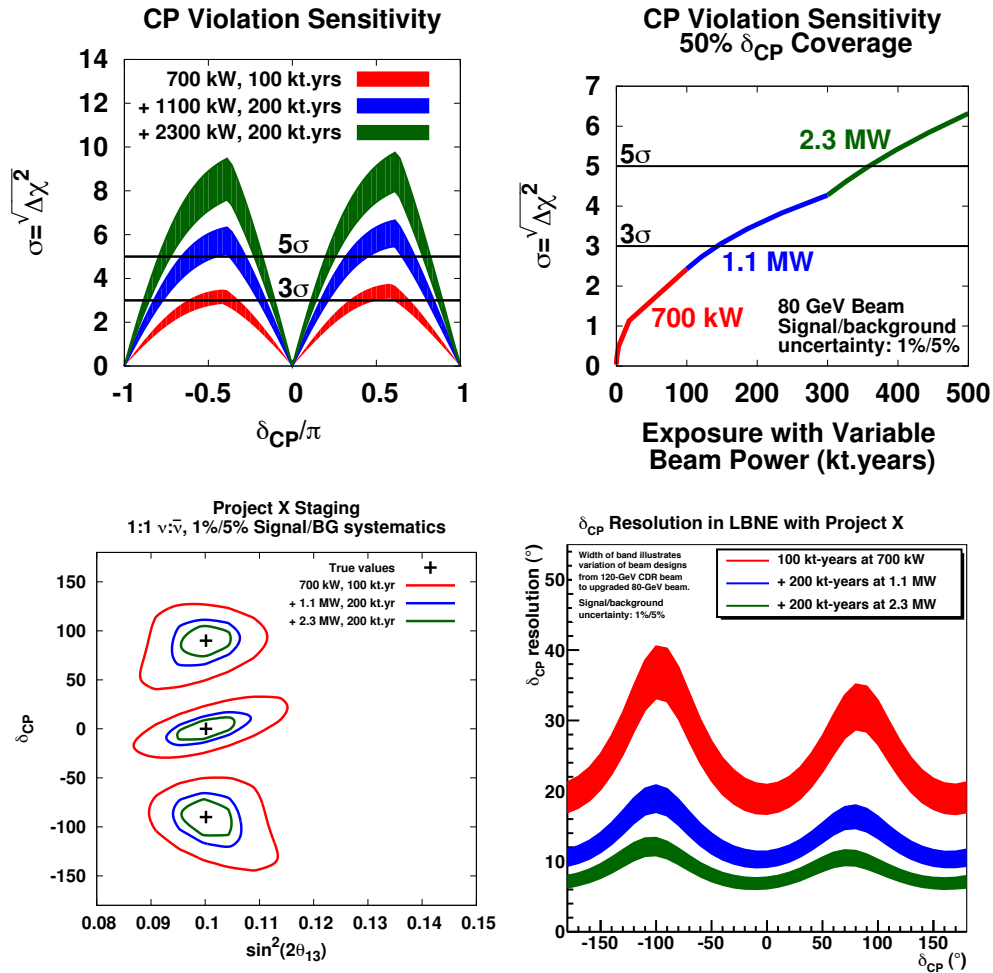


**Figure 1-11.**  $CP$  violation sensitivity as a function of  $\delta_{CP}$  (top left) and exposure for 50% coverage of the full  $\delta_{CP}$  range (top right). Also shown are the projected precision on the measurement of  $\delta_{CP}$  for various true points in the  $\delta_{CP}$ - $\sin^2 2\theta_{13}$  plane (bottom left) and as a function of  $\delta_{CP}$  (bottom right). All plots show the increasing precision possible in a staged long-baseline neutrino program in LBNE starting from nominal 700kW running (red), through 1.1 MW using Project X Stage 1 (blue), to 2.3 MW with Project X Stage 2 (green).

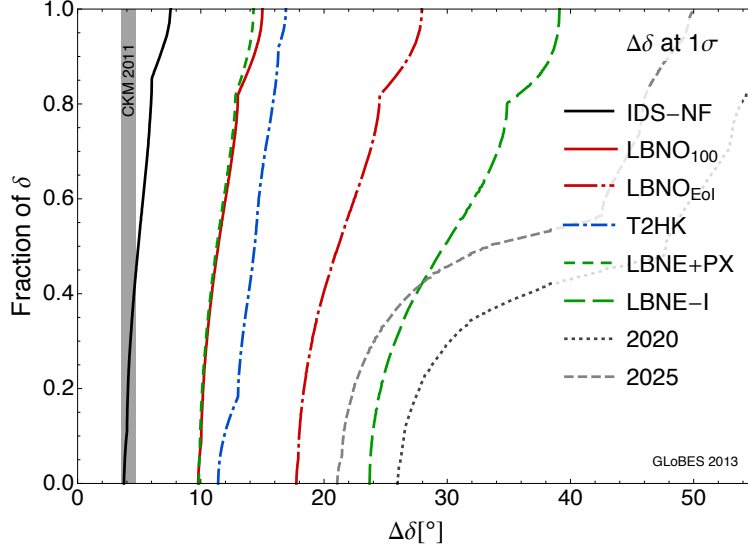


**Figure 1-12.** Projected precision for a CP measurement. Shown is the fraction of all possible true values of  $\delta_{CP}$  as a function of the  $1\sigma$  error in the measurement of  $\delta_{CP}$ . A CP fraction of 1 implies that this precision will be reached for all possible CP phases, whereas a CP fraction of 0 means that there is only one value of  $\delta_{CP}$  for which the measurement will have that precision. The various lines are for a variety of possible experiments as labeled in the legend and explained in the text. The vertical gray shaded area, labeled “CKM 2011”, indicates the current errors on the CP phase in the CKM matrix. This calculation includes near detectors and assumes consistent flux and cross section uncertainties across different setups. Plot courtesy of P. Coloma.

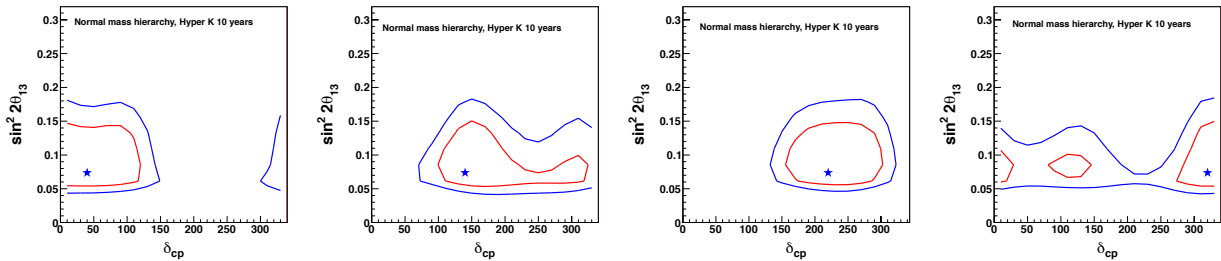


**Figure 1-13.** Expected sensitivities for  $\delta$  and  $\sin^2 2\theta_{13}$  at 90% CL (red) and 99% CL (blue) with a livetime of 10 Hyper-K years. Stars in the contours represent the true parameters. Normal mass hierarchy is assumed. Figure from [81].

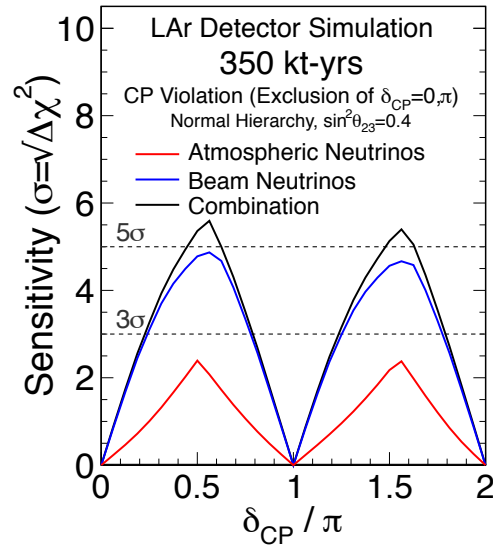


**Figure 1-14.** Sensitivity to CP violation as a function of  $\delta_{CP}$  for a liquid argon detector showing the results of combining information from both beam (blue) and atmospheric (red) neutrinos. Plot courtesy of A. Blake.

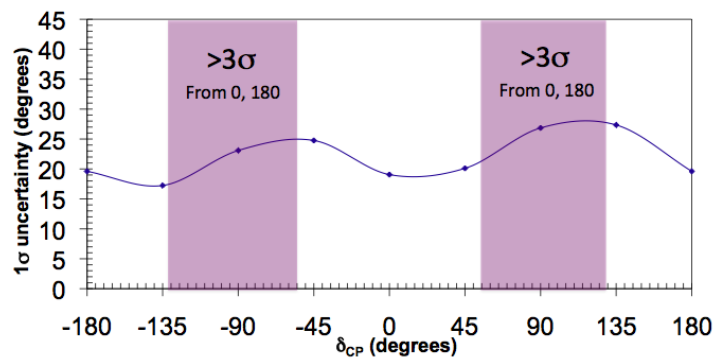


**Figure 1-15.** Sensitivity of a CP search for DAE $\delta$ ALUS combined with LENA [80].

## 1.6 The Nature of the Neutrino – Majorana versus Dirac

With the realization that neutrinos are massive, there is an increased interest in investigating their intrinsic properties. Understanding the neutrino mass generation mechanism, the absolute neutrino mass scale, and the neutrino mass spectrum are some of the main focuses of future neutrino experiments. Whether neutrinos are Dirac fermions (*i.e.*, exist as separate massive neutrino and antineutrino states) or Majorana fermions (neutrino and antineutrino states are equivalent) is a key experimental question, the answer to which will guide the theoretical description of neutrinos.

All observations involving leptons are consistent with their appearance and disappearance in particle anti-particle pairs. This property is expressed in the form of lepton number,  $L$ , being conserved by all fundamental forces. We know of no fundamental symmetry relating to this empirical conservation law. Neutrinoless double-beta decay, a weak nuclear decay process in which a nucleus decays to a different nucleus emitting two beta-rays and no neutrinos, violates lepton number conservation by two units and thus, if observed, requires a revision of our current understanding of particle physics. In terms of field theories, such as the Standard Model, neutrinos are assumed to be massless and there is no chirally right-handed neutrino field. The guiding principles for extending the Standard Model are the conservation of electroweak isospin and renormalizability, which do not preclude each neutrino mass eigenstate  $\nu_i$  to be identical to its antiparticle  $\bar{\nu}_i$ , or a Majorana particle. However,  $L$  is no longer conserved if  $\nu = \bar{\nu}$ . Theoretical models, such as the seesaw mechanism that can explain the smallness of neutrino mass, favor this scenario. Therefore, the discovery of Majorana neutrinos would have profound theoretical implications in the formulation of a new Standard Model while yielding insights into the origin of mass itself. If neutrinos are Majorana particles, they may fit into the leptogenesis scenario for creating the baryon asymmetry, and hence ordinary matter, of the universe.

As of yet, there is no firm experimental evidence to confirm or refute this theoretical prejudice. Experimental evidence of neutrinoless double-beta ( $0\nu\beta\beta$ ) decay would establish the Majorana nature of neutrinos. It is clear that  $0\nu\beta\beta$  experiments sensitive at least to the mass scale indicated by the atmospheric neutrino oscillation results are needed.

For  $0\nu\beta\beta$  decay the summed energy of the emitted electrons is mono-energetic. Observation of a sharp peak at the  $\beta\beta$  endpoint would thus quantify the  $0\nu\beta\beta$  decay rate, demonstrate that neutrinos are Majorana particles, indicate that lepton number is not conserved, and, paired with nuclear structure calculations, provide a measure of an effective Majorana mass,  $\langle m_{\beta\beta} \rangle$ . There is consensus within the neutrino physics community that such a decay peak would have to be observed for at least two different decaying isotopes at two different energies to make a credible claim for  $0\nu\beta\beta$  decay.

In more detail, the observed half-life can be related to an effective Majorana mass according to  $(T_{1/2,0\nu\beta\beta})^{-1} = G_{0\nu} |M_{0\nu}|^2 \langle m_{\beta\beta} \rangle^2$ , where  $\langle m_{\beta\beta} \rangle^2 \equiv |\sum_i U_{ei}^2 m_i|^2$ .  $G_{0\nu}$  is a phase space factor,  $m_i$  is the mass of neutrino mass eigenstate  $\nu_i$ , and  $M_{0\nu}$  is the transition nuclear matrix element. The matrix element has significant nuclear theoretical uncertainties, dependent on the nuclide under consideration.

In the standard three-massive-neutrinos paradigm,

$$\langle m_{\beta\beta} \rangle = |\cos^2 \theta_{12} \cos^2 \theta_{13} e^{-2i\xi} m_1 + \sin^2 \theta_{12} \cos^2 \theta_{13} e^{-2i\zeta} m_2 + \sin^2 \theta_{13} e^{-2i\delta} m_3|. \quad (1.13)$$

If none of the neutrino masses vanish,  $\langle m_{\beta\beta} \rangle$  is a function of not only the oscillation parameters  $\theta_{12,13}, \delta$  and the neutrino masses  $m_{1,2,3}$  but also the two Majorana phases  $\xi, \zeta$ . Neutrino oscillation experiments indicate that at least one neutrino has a mass of  $\sim 45$  meV or more. As a result and as shown in Fig. 1-16, in the inverted hierarchy mass spectrum with  $m_3 = 0$  meV,  $\langle m_{\beta\beta} \rangle$  is between 10 and 55 meV depending on the values of the Majorana phases. This region is sometimes referred to as the atmospheric mass scale region. Exploring this region requires a sensitivity to half-lives exceeding  $10^{27}$  years. This is a challenging

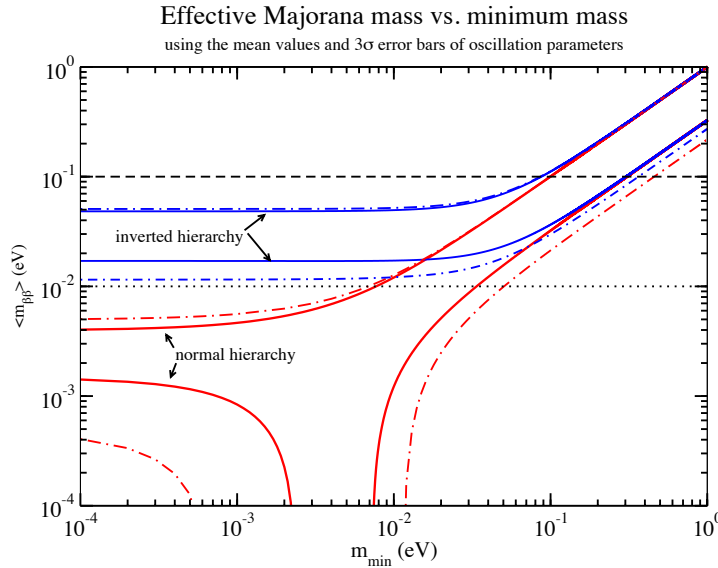


**Figure 1-16.** Allowed values of  $\langle m_{\beta\beta} \rangle$  as a function of the lightest neutrino mass for the inverted and normal hierarchies. The regions defined by the solid curves correspond to the best-fit neutrino mixing parameters from [98] and account for the degeneracy due to the unknown Majorana phases. The regions defined by the dashed-dotted curves correspond to the maximal allowed regions including mixing parameter uncertainties as evaluated in [98]. The dashed line shows expected sensitivity of next-generation  $\sim 100$  kg class experiments and the dotted line shows potential reach of multi-ton scale future experiments.

872 goal requiring several ton-years of exposure and very low backgrounds. The accomplishment of this goal  
 873 requires a detector at the ton scale of enriched material and a background level below 1 count/(ton y) in the  
 874 spectral region of interest (ROI). Very good energy resolution is also required.

875 There is one controversial result from a subset of collaborators of the Heidelberg-Moscow experiment, who  
 876 claim a measurement of the process in  $^{76}\text{Ge}$ , with 70 kg-years of data [99]. These authors interpret the  
 877 observation as giving an  $\langle m_{\beta\beta} \rangle$  of 440 meV. Recent limits using the isotope  $^{136}\text{Xe}$  from EXO-200 and  
 878 KamLAND-Zen (see below) are in tension with this  $\langle m_{\beta\beta} \rangle$  regime.

879 There is a large number of current neutrinoless double-beta decay search efforts, employing very different  
 880 techniques; a recent review is [100]. Here we will highlight some for which there is a component of effort from  
 881 physicists based in the US. These represent different kinds of detectors and experimental approaches [101,  
 882 102, 103, 104, 105, 106, 107, 108, 109, 110].

883 The MAJORANA [111, 112, 113, 107] experiment employs the germanium isotope  $^{76}\text{Ge}$ , to be enriched. The  
 884 current phase of the experiment is the “DEMONSTRATOR”, which will employ 30 kg of Ge enriched to 86%  
 885  $^{76}\text{Ge}$  and 10 kg of Ge P-type point contact detectors, is being constructed underground at the Sanford  
 886 Underground Research Facility (SURF). It will have first data in 2013 with data from enriched detectors  
 887 in 2014. The MAJORANA collaboration is planning a ton-scale effort in collaboration with its European  
 888 counterpart GERDA.

889 The “bolometric” CUORE experiment [114, 106], located at Gran Sasso National Laboratory in Italy, em-  
 890 ploys  $^{130}\text{Te}$  in the form of natural  $\text{TeO}_2$  crystals. This is a cryogenic setup, operated at temperatures around

891 10 mK, that determines the energy deposit via temperature rise measured with thermistors. Bolometric  
892 detectors are characterized by excellent energy resolution (5 keV FWHM has been achieved) and high  
893 efficiency for electrons from the double-beta decay. The prototype of this experiment, Cuoricino, ran from  
894 2003-2008 with 11.3 kg of  $^{130}\text{Te}$  mass. The first stage of CUORE, CUORE-0, is currently operating with  
895 a  $^{130}\text{Te}$  mass of 11 kg, and the full CUORE detector plans commencing operations in 2014 with 206 kg.  
896 CUORE aims at the sensitivity to the  $0\nu\beta\beta$  lifetime of  $2 \times 10^{26}$  after five years of operation, which would  
897 correspond to about the middle of the Inverted hierarchy region.

898 The EXO experiment [109] makes use of  $^{136}\text{Xe}$ , which double-beta decays as  $^{136}\text{Xe} \rightarrow ^{136}\text{Ba}^{++} + e^{-} + e^{-}$ . The  
899 first version of EXO, EXO-200, is currently taking data at the Waste Isolation Pilot Plant in New Mexico  
900 with 200 kg of xenon enriched to 80% in the isotope 136. A time projection chamber is used to detect  
901 both scintillation light from the interaction and ionization energy deposited by the electrons in the xenon,  
902 which is used in the liquid phase. EXO-200 reported the first observation of the two-neutrino double-beta  
903 decay [115] in  $^{136}\text{Xe}$  and subsequently a limit on the neutrinoless double beta decay [116] in  $^{136}\text{Xe}$ . The EXO  
904 collaboration is planning a 5-ton detector called nEXO that builds on the success of the EXO-200 detector.  
905 The expected nEXO sensitivity to the  $0\nu\beta\beta$  half-life is  $2.5 \times 10^{27}$  years after 10 years of operation. The EXO  
906 collaboration's novel idea for an upgrade is the use of barium tagging: the principle is to reduce backgrounds  
907 by identifying the resulting nucleus by laser spectroscopy [117]. This ambitious plan – to tag a single ion in 5  
908 tons of xenon – is currently under development, and there are several schemes under development, including  
909 gaseous versions of EXO. The incorporation of barium tagging will improve the nEXO sensitivity to the  $0\nu\beta\beta$   
910 half-life by approximately an order of magnitude.

911 Another ambitious idea for a double-beta decay experiment is SNO+ [35, 101]. SNO+ is an experiment at  
912 SNOLAB in Canada which plans to refill the acrylic vessel of SNO with liquid scintillator. This experiment  
913 would in addition provide a rich physics program of solar neutrino, geoneutrino and supernova neutrino  
914 physics (see Sec. 1.10). SNO+ plans to load the scintillator with 0.3% Te, which after one year of data  
915 should give them a 90% C.L. sensitivity of approximately  $4 \times 10^{25}$  years (neutrino mass sensitivity of 70 to  
916 100 meV). There is an R&D effort underway to increase the amount of Te loaded into the scintillator, which  
917 could allow complete coverage of the inverted hierarchy.

918 KamLAND-Zen [118] (the Kamioka Liquid Anti-Neutrino Detector, ZERo Neutrino double-beta decay ex-  
919 periment) is an extension of the KamLAND[119] experiment. KamLAND is a 6.5-m radius balloon filled  
920 with 1000 tons of liquid scintillator, surrounded by 3000 tons of mineral oil and submerged inside a 9-m  
921 radius stainless-steel sphere with PMTs mounted on the wall. In 2011, the collaboration added an additional  
922 low-background miniballoon into the inner sphere that contains 13 tons of liquid scintillator loaded with  
923 330 kg of dissolved Xe gas enriched to 91% in  $^{136}\text{Xe}$ . The initial results include an improved limit on  
924 neutrinoless double-beta decay for  $^{136}\text{Xe}$  and a measurement of two-neutrino double-beta decay that agrees  
925 with the recent EXO-200 result [120]. The collaboration is currently in the process of purifying the Xe-LS  
926 of a problematic background observed in the first phase of data taking. The collaboration has an additional  
927 400 kg of enriched Xe in hand and is considering options to upgrade the detector with a larger-size internal  
928 balloon.

929 NEXT [121, 122, 103] (Neutrino Experiment with Xenon TPC) intends to use  $>100$  kg of Xe enriched to  
930  $\sim 90\%$  in  $^{136}\text{Xe}$ . The detector will be a moderate-density gas TPC  $\sim 0.08$  g/cm<sup>3</sup> that will detect primary and  
931 secondary scintillation light. By operating at low pressures ( $\sim 15$  bar), the design should not only provide  
932 good energy resolution, but also permit tracking that allows fairly detailed track reconstruction to confirm  
933 that candidate events involve two electrons moving in opposite directions. The collaboration has recently  
934 demonstrated impressive 1% resolution at 662 keV in a limited fiducial volume device. Construction started  
935 in 2012 with commissioning scheduled to start in 2014. It will operate at the Laboratorio Subterráneo de  
936 Canfranc (LSC) in Spain.

937 The SuperNEMO [123, 102] proposal builds on the great success of the NEMO-3 (Neutrino Ettore Majorana  
 938 Observatory) experiment, which measured two-neutrino double-beta decay rates and set some of the most  
 939 stringent constraints for zero-neutrino double beta transitions for seven isotopes [124]. NEMO-3 has provided  
 940 some of the best two-neutrino double-beta decay data to date, including information on single-electron energy  
 941 distributions and opening angles. The design uses calorimetry to measure energies and timing, and tracking  
 942 to provide topological and kinematical information about the individual electrons. SuperNEMO will improve  
 943 on NEMO-3 by using a larger mass of isotope, lowering backgrounds, and improving the energy resolution.  
 944 The present design is for 100 kg of  $^{82}\text{Se}$ , but other isotopes, like  $^{150}\text{Nd}$  or  $^{48}\text{Ca}$ , are also being considered. It  
 945 will have a modular design of 20 thin-source planes of  $40\text{ mg/cm}^2$  thickness. Each source will be contained  
 946 within a Geiger-mode drift chamber enclosed by scintillator and phototubes. Timing measurements from  
 947 digitization of the scintillator and drift chamber signals will provide topological information such as the  
 948 event vertex and particle directionality. The modules will be surrounded by passive shielding. A one-module  
 949 demonstrator with 7 kg of  $^{82}\text{Se}$  is planned to be commissioned in 2014. One of the Demonstrator's goal is  
 950 to reach a zero-background regime in the energy region of interest around the double-beta-decay transition  
 951 energy (2.8–4.5 MeV for  $^{82}\text{Se}$ ,  $^{150}\text{Nd}$ , and  $^{48}\text{Ca}$ , respectively). The complete experiment will be ready by the  
 952 end of the decade in an extension of the LSM Modane in the Fréjus Tunnel in France. Its design sensitivity  
 953 for the  $0\nu\beta\beta$  half-life of  $^{82}\text{Se}$  is  $10^{26}$  yr, in a 500 kg·yr exposure.

954 The current and next-generation experiments are of 10-100 kg masses; these have sensitivities down to  
 955 about 100 meV. Further ton-scale experiments are planned for the generation beyond that: these should  
 956 have sensitivities reaching the 10 meV or smaller scale. Reaching this regime will be very interesting in  
 957 its complementarity with oscillation experiments: if independent oscillation experiments (or data from  
 958 supernovae or colliders) determine the mass hierarchy to be inverted, and there is no  $0\nu\beta\beta$  decay signal  
 959 at the 10 meV scale, then neutrinos must be Dirac (assuming Nature is not too diabolical). If a signal is  
 960 observed at the few meV scale, then not only will we know that neutrinos are Majorana, but we will also  
 961 know that the hierarchy must be normal, even in the absence of an independent determination.

962 It is important to understand that several experiments using different isotopes are in order, at each step of  
 963 sensitivity. This is because different isotopes involve different matrix elements with their uncertainties. In  
 964 addition, unknown small-probability gamma transitions may occur at or near the end point of a particular  
 965 isotope, but it is very unlikely that they occur for *every* double-beta decay emitter. Finally, and maybe most  
 966 importantly, different isotopes generally correspond to radically different techniques, and since neutrinoless  
 967 double-beta decay searches require exceedingly low backgrounds, it is virtually impossible to decide *a priori*  
 968 which technique will truly produce a background-free measurement. The long-term future for double-beta  
 969 decay experiments will depend on what is observed: if no experiments, or only some experiments, see a signal  
 970 at the 100 kg scale, then ton-scale experiments are in order. If a signal is confirmed, the next generation  
 971 of detectors may be low-energy trackers, in order to better investigate the  $0\nu\beta\beta$  mechanism by separately  
 972 measuring the energies of each electron as well as their angular correlations.

Experiment	Isotope	Mass	Technique	Status	Location
AMoRE[125, 126]	$^{100}\text{Mo}$	50 kg	$\text{CaMoO}_4$ scint. bolometer crystals	Devel.	Yangyang
CANDLES[127]	$^{48}\text{Ca}$	0.35 kg	$\text{CaF}_2$ scint. crystals	Prototype	Kamioka
CARVEL[128]	$^{48}\text{Ca}$	1 ton	$\text{CaF}_2$ scint. crystals	Devel.	Solotvina
COBRA[129]	$^{116}\text{Cd}$	183 kg	$^{enr}\text{Cd}$ CZT semicond. det.	Prototype	Gran Sasso
CUORE-0[114]	$^{130}\text{Te}$	11 kg	$\text{TeO}_2$ bolometers	Constr. (2013)	Gran Sasso
CUORE[114]	$^{130}\text{Te}$	203 kg	$\text{TeO}_2$ bolometers	Constr. (2014)	Gran Sasso
DCBA[130]	$^{150}\text{Nd}$	20 kg	$^{enr}\text{Nd}$ foils and tracking	Devel.	Kamioka
EXO-200[115, 116]	$^{136}\text{Xe}$	200 kg	Liq. $^{enr}\text{Xe}$ TPC/scint.	Op. (2011)	WIPP
nEXO[117]	$^{136}\text{Xe}$	5 t	Liq. $^{enr}\text{Xe}$ TPC/scint.	Proposal	SNOLAB
GERDA[131]	$^{76}\text{Ge}$	$\approx 35$ kg	$^{enr}\text{Ge}$ semicond. det.	Op. (2011)	Gran Sasso
GSO[132]	$^{160}\text{Gd}$	2 t	$\text{Gd}_2\text{SiO}_5:\text{Ce}$ crys. scint. in liq. scint.	Devel.	
KamLAND-Zen[118, 120]	$^{136}\text{Xe}$	400 kg	$^{enr}\text{Xe}$ dissolved in liq. scint.	Op. (2011)	Kamioka
LUCIFER[133, 134]	$^{82}\text{Se}$	18 kg	$\text{ZnSe}$ scint. bolometer crystals	Devel.	Gran Sasso
MAJORANA [111, 112, 113]	$^{76}\text{Ge}$	30 kg	$^{enr}\text{Ge}$ semicond. det.	Constr. (2013)	SURF
MOON [135]	$^{100}\text{Mo}$	1 t	$^{enr}\text{Mo}$ foils/scint.	Devel.	
SuperNEMO-Dem[123]	$^{82}\text{Se}$	7 kg	$^{enr}\text{Se}$ foils/tracking	Constr. (2014)	Fréjus
SuperNEMO[123]	$^{82}\text{Se}$	100 kg	$^{enr}\text{Se}$ foils/tracking	Proposal (2019)	Fréjus
NEXT [121, 122]	$^{136}\text{Xe}$	100 kg	gas TPC	Devel. (2014)	Canfranc
SNO+[136, 137, 35]	$^{130}\text{Te}$	800 kg	Te-loaded liq. scint.	Constr. (2013)	SNOLAB

**Table 1-4.** A summary list of neutrinoless double-beta decay proposals and experiments.

## 973 1.7 Weighing Neutrinos

### 974 1.7.1 Kinematic neutrino mass measurements

975 The neutrino’s absolute mass cannot be determined by oscillation experiments, which give information only  
 976 on mass differences. The neutrino’s rest mass has a small but potentially measurable effect on its kinematics,  
 977 in particular on the phase space available in low-energy nuclear beta decay. The effect is indifferent to the  
 978 distinction between Majorana and Dirac masses, and independent of nuclear matrix element calculations.

979 Two nuclides are of major importance to current experiments: tritium ( ${}^3\text{H}$  or T) and  ${}^{187}\text{Re}$ . The particle  
 980 physics is the same in both cases, but the experiments differ greatly. Consider the superallowed decay  
 981  ${}^3\text{H} \rightarrow {}^3\text{He} + e^- + \bar{\nu}_e$ . The electron energy spectrum has the form:

$$dN/dE \propto F(Z, E)p_e(E + m_e)(E_0 - E)\sqrt{(E_0 - E)^2 - m_\nu^2} \quad (1.14)$$

982 where  $E$ ,  $p_e$  are the electron energy and momentum,  $E_0$  is the Q-value, and  $F(Z, E)$  is the Fermi function.  
 983 If the neutrino is massless, the spectrum near the endpoint is approximately parabolic around  $E_0$ . A finite  
 984 neutrino mass makes the parabola “steeper”, then cuts it off  $m_\nu$  before the zero-mass endpoint. The value  
 985 of  $m_\nu$  can be extracted from the shape without knowing  $E_0$  precisely, and without resolving the cutoff.

986 The flavor state  $\nu_e$  is an admixture of three mass states  $\nu_1$ ,  $\nu_2$ , and  $\nu_3$ . Beta decay yields a superposition  
 987 of three spectra, with three different endpoint shapes and cutoffs, whose relative weights depend on the  
 988 magnitude of elements of the mixing matrix. Unless the three endpoint steps are fully resolved, the spectrum  
 989 is well approximated by the single-neutrino spectrum with an effective mass  $m_\beta^2 = \sum_i U_{ei}^2 m_i^2$ . Past tritium  
 990 experiments have determined  $m_\beta < 2.0$  eV.

991 To measure this spectrum distortion, any experiment must have the following properties:

- 992 • High energy resolution—in particular, a resolution function lacking high-energy tails—to isolate the  
 993 near-endpoint electrons from the more numerous low-energy electrons.
- 994 • An extremely well-known spectrometer resolution. The neutrino mass parameter covaries very strongly  
 995 with the detector resolution.
- 996 • The ability to observe a very large number of decays, with high-acceptance spectrometers and/or  
 997 ultra-intense sources, in order to collect adequate statistics in the extreme tail of a rapidly-falling  
 998 spectrum.

### 999 1.7.2 Upcoming experiments

1000 **KATRIN** The KATRIN experiment [138, 139], now under construction, will attempt to extract the  
 1001 neutrino mass from decays of gaseous  $\text{T}_2$ . KATRIN achieves high energy resolution using a MAC-E (Magnetic  
 1002 Adiabatic Collimation-Electrostatic) filter. In this technique, the  $\text{T}_2$  source is held at high magnetic field.  
 1003 Beta-decay electrons within a broad acceptance cone are magnetically guided towards a low-field region; the  
 1004 guiding is adiabatic and forces the electrons’ momenta nearly parallel to  $B$  field lines. In the parallel region,  
 1005 an electrostatic field serves as a sharp energy filter. Only the highest-energy electrons can pass the filter and

reach the detector, so MAC-E filters can tolerate huge low-energy decay rates without encountering detector rate problems. In order to achieve high statistics, KATRIN needs a very strong source, supplying  $10^{11}$   $e^-/s$  to the spectrometer acceptance. This cannot be done by increasing the source thickness, which is limited by self-scattering, so the cross-sectional area of the source and spectrometer must be made very large,  $53\text{ cm}^2$  and  $65\text{ m}^2$  respectively. As proposed, KATRIN anticipates achieving a neutrino mass exclusion limit down to  $0.2\text{ eV}$  at 95% confidence, or  $0.35\text{ eV}$  for a 3-sigma discovery.

KATRIN is currently under construction. As of March 2013, the KATRIN spectrometer (i.e. the MAC-E filter) is fully instrumented, baked, and pumped down to  $6 \times 10^{-11}$  mbar. The detector system is operational. The spectrometer/detector system will be calibrated with an electron gun starting in summer 2013. The tritium source is on-track for installation in 2014, and data-taking will begin in late 2015.

**Project 8** Project 8 is a new technology for pursuing the tritium endpoint [140]; it anticipates providing a roadmap towards a large tritium experiment with new neutrino mass sensitivity, via a method with systematic errors largely independent of the MAC-E filter method. In Project 8, a low-pressure gaseous tritium source is stored in a magnetic bottle. Magnetically-trapped decay electrons undergo cyclotron motion for  $\sim 10^6$  orbits. This motion emits microwave radiation at frequency  $\omega = qB/\gamma m$ , where  $\gamma$  is the Lorentz factor. A measurement of the frequency can be translated into an electron energy. A prototype, now operating at the University of Washington, is attempting to detect and characterize single conversion electrons from a  $^{83m}\text{Kr}$  conversion electron calibration source. The prototype is intended to help answer a number of technical questions, including the merits of various magnetic-trap configurations for the electrons, waveguide vs. cavity configurations for the microwaves, and questions about data analysis techniques.

The Project 8 collaboration will follow up on this prototype by preparing detailed proposals for larger experiments. A first experiment would aim for few-eV neutrino mass sensitivity while precisely measuring other parameters of the decay spectrum. A larger followup experiment would extend the sensitivity down to the limits of the technique.

**Microcalorimeter methods** While most of the neutrino-mass community is focused on tritium, there are several other nuclides of potential experimental interest. Tritium is the only low-energy beta decay nuclide whose decay rate (and low atomic number) permits the creation of thin, high-rate sources. If one can detect decays in a cryogenic microcalorimeter, the requirement of a thin source is removed, and one can explore lower-energy decays. For a neutrino mass  $m_\nu$ , and a beta-decay energy  $E_0$ , the fraction of decays in the signal region scales as  $(m_\nu/E_0)^3$ . The best-known candidate is  $^{187}\text{Re}$ , whose beta-decay endpoint is unusually low at  $2.469\text{ keV}$ . However, the long lifetime of  $^{187}\text{Re}$  forces any such experiment to instrument a very large total target mass, and the low-temperature properties of Re are unfavorable.

Another candidate,  $^{163}\text{Ho}$ , is somewhat more promising. In the EC decay  $^{163}\text{Ho} \rightarrow ^{163}\text{Dy}$ , the inner bremsstrahlung spectrum is sensitive to the neutrino mass. Speculation [141] that atomic effects might enhance the endpoint phase space has been largely resolved. At the moment, however, even ambitious microcalorimeter proposals require long data-taking periods to accumulate statistics with sub-eV sensitivity, and the systematic errors are underexplored.

**PTOLEMY** The PTOLEMY experiment [142] at Princeton is attempting to combine many different technologies in a single tritium-endpoint spectrometer. While its primary goal is the detection of relic neutrinos, as discussed in Sec. 1.10.1, its measurements would certainly be relevant to a direct search for neutrino masses. The PTOLEMY design uses a thin surface-deposition tritium source, which in a future design is planned to reach  $100\text{ g}$ . Tritium beta electrons are accelerated into a static MAC-E filter which

discards all but the last 50–150 eV of the spectrum. The remaining electrons, now at a manageable event rate, are time-tagged by detection of their RF cyclotron radiation in a long solenoid. Finally, the electrons are decelerated to energies below 1 keV before detection in a cryogenic microcalorimeter. The calorimeter provides both energy information at 0.1 eV resolution, and time-of-flight information in correlation with the RF tagger. PTOLEMY installed a small technology-validation prototype at the Princeton Plasma Physics Laboratory in February 2013. The collaboration plans to use the prototype to measure the spectrum of tritium deposited on different substrates including titanium, gold, diamond, and graphene.

Several of PTOLEMY’s methods are untested and may present serious practical challenges. The use of a solid-state source will require a careful roadmap towards answering systematic-error questions.

**Cosmological probes** Another way of addressing the question of absolute neutrino masses connects to the cosmic frontier. The field of observational cosmology now has a wealth of data. Global fits to the data – large-scale structure, high-redshift supernovae, cosmic microwave background, and Lyman  $\alpha$  forest measurements – yield limits on the sum of the three neutrino masses of less than about 0.3-0.6 eV, although specific results depend on assumptions. Future cosmological measurements will further constrain the absolute mass scale. References [143, 144, 145] are recent reviews. The Planck experiment has very recently published new global cosmology fits, including strong neutrino mass constraints, discussed in Sec. [?].

### 1.7.3 Mass-measurement milestones and their physics implications

There is substantial complementarity between kinematic measurements, neutrinoless double beta decay measurements, and cosmological constraints.

Kinematic measurements are sensitive to  $m_\beta$ , a simple mixing-weighted sum with a nonzero lower bound. Neutrinoless double beta decay is either (a) insensitive to  $m_{\beta\beta}$ , if neutrinos are Dirac particles, or (b) if neutrinos are Majorana, sensitive to  $m_{\beta\beta}$ , a quantity which incorporates masses, mixing angles, and complex phases, and may in certain cases be zero. Cosmological probes are insensitive to the simple sum of masses, independent of mixing angles and symmetries, but this sensitivity could be garbled by changes to the cosmological assumptions, including (but not limited to) new fundamental physics.

One worthwhile question is, under what circumstances do direct measurements resolve the neutrino mass hierarchy? See Fig. 1-17. Direct measurements based on beta decay are intrinsically capable of unambiguous determination of the hierarchy because they can identify the three masses weighted by their electron flavor content. However, the mass resolution to make such a measurement is well beyond present capabilities for any choice of mass or hierarchy. A measurement at the achievable sensitivity represented by KATRIN, 200 meV, would show that neutrinos have a nearly degenerate hierarchy, perhaps even more interesting from the theoretical standpoint than the level ordering. In the foreseeable future, new ideas such as Project 8 may be able to reach the 50 meV level. Non-observation of the mass at this level would show that the hierarchy is normal.

### 1.7.4 Future progress and needs for absolute neutrino mass measurements

The field of direct neutrino mass determination, with KATRIN leading the push to  $\sim 0.2$  eV sensitivity, is balancing both statistical and systematic errors. Experiments aiming for lower masses, including Project 8 and PTOLEMY, take it for granted that large statistical power is needed. However, attention must be

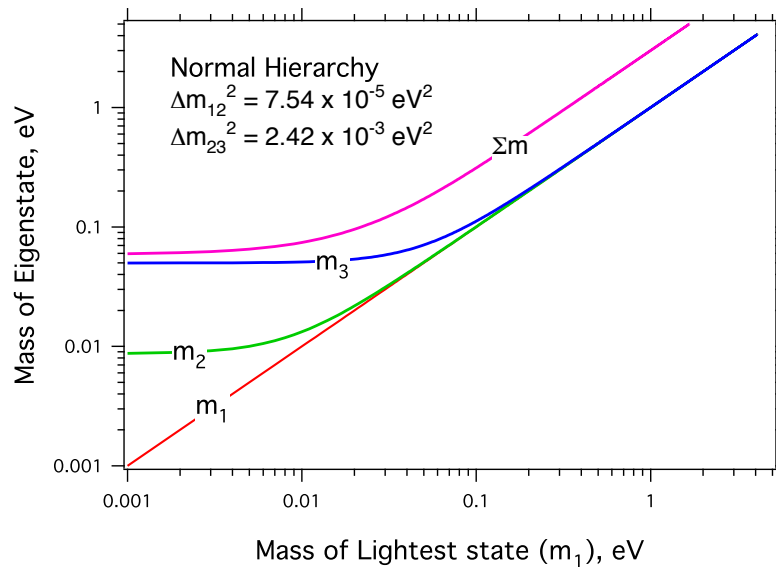


**Figure 1-17.** For normal hierarchy,  $m_\beta$  vs.  $m_{min}$  and component mass eigenstates.

1086 paid to systematics. One systematic error in particular, the molecular excited-state distribution of the  
 1087 daughter ion (in  $T_2 \rightarrow (T \ ^3\text{He})^{+*} + e^- + \bar{\nu}_e$ ) produces an irreducible smearing of all  $T_2$  decay spectra; this  
 1088 smearing is presently unmeasured, and known (with an uncertainty difficult to quantify) from quantum  
 1089 theory. The effect is present in common in KATRIN, Project 8, and any future  $T_2$ -based experiment. The  
 1090 field would benefit from an experimental verification or a theory cross-check on these excited-state spectra.  
 1091 Technologies allowing high-purity atomic  $T_0$  sources would be an end-run around this uncertainty. Most  
 1092 other systematic errors in  $T_2$  experiments are technology-specific, which is important for robust comparisons  
 1093 between experiments.

1094 On the microcalorimeter side, the field is benefiting from decades of hard work, largely on the astrophysics  
 1095 side, in developing microcalorimeter arrays. The discovery of the favorable  $^{163}\text{Ho}$  spectrum highlights the  
 1096 need to complete a search for other candidate nuclides, including high-precision mass measurements to resolve  
 1097 ambiguities about several low-Q decays.

## 1098 1.8 Neutrino Scattering

### 1099 1.8.1 Introduction

1100 Predictions for the rates and topologies of neutrino interactions with matter are a crucial component in many  
 1101 current investigations within nuclear and astroparticle physics. Ultimately, we need to measure neutrino-  
 1102 matter interactions precisely to enable adequate understanding of high-priority physics including neutrino  
 1103 oscillations, supernova dynamics, and dark matter searches. Precise knowledge of such neutrino interactions  
 1104 is an absolute necessity for future measurements of the masses and mixings mediating neutrino oscillations.  
 1105 To enable further progress in neutrino physics, we eventually need to understand, fairly completely, the  
 1106 underlying physics of the neutrino weak interaction within a nuclear environment. This completeness is  
 1107 required so that we can reliably apply the relevant model calculations across the wide energy ranges and  
 1108 varying nuclei necessary for our neutrino investigations.

1109 Neutrino cross-section uncertainties are already becoming a limiting factor in the determination of neutrino  
 1110 oscillation parameters in many experiments. Furthermore, experiments using heavier nuclear targets to  
 1111 increase their signal yields have to contend with the presence of significant nuclear effects impacting both  
 1112 the interaction cross sections and observed final states. Such nuclear effects also impact the reconstruction  
 1113 of the incoming neutrino energy, a key quantity in the determination of neutrino oscillation parameters.  
 1114 Understanding these neutrino-nucleus scattering processes directly affects how well one can separate signal  
 1115 from background. Uncertainties in both the neutrino interaction cross sections and associated nuclear effects  
 1116 must be understood to maximize the sensitivity of an experiment to neutrino oscillations. Of course,  
 1117 depending on the detector, the scientific question being asked, and the oscillation parameters, different  
 1118 cross-section uncertainties can take on different levels of importance. For example, careful control of  
 1119 neutrino/antineutrino cross section differences will be particularly important in establishing CP violation  
 1120 in the neutrino sector [146]. In fact, since  $|U_{e3}|$  is larger than minimal assumptions, such systematic  
 1121 uncertainties become even more important because the expected neutrino/antineutrino asymmetry becomes  
 1122 increasingly smaller for larger  $|U_{e3}|$ .

1123 In addition to the goal of better understanding neutrino-nucleus interactions for more precise oscillation  
 1124 measurements, we also need this physics under control for understanding the dynamics of supernovae. The  
 1125 physics of core-collapse supernova is not yet well-understood. Neutrinos are likely very important in the  
 1126 dynamics of supernovae as well as valuable probes into their inner workings. Supernova neutrinos can also  
 1127 be used to measure oscillations as they travel from source to large detectors on earth, if we can accurately  
 1128 quantify their interactions with nuclei within these large detectors.

1129 These and related physics topics are most easily categorized according to the energy of the incident neutrino.  
 1130 The 0.2-10 GeV energy range (called “intermediate-energy” here) is of most relevance to current and planned  
 1131 meson decay-in-flight (DIF) neutrino beams such as those being used currently for ICARUS, MicroBooNE,  
 1132 MINOS, NOvA, OPERA, T2K, and in the future for LBNE. In addition, a beam from stored muons such  
 1133 as in a muon-factory or the currently proposed nuSTORM facility [147] would also elucidate this regime.  
 1134 The 10-100 MeV range (“low-energy”) is relevant for supernova neutrino studies. Such low energy neutrinos  
 1135 can be produced in intense beams of lower energy protons that create copious pions that decay at rest  
 1136 (DAR). The physics of interest that is categorized by these energy ranges (with some overlap between them)  
 1137 corresponds to the type of neutrino source.

## 1138 1.8.2 Intermediate-Energy Regime

1139 In the 0.2-10 GeV neutrino energy regime, neutrino interactions are a complex combination of quasi-elastic  
 1140 scattering, resonance production, and deep inelastic scattering processes, each of which has its own model and  
 1141 associated uncertainties. Solar and reactor oscillation experiments operating at very low neutrino energies  
 1142 and scattering experiments at very high energies have enjoyed very precise knowledge of their respective  
 1143 neutrino interaction cross sections (at the few-percent level) for the detection channels of interest. However,  
 1144 the same is not true for the relevant intermediate energy regime. In this region, the cross sections even off  
 1145 free nucleons are not very well measured (at the 10 – 40% level) and the data are in frequent conflict with  
 1146 theoretical predictions. Furthermore, the nuclear effects ranging from multi-nucleon-target initial states to  
 1147 complex final-state interactions are still quite poorly known. Figure 1-18 shows existing measurements of  
 1148 charged-current neutrino cross sections in the relevant energy range. Such measurements form the foundation  
 1149 of our knowledge of neutrino interactions and provide the basis for simulations in present use.

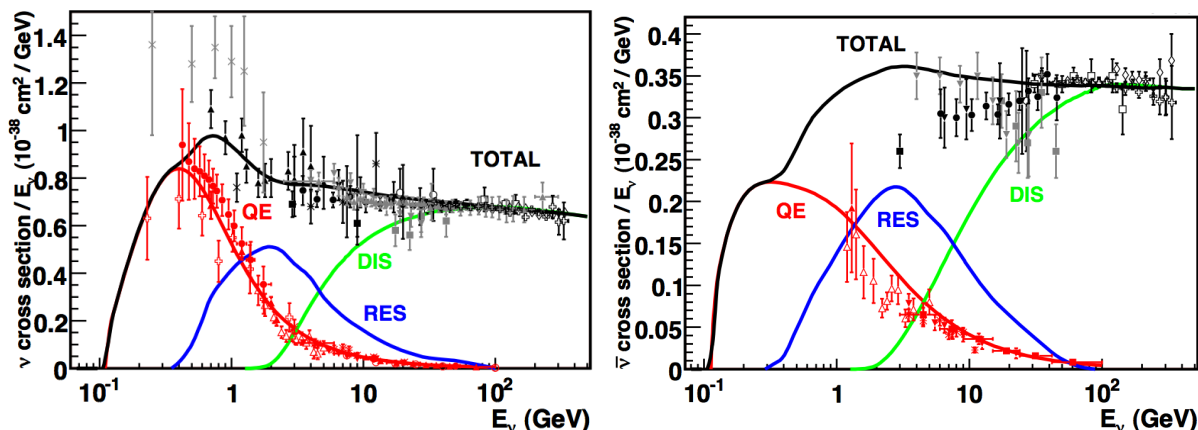


**Figure 1-18.** Existing muon neutrino (left) and antineutrino (right) charged-current cross section measurements [30] and predictions [148] as a function of neutrino energy. The contributing processes in this energy region include quasi-elastic (QE) scattering, resonance production (RES), and deep inelastic scattering (DIS). The error bars in the intermediate energy range reflect the uncertainties in these cross sections (typically 10 – 40%, depending on the channel).

1150 There has been renewed interest and progress in neutrino interaction physics in the last ten years because  
 1151 of recent efforts to understand and predict signal and background rates in neutrino oscillation searches in  
 1152 few-GeV beams. One of several intriguing results from these new data comes from recent measurements  
 1153 of quasi-elastic (QE) scattering. QE scattering is a simple reaction historically thought to have a well-  
 1154 known cross section; this is one reason why it is chosen as the signal channel in many neutrino oscillation  
 1155 experiments. Interestingly, the neutrino QE cross section recently measured on carbon at low energy by  
 1156 the MiniBooNE experiment is about 40% higher than the most widely used predictions [149] and is even  
 1157 larger than the free nucleon scattering cross section in some energy regions [150]. Similar effects are seen  
 1158 for antineutrinos [151]. These results are surprising because nuclear effects have always been expected to  
 1159 reduce the cross section, not enhance it. A recent QE cross section measurement from NOMAD at higher  
 1160 energies does not exhibit such an enhancement [152]. A possible reconciliation between the two classes of  
 1161 measurements has suggested that previously-neglected nuclear effects could in fact significantly increase the  
 1162 QE cross section on nuclei at low energy [153]. A similar enhancement has been observed in electron-nucleus  
 1163 scattering [154]. If true, this radically changes our thinking on nuclear effects and their impact on low-energy

1164 neutrino interactions. This revelation has been the subject of intense theoretical scrutiny and experimental  
1165 investigation over the past year or more (see for example, [155, 156, 157, 158]).

1166 In the so-called resonance/transition region, the channels of interest are mainly hadronic resonances with  
1167 the most important being the  $\Delta(1232)$ . Typical final states are those with a single pion. During the last five  
1168 years, several new pion production measurements have been performed. In all of them, the targets were nuclei  
1169 (most often carbon). As one example, the MiniBooNE experiment recently measured a comprehensive suite  
1170 of CC  $1\pi^+$ , CC  $1\pi^0$ , and NC  $1\pi^0$  production cross sections [159]. A variety of flux-integrated differential cross  
1171 sections, often double differential, were reported for various final state particle kinematics. The cross-section  
1172 results differ from widely-used predictions at the 20% level or more.

1173 There are several efforts currently producing results that will add significantly to the available data and to  
1174 the underlying physics understanding. The MINERvA experiment in the 1-10 GeV NuMI beam at Fermilab  
1175 has very recently published results on QE scattering measured with a precise tracking detector from both  
1176 neutrino and antineutrinos on carbon [157, 158]. The near detectors of the T2K [160] experiment in Japan  
1177 are also measuring neutrino-nucleus interactions as part of their oscillation measurement program. T2K  
1178 has recently reported total cross sections for neutrino CC inclusive scattering [160]. Additional results on  
1179 exclusive channels from MINERvA and both the T2K and NOvA near detectors will be forthcoming in the  
1180 near future.

1181 The MINERvA experiment will also perform the first studies of nuclear effects in neutrino interactions using a  
1182 suite of nuclear targets including He, C, O (water), Fe, and Pb in addition to a large quantity of scintillator  
1183 CH. Analysis of neutrino scattering processes from these varying nuclei are already underway. Another  
1184 possible step in the MINERvA program is the addition of a deuterium target [161] which is currently under  
1185 review. This is an intriguing, albeit challenging, possibility as it will allow nuclear effects in these processes  
1186 to be separated from the bare-nucleon behavior.

1187 All current accelerator-based neutrino experiments use a meson-decay beam either on-axis or off-axis to  
1188 narrow the energy spread of the beam. The uncertainty in the neutrino flux normalization and spectral  
1189 shape will ultimately limit our understanding of the underlying physics of neutrino interactions and the  
1190 ability to conduct precision neutrino oscillation measurements. Because of these uncertainties, an improved  
1191 understanding of our neutrino beams is paramount. For these beams, some improvement in the knowledge  
1192 of the neutrino flux is possible through meson-production experiments that determine the underlying meson  
1193 momentum and angular distributions. These can then be combined with detailed simulations of the neutrino  
1194 beamline optics. Current neutrino fluxes are known to the 10% level with a goal to reach the 5% level or  
1195 better.

1196 Additional experiments in beams of different energies provide a valuable cross-check on the underlying energy  
1197 dependence of physics models as well as the background calculations of the experiments. For example, the  
1198 NOvA experiment, which will soon run in the NuMI off-axis neutrino beam, offers a unique opportunity  
1199 to add to the world's neutrino interaction data by measuring cross sections with its near detector as well  
1200 as with a possible upgrade to a relatively-inexpensive fine-grained detector such as the proposed SciNOvA  
1201 experiment [162, 161].

1202 A potentially transformative next step beyond meson-decay beams as sources of neutrinos would be the  
1203 use of circulating muon beams. The muons may be either uncooled and unaccelerated as in the case of  
1204 nuSTORM [147] or both cooled and accelerated as in the case of a Neutrino Factory. These facilities will  
1205 yield a flux of neutrinos known to better than 1%, thus allowing large gains in our understanding of neutrino  
1206 interaction processes. Another significant advantage of these muon-decay-based neutrino sources would be  
1207 the availability, for the first time, of an intense and well-known source of electron-(anti)neutrinos. Such

1208 beams would allow the measurement of  $\nu_e$ -nucleus cross sections, which have not been historically well  
1209 measured and are of great importance to future  $\nu_\mu \rightarrow \nu_e$  oscillation experiments.

1210 In addition to beam improvements, up-and-coming detector technologies such as LAr TPCs will both provide  
1211 increased tracking precision for better final-state exclusivity as well as measurements specifically on argon.  
1212 Understanding interactions on argon is obviously crucial for oscillation measurements in LBNE given that  
1213 the far detector of choice is a LAr TPC. New neutrino scattering measurements on argon are already being  
1214 reported by ArgoNeuT which ran in the NuMI beam in 2009–2010 [163]. The near-future MicroBooNE  
1215 experiment which will begin taking data in an  $\approx 1$  GeV neutrino beam starting in 2014 will further boost  
1216 this effort in the next few years. In addition, other efforts with imminent,  $\approx 10$  ton LAr TPCs [161] in an  
1217 existing beam such as NuMI, can also provide more information on reconstruction and final-state topology  
1218 to further this effort.

1219 However, in order to adequately map out the complete nuclear dependence of the physics, there is need to  
1220 have multiple nuclear targets to measure the nuclear effects combined with a precision tracker. For this an  
1221 attractive follow-on to MINERvA would be a straw-tube/transition-radiation detector that employs multiple  
1222 nuclear targets (including argon) simultaneously in the same beam such as that proposed for one of the LBNE  
1223 near-detector options [161].

### 1224 1.8.3 Low-Energy Regime

1225 The 10-100 MeV neutrino energy range addresses a varied set of topics at the forefront of particle physics  
1226 such as supernovae, dark matter, and nuclear structure. Low-energy neutrino scattering experiments are  
1227 possibilities at currently-existing high-intensity proton sources such as the ORNL SNS or the Fermilab  
1228 Booster neutrino beam line. They should also be considered at future facilities such as Project-X at Fermilab.

#### 1229 1.8.3.1 Supernova neutrino physics

1230 The multiple physics signatures and expected neutrino fluxes from a core-collapse signature are described in  
1231 Sec. 1.10.2.1. To get the most from the next supernova neutrino observation, it will be critical to understand  
1232 the interactions of neutrinos with matter in the tens-of-MeV energy range [164, 165].

1233 A stopped-pion source provides a monochromatic source of 30 MeV  $\nu_\mu$ 's from pion decay at rest, followed on  
1234 a 2.2  $\mu$ s timescale by  $\bar{\nu}_\mu$  and  $\nu_e$  with a few tens of MeV from  $\mu$  decay. The  $\nu$  spectrum matches the expected  
1235 supernova spectrum reasonably well (see Fig. 1-19). A  $\sim 1$  GeV, high-intensity, short-pulse-width, proton  
1236 beam is desirable for creating such a  $\nu$  source. Prior examples used for neutrino physics include LANSCE  
1237 and ISIS. A rich program of physics is possible with such a stopped-pion  $\nu$  source, including measurement  
1238 of neutrino-nucleus cross sections in the few tens of MeV range in a variety of targets relevant for supernova  
1239 neutrino physics. This territory is almost completely unexplored: so far only  $^{12}\text{C}$  has been measured at the  
1240 10% level.

1241 A pion DAR neutrino source such as that currently available at the ORNL SNS neutron spallation target  
1242 would be an excellent source of neutrinos for this physics on a variety of nuclei relevant for supernova [166,  
1243 167]. In addition, this source would allow specific studies to better understand the potential of a large LAr  
1244 detector such as that proposed for LBNE. In particular, low-energy neutrino-argon cross sections, required  
1245 for supernova detection in a large LAr detector could be measured with a near future prototype  $\approx 10$  ton  
1246 LAr detector [165, 168]. In the farther future, the high-intensity FNAL Project-X 1-3 GeV Linac would also  
1247 provide a potential site for these experiments.

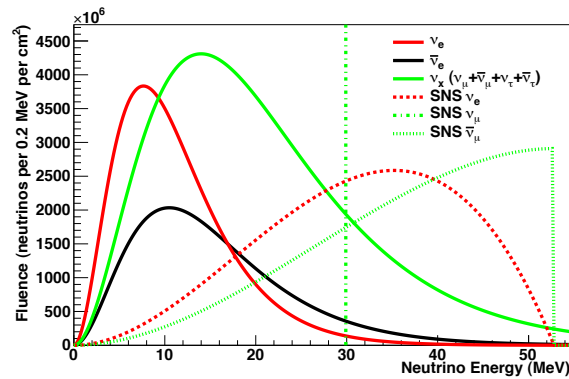


**Figure 1-19.** Solid lines: typical expected supernova spectrum for different flavors; fluence integrated over the  $\sim 15$ -second burst. Dashed and dotted lines: SNS spectrum; integrated fluence for one day at 30 m from the SNS target.

### 1248 1.8.3.2 Coherent elastic neutrino-nucleus scattering

1249 Coherent elastic neutrino-nucleus scattering (CENNS), a process in which the target nucleus recoils coherently via a collective neutral current exchange amplitude with a neutrino or antineutrino, is a long-sought prediction of the Standard Model. Although the process is well predicted by the Standard Model and has a comparatively large cross section ( $10^{-39}$  cm<sup>2</sup>) in the relevant energy region (0  $\sim$  50 MeV), CENNS has never been observed before as the low-energy nuclear recoil signature is difficult to observe. Numerous groups world-wide are now working to detect this elusive process [169]. Only a few sources, in particular nuclear reactors and spallation neutrino sources, produce the required 1-50 MeV energies of the neutrinos in sufficient quantities for a definitive first measurement. Above this energy, the de Broglie wavelength of the neutrino approaches that of the individual nucleon and the coherent interaction strength diminishes.

1258 A modest sample of a few hundred events collected with a keV-scale-sensitive dark-matter-style detector could improve upon existing non standard neutrino interaction parameter sensitivities by an order of magnitude or more. A deviation from the  $\sim 5\%$  predicted cross section could be an indication of new physics [170, 171]. Either way, the cross section is relevant for understanding the evolution of core-collapse supernovae, characterizing future burst supernova neutrino events collected with terrestrial detectors, and a measurement of the process that will ultimately set the background limit to direct WIMP searches with detectors at approximately the ten-ton scale [172, 173]. Proposals have arisen to probe nuclear structure [174] owing to the sensitivity of the coherent scatter process to the number of neutrons in the nucleus, and to search for sterile neutrinos [175, 176] by exploiting the flavor-blind nature of the process. There are also potentially practical applications, as described in Sec. 1.11.1.2.

1268 Well-defined neutrino sources are an essential component to measure CENNS. If a near, low-background location can be identified, this experiment may be performed, at the Spallation Neutron Source at Oak Ridge National Laboratory [167, 177]. As an alternative, there may be an opportunity to utilize the existing FNAL 8 GeV proton source at a far off-axis location [178].

#### 1.8.4 Required Theoretical/Phenomenological Work

A strong effort in theory/phenomenology/modeling is requisite to profit from improved measurements in neutrino experiments. While there is a healthy community working on the subject of neutrino-nucleus interactions in Europe, there is a dearth of phenomenologists in the U.S. able to address the pressing theoretical questions needed to fully understand this subject and apply it to the interpretation of experimental data. Even in Europe, the funding for phenomenology work is not necessarily tied to neutrino-nucleus scattering but to other more European-centric physics projects. There is a critical need within the U.S. physics community to devote time and resources to a theoretical/phenomenological understanding of neutrino-nucleus scattering. This naturally directly calls for a united effort of both the particle and nuclear physics communities to better support these efforts [179]. There are numerous ideas that have been put forth by both experimentalists and theorists for how best to proceed [180, 181]. They include suggestions for improvements to neutrino event generators with more sophisticated underlying calculations for neutrino interactions on nuclei as well as the formation.

## 1.9 Beyond the Standard Paradigm – Anomalies and New Physics

Neutrinos moved beyond the standard model years ago with the discovery of neutrino oscillations, which implied the existence of neutrino mass. Much of the oscillation data can be described by a three-neutrino paradigm. However, there are intriguing anomalies that cannot be accommodated within this paradigm, and suggest new physics beyond it. In particular, the marginal yet persistent evidence of oscillation phenomena around  $\Delta m^2 \sim 1 \text{ eV}^2$ , which is not consistent with the well-established solar and atmospheric  $\Delta m^2$  scales, is often interpreted as evidence for one or more additional neutrino states, known as sterile neutrinos. Beyond the sterile neutrino, new physics may appear through a broad array of mechanisms collectively known as non-standard interactions (NSI). Typically, searches for these effects occur in experiments designed to study standard phenomena. One type of NSI that has been the subject of dedicated searches in the past and may play a role in the future program is the neutrino magnetic moment. In the following sections we will discuss the prospects for neutrino experiments sensitive to anomalies and new physics over the next several years.

### 1.9.1 Sterile Neutrinos

Data from a variety of short-baseline experiments, as well as astrophysical observations and cosmology, hint at the existence of additional neutrino mass states beyond the three active species in the standard model (see for example [60]). The implications of these putative sterile neutrino states would be profound, and would change the paradigm of the standard model of particle physics. As a result, great interest has developed in testing the hypothesis of sterile neutrinos and providing a definitive resolution to the question: do light sterile neutrinos exist?

Recently, a number of tantalizing results (anomalies) have emerged from short-baseline neutrino oscillation experiments that cannot be explained by the current three-neutrino paradigm. These anomalies, which are not directly ruled out by other experiments, include the excess of  $\bar{\nu}_e$  events ( $3.8 \sigma$ ) observed by the LSND experiment [182], the  $\nu_e$  ( $3.4 \sigma$ ) and  $\bar{\nu}_e$  ( $2.8 \sigma$ ) excesses observed by MiniBooNE [183] particularly at low-energy in  $\nu_e$  mode [184], the deficit of  $\bar{\nu}_e$  events ( $0.937 \pm 0.027$ ) observed by reactor neutrino experiments [185], and the deficit of  $\nu_e$  events ( $0.86 \pm 0.05$ ) observed in the SAGE and GALLEX radioactive source experiments [186].

Although there may be several possible ways to explain these anomalies, the simplest explanation is the  $3+N$  sterile neutrino model, in which there are three light, mostly active neutrinos and  $N$ , mostly sterile neutrinos which mix with the active flavors. For  $N > 1$ , these models allow for CP-violating effects in short-baseline appearance experiments. The world's oscillation data can be fit to these  $3+N$  models resulting in allowed regions that close at 95% CL or better, as shown in Fig. 1-20 and 1-21 for the  $3+1$  model. Still, significant tension exists between the appearance and disappearance data [187], particularly due to the absence of  $\nu_\mu$  disappearance in the  $\Delta m^2 \sim 1 \text{ eV}^2$  region [188, 189], a key prediction of the  $3+N$  models.

Beyond particle physics, there are hints of additional neutrinos coming from cosmology. Fits to astrophysical data sets (including the cosmic microwave background (CMB), large scale structure, baryon acoustic oscillations and Big Bang nucleosynthesis) are sensitive to the effective number of light degrees of freedom ( $N_{eff}$ ) (which in the standard model is equivalent to saying the effective number of neutrino families, although in principle this could include other types of light, weakly-coupled states). Prior to the release of the Planck data in 2013, there was an astonishing trend that such fits, conducted by different groups and involving differing mixes of data sets and assumptions, tended to favor  $N_{eff}$  closer to 4 than 3 [60]. With the release of Planck data [190] new more precise fits to  $N_{eff}$  are now more consistent with 3. The Planck Collaboration fit values range from  $3.30 \pm 0.52$  (95% CL) to  $3.62 \pm 0.49$  (95% CL) depending on which other data sets

are included in the fit. The pre-Planck fits used the full-sky WMAP [191] data set for the first three peaks of the the CMB angular power spectrum, but and typically relied on narrow-sky, high angular resolution observations by the South Pole Telescope [192], or the Atacama Cosmology Telescope [193] for the next four peaks. The Planck mission combined a full-sky survey with high angular resolution, and was, for the first time, able to measure the first seven peak in the spectrum with one apparatus. The Planck Collaboration believes that a miscalibration in the stitched together spectra was responsible for the anomalously high value of  $N_{eff}$  found in the earlier fits [190]. While the new fits to  $N_{eff}$  are now more consistent with 3 light degrees of freedom, they are still high. Generally the Plank fits seem to rule out  $N_{eff} \geq 4$ , but they are still consistent with one or more sterile neutrino states that were not fully thermalized.

For a comprehensive review of light sterile neutrinos including the theory, the cosmological evidence, and the particle physics data see Ref. [60].

In order to determine if these short-baseline anomalies are due to neutrino oscillations in a  $3 + N$  sterile neutrino model, future short-baseline experiments are needed. These experiments should have robust signatures for electron and/or muon neutrino interactions and they should be capable of measuring the  $L/E$  dependence of the appearance or disappearance effect. Several ways of measuring  $L/E$  dependence have been proposed including: 1) placing a large detector close to a source of low-energy neutrinos from a reactor, cyclotron or intense radioactive source and measuring the  $L/E$  dependence of the  $\bar{\nu}_e$  disappearance with a single detector, 2) positioning detectors at two or more baselines from the neutrino source, and 3) measuring the  $L/E$  dependence of high energy atmospheric neutrinos, where strong matter effects are expected, in particular close to the matter resonance expected for the sterile  $\Delta m^2$  in the Earth’s core. In addition, experiments sensitive to neutral current interactions, in which active flavor disappearance would be a direct test of the sterile hypothesis, are needed.

Finally, it is important to note that satisfactorily resolving these short-baseline anomalies, even if unrelated to sterile neutrinos, is very important for carrying out the 3-flavor neutrino oscillation program described earlier. The 2 to 3  $\sigma$  effects reported at the sub-percent to the several-percent level, are similar in scale and effect to the  $CP$ -violation and mass hierarchy signals being pursued in long-baseline experiments.

### 1.9.1.1 Projects and Proposals with Radioactive Neutrino Sources

Proposals to use radioactive neutrino sources to search for sterile neutrino oscillations actually predate the “gallium anomaly” [205]. Perhaps the most intriguing opportunity with the source experiments is the possibility of precision oscillometry – the imaging, within one detector, the oscillation over multiple wavelengths in  $L/E$ . Therefore this approach would likely be the best way to deconvolve the multiple frequencies expected if there are two or more sterile neutrino states. Typically these proposals are built around existing detectors with well-measured backgrounds, where the new effort involves creating a source and delivering it to the detector. There are two types of sources actively under consideration: 1)  $^{51}\text{Cr}$ , an electron capture isotope which produces a  $\nu_e$  of 750 keV, and 2)  $^{144}\text{Ce}$ - $^{144}\text{Pr}$ , where the long-lived  $^{144}\text{Ce}$  ( $\tau_{1/2} = 285$  days)  $\beta$ -decays producing a low energy  $\bar{\nu}_e$  of no interest, while the daughter isotope,  $^{144}\text{Pr}$ , rapidly  $\beta$ -decays producing a  $\bar{\nu}_e$  with a 3 MeV endpoint. Since  $^{51}\text{Cr}$  neutrinos are mono-energetic, with no need to reconstruct the neutrino energy, they can be detected by charged-current, neutral-current or elastic scattering.  $^{144}\text{Pr}$  neutrinos, on the other hand which are emitted with a  $\beta$  spectrum, and must be detected via a charged-current process such as inverse  $\beta$ -decay.

Proposals actively under consideration include SOX [196] based on the Borexino detector, Ce-LAND [194] based on the KamLAND detector, and a Daya Bay Source experiment [195]. SOX is considering both  $^{51}\text{Cr}$  and  $^{144}\text{Ce}$ - $^{144}\text{Pr}$  phases. In the  $^{51}\text{Cr}$  phase, a source of up to 10 MCi is placed about 8 m from the center

**Table 1-5.** *Proposed sterile neutrino searches.*

Experiment	$\nu$ Source	$\nu$ Type	Channel	Host	Cost Category <sup>1</sup>
Ce-LAND [194]	$^{144}\text{Ce}$ - $^{144}\text{Pr}$	$\bar{\nu}_e$	disapp.	Kamioka, Japan	small <sup>2</sup>
Daya Bay Source [195]	$^{144}\text{Ce}$ - $^{144}\text{Pr}$	$\bar{\nu}_e$	disapp.	China	small
SOX [196]	$^{51}\text{Cr}$	$\nu_e$	disapp.	LNGS, Italy	small <sup>2</sup>
	$^{144}\text{Ce}$ - $^{144}\text{Pr}$	$\bar{\nu}_e$	disapp.		
US Reactor [197]	Reactor	$\bar{\nu}_e$	disapp.	US <sup>3</sup>	small
Stereo	Reactor	$\bar{\nu}_e$	disapp.	ILL, France	NA <sup>4</sup>
DANSS [198]	Reactor	$\bar{\nu}_e$	disapp.	Russia	NA <sup>4</sup>
OscSNS [199]	$\pi$ -DAR	$\bar{\nu}_\mu$	$\bar{\nu}_e$ app.	ORNL, US	medium
LAr1 [200]	$\pi$ -DIF	$\bar{\nu}_\mu^{(-)}$	$\bar{\nu}_e^{(-)}$ app.	Fermilab	medium
MiniBooNE+ [201]	$\pi$ -DIF	$\bar{\nu}_\mu^{(-)}$	$\bar{\nu}_e^{(-)}$ app.	Fermilab	small
MiniBooNE II [202]	$\pi$ -DIF	$\bar{\nu}_\mu^{(-)}$	$\bar{\nu}_e^{(-)}$ app.	Fermilab	medium
ICARUS/NESSiE [203]	$\pi$ -DIF	$\bar{\nu}_\mu^{(-)}$	$\bar{\nu}_e^{(-)}$ app.	CERN	NA <sup>4</sup>
IsoDAR [96]	$^8\text{Li}$ -DAR	$\bar{\nu}_e$	disapp.	Kamioka, Japan	medium
$\nu$ STORM [147]	$\mu$ Storage Ring	$\bar{\nu}_e^{(-)}$	$\bar{\nu}_\mu^{(-)}$ app.	Fermilab/CERN	large

<sup>1</sup> Rough recost categories: small: <\$5M, medium: \$5M-\$50M, large: \$50M-\$300M.

<sup>2</sup> US scope only.

<sup>3</sup> Multiple sites are under consideration [204].

<sup>4</sup> No US participation proposed.

1370 of the detector. This phase takes advantage of Borexino’s demonstrated ability to see the  $\nu_e - e$  elastic  
1371 scattering of 861 keV,  $^7\text{Be}$  solar neutrino [206]. Later phases may involve a  $^{144}\text{Ce}$ - $^{144}\text{Pr}$  source which could  
1372 be located either inside or outside the detector, the former requiring major modifications to the Borexino  
1373 detector. The Ce-LAND and the Daya Bay Source proposals are both based on  $^{144}\text{Ce}$ - $^{144}\text{Pr}$ . In the Daya  
1374 Bay Source proposal, a 500 kCi source is placed in between the four 20-ton antineutrino detectors at the  
1375 Daya Bay far site. With Ce-LAND, a 75 kCi source could be placed either outside the detector, 9.5 m from  
1376 the center, or inside the detector (only after the KamLAND-Zen  $\beta\beta_{0\nu}$  run is complete). The sensitivity for  
1377 these proposals is shown in Fig. 1-20a.

1378 There is also the possibility of a sterile neutrino measurement based on the combination of a  $^{51}\text{Cr}$  source with  
1379 cryogenic solid state bolometers, to detect all active neutrino flavors through neutral current CENNS [175]  
1380 (see Sec. 1.8.3.2). This proposal, known as RICOCHET, would be a direct test of the sterile hypothesis since  
1381 the neutral current is equally sensitive to all active flavors, but blind to sterile neutrinos.

### 1382 1.9.1.2 Projects and Proposals that Directly Address the Reactor Anomaly

1383 The apparent deficit of neutrinos in short-baseline reactor neutrino experiments, known as the reactor  
1384 anomaly is result of two distinct lines of analysis: the theoretical calculations of the reactor antineutrino  
1385 flux [207, 208, 209, 210], which are based on measurements of the  $\beta$ -spectra from the relevant fission  
1386 isotopes [207, 208], and the reactor antineutrino measurements [211, 212, 213, 214, 215, 216, 217, 218, 219].  
1387 The anomaly [185] emerges in the comparison of these two analyses, and as such, both improved flux

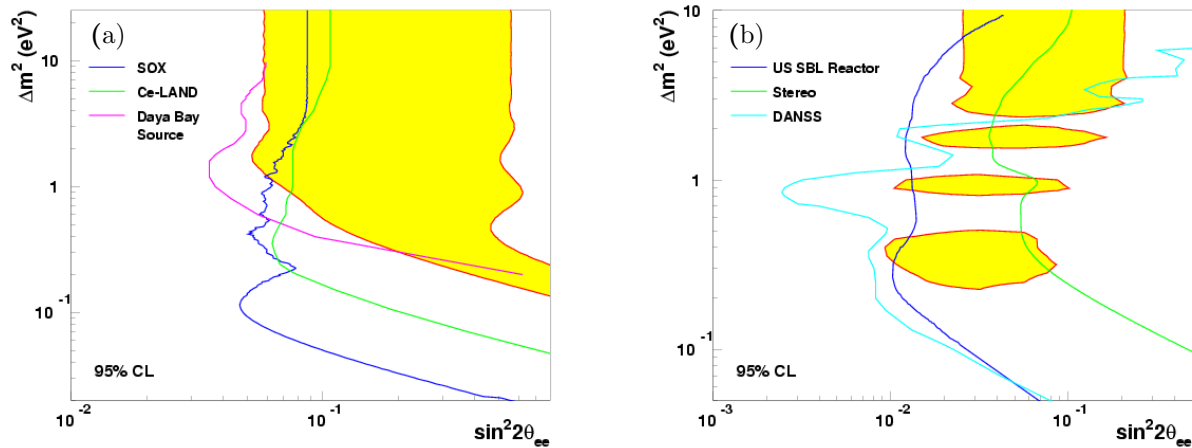


**Figure 1-20.** Collaboration-reported sensitivity curves for proposed source (a) and reactor (b) experiments plotted against the global fits [187] for the gallium anomaly and reactor anomaly respectively.

1388 calculations (and the underlying  $\beta$ -spectra measurements) and new reactor antineutrino measurements are  
 1389 needed.

1390 The most direct proof of a sterile neutrino solution to the reactor anomaly would be to observe a spectral  
 1391 distortion in the antineutrino rate that varies as a function of distance from the reactor core. There are  
 1392 several projects and proposals from all over the world to search for this effect, including: Stereo [60] at ILL  
 1393 in France and DANSS [198] at the Kalinin Power Plant in Russia, to name two. In the US, the parties  
 1394 interested in this measurement have organized into a single collaboration [197] that is investigating several  
 1395 potential sites [204] and detector technologies [220]. A compact reactor core is highly desirable to reduce  
 1396 the smearing and uncertainty in  $L$ , which makes power reactors less attractive. In addition, new detector  
 1397 designs with better spatial resolution, improved background rejection and better neutron tagging may be  
 1398 needed.

1399 On the antineutrino flux side, the existing reactor  $\theta_{13}$  experiments, such as Daya Bay [221], with their  
 1400 high-statistics near detectors, at baselines far enough to average out any spectral distortions from sterile  
 1401 oscillations, will provide the world's best data on reactor fluxes, ensuring that the uncertainty on the reactor  
 1402 anomaly is dominated by the flux calculation. New measurements of the  $\beta$ -spectra of the fission isotopes [222],  
 1403 would be helpful in further reducing the uncertainty on the flux calculation, but theoretical uncertainties  
 1404 from effects such as weak magnetism [210] will ultimately limit this approach.

### 1405 1.9.1.3 Projects and Proposals with Accelerator Induced Neutrinos

1406 There are a number of proposals involving Fermilab's Booster Neutrino Beam (BNB) which are relevant to the  
 1407 sterile neutrino question. The MicroBooNE experiment, which is currently under construction right upstream  
 1408 of MiniBooNE, will use the fine grain tracking of its 170-ton LAr TPC to study, in detail, the interaction  
 1409 region of events corresponding to the MiniBooNE low-energy excess, and may help to determine if these  
 1410  $\nu_\mu \rightarrow \nu_e$  oscillation candidates are really  $\nu_e$  charged current quasielastic events as assumed by MiniBooNE.  
 1411 Similarly, the proposed MiniBooNE+ [201] would look for neutron captures following  $\nu_e$  candidate events. In  
 1412 the MiniBooNE energy range, the production of free neutrons in a neutrino interaction is strongly correlated

1413 with the charged current. MiniBooNE+ would attempt to detect these neutrons by adding scintillator to  
 1414 the MiniBooNE detector making it sensitive to the 2.2 MeV gammas produced when a neutron captured  
 1415 on hydrogen. This neutron tagging capability would be used to study whether the MiniBooNE low-energy  
 1416 excess events are truly  $\nu_e$  events as the oscillation hypothesis requires. The MiniBooNE II proposal [202],  
 1417 to either build a new near detector or move the existing MiniBooNE detector to a near location, is also  
 1418 intended as a test of MiniBooNE excess. The presence of a near detector may help to confirm or refute the  
 1419 baseline dependence of the excess. The LAr1 proposal [200] is a multi-baseline proposal for the BNB which  
 1420 is based on LAr. It would add a 25-ton, “MicroLAr” detector at 100 m and a 3 kton, “LAr1”, detector at  
 1421 700 m to the existing MicroBooNE detector, which is at a baseline of 470 m. The projected sensitivity of  
 1422 this three detector combination is shown in Fig. 1-21b. There is also a less ambitious proposal to add just  
 1423 the MicroLAr near detector [223]. In Fermilab’s NuMI beam line the MINOS+ experiment [69] will search  
 1424 for muon neutrino disappearance caused by oscillations to  $\nu_s$ .

1425 There is also a proposal at CERN for a two detector LAr TPC known as ICARUS/NESSiE [203]. In this  
 1426 proposal, the ICARUS T600 LAr TPC would be moved from Gran Sasso and set 1600 m downstream  
 1427 from a new neutrino beam extracted from the CERN-SPS. A second, smaller LAr TPC would be built at  
 1428 300 m. Additionally a muon spectrometer would be installed behind each TPC. The projected sensitivity of  
 1429 ICARUS/NESSiE is shown in Fig. 1-21b.

1430 The Spallation Neutron Source (SNS) at Oak Ridge National Laboratory is also an intense and well-  
 1431 understood source of neutrinos from  $\pi^+$  and  $\mu^+$  decays-at-rest in much the same way that LAMPF produced  
 1432 neutrinos for LSND [224]. As such it is an excellent place to make a direct test of LSND. The OscSNS [199]  
 1433 proposal would build an 800-ton detector approximately 60 m from the SNS beam dump. OscSNS could  
 1434 improve upon LSND in at least three specific ways: 1) the lower duty factor of the SNS significantly reduces  
 1435 cosmic backgrounds, 2) the detector would be placed upstream of the beam lowering the possibility of  
 1436 non-neutrino, beam-correlated backgrounds, and 3) gadolinium-doped scintillator may be used to capture  
 1437 neutrons, providing a more robust tag of inverse  $\beta$ -decay. In addition to  $\bar{\nu}_e$  appearance, OscSNS would  
 1438 search for  $\nu_\mu$  and  $\nu_e$  disappearance. The projected sensitivity of the OscSNS  $\bar{\nu}_e$  appearance search is shown  
 1439 in Fig. 1-21b.

1440 IsoDAR [96] is a proposal to use a low-energy, high-power cyclotron to produce  $^8\text{Li}$ , which  $\beta$ -decays producing  
 1441 a  $\bar{\nu}_e$  with an endpoint of 13 MeV. This cyclotron would be placed near the KamLAND detector which would  
 1442 detect the  $\bar{\nu}_e$  via inverse  $\beta$ -decay. This arrangement would be sensitive to the disappearance of  $\bar{\nu}_e$ , and, given  
 1443 the low-energy of the neutrinos and 13-m diameter detector, it should be capable of precision oscillometry.  
 1444 The projected sensitivity of IsoDAR is shown in Fig. 1-21a.

1445 The nuSTORM [147] proposal, to build a racetrack-shaped muon storage ring, to provide clean and well-  
 1446 characterized beams of  $\nu_e$  and  $\bar{\nu}_\mu$  (or  $\bar{\nu}_e$  and  $\nu_\mu$  if  $\mu^-$  are stored). These beams would enable extremely  
 1447 precise searches for sterile neutrino oscillations in four neutrino types, in both appearance and disappearance  
 1448 channels. The most powerful and unprecedented capability of nuSTORM would be to search for  $(\bar{\nu}_\mu^{\prime})$  appear-  
 1449 ance. The nuSTORM beams are essentially free of intrinsically-produced wrong sign/wrong flavor neutrinos  
 1450 which are unavoidable in pion decay-in-flight beams. On the other hand muon storage rings simultaneously  
 1451 produce  $\nu_e$  and  $\bar{\nu}_\mu$ , so it essential to have magnetic detectors to distinguish between  $\bar{\nu}_\mu$  from oscillation  
 1452 and  $\nu_\mu$  from the beam. The proposed nuSTORM project has near and far magnetized iron detectors, but  
 1453 future upgrades could include magnetized LAr TPCs. NuSTORM is a facility which, in addition to sterile  
 1454 neutrino searches, would make neutrino cross-section measurements critical to the long-baseline program (see  
 1455 Sec. 1.8) and conduct neutrino factory R&D, yet it is based on existing accelerator technology. Proposals for  
 1456 nuSTORM are currently being considered by both Fermilab [225] and CERN [226]. The projected sensitivity  
 1457 of the nuSTORM  $(\bar{\nu}_e^{\prime}) \rightarrow (\bar{\nu}_\mu^{\prime})$  search is shown in Fig. 1-21b.

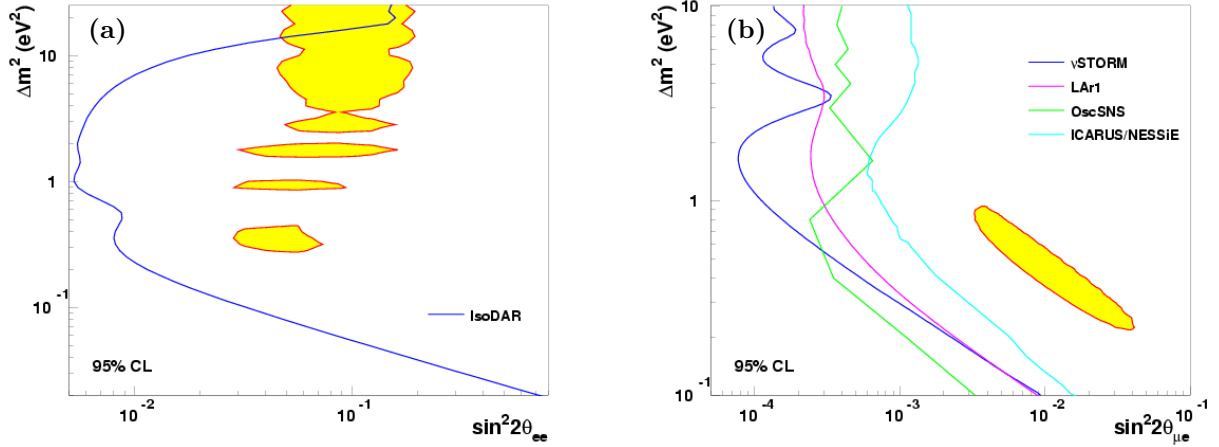


**Figure 1-21.** Collaboration-reported sensitivity curves for proposed accelerator-based experiments sensitive to  $\nu_e$  and  $\bar{\nu}_e$  disappearance (a) and appearance which includes  $\nu_\mu \rightarrow \nu_e$  and  $\nu_e \rightarrow \nu_\mu$  in both neutrinos and antineutrinos, (b) plotted against the global fits [187].

#### 1458 1.9.1.4 Sensitivity from Atmospheric Neutrinos

1459 The disappearance of atmospheric  $\nu_\mu$  in the 0.5 to 10 TeV energy range can be enhanced by matter effects in  
 1460 the Earth’s core for the case of a sterile neutrino with  $\Delta m^2 \sim 1 \text{ eV}^2$  [227, 228]. Such neutrinos are observed  
 1461 by the IceCube experiment [229] at the South Pole, which can measure or set limits on the muon to sterile  
 1462 mixing amplitude by studying the zenith angle (effectively  $L$ ) and energy dependence of any disappearance  
 1463 effect.

#### 1464 1.9.2 Non-Standard Interactions

1465 Neutrino experiments in general, and neutrino oscillation experiments in particular, are also very sensitive  
 1466 to new, heavy degrees of freedom that mediate new “weaker-than-weak” neutral current interactions. These  
 1467 so-called non-standard interactions (NSI) between neutrinos and charged fermions modify not only neutrino  
 1468 production and detection, but also neutrino propagation through matter effects. In a little more detail, NSI  
 1469 are described by effective operators proportional to, for example,  $G_F \epsilon_{\alpha\beta}^f \nu_\alpha \gamma_\mu \nu_\beta \bar{f} \gamma^\mu f$ , where  $\nu_{\alpha,\beta} = \nu_{e,\mu,\tau}$ ,  $f$   
 1470 are charged fermions ( $e, u, d, \mu, s, \dots$ ),  $G_F$  is the Fermi constant, and  $\epsilon$  are dimensionless couplings.<sup>6</sup> When  
 1471  $f$  is a first-generation fermion, the NSI contribute to neutrino detection and production at order  $\epsilon^2$  (ignoring  
 1472 potential interference effects between the standard model and the NSI). On the other hand, the NSI also  
 1473 contribute to the forward-scattering amplitude for neutrinos propagating in matter, modifying the neutrino  
 1474 dispersion relation and hence its oscillation length and mixing parameters. These modified matter effects are  
 1475 of order  $\epsilon^1$  and potentially more important than the NSI effects at production or detection. Furthermore, for  
 1476  $\alpha \neq \beta$ , the NSI-related matter effects lead to  $P_{\alpha\beta} \neq \delta_{\alpha\beta}$  in the very short baseline limit ( $L \rightarrow 0$ ), which are  
 1477 not present in the standard model case. More information – including relations to charged-lepton processes  
 1478 – current bounds, and prospects are discussed in detail in, for example, [230, 231], and references therein.

<sup>6</sup>  $\epsilon \sim 1$  ( $\ll 1$ ) implies that the new physics effects are on the order of (much weaker than) those of the weak interactions.

### 1479 1.9.3 Neutrino Magnetic Moment

1480 In the minimally-extended standard model, the neutrino magnetic moment (NMM) is expected to be very  
 1481 small ( $\mu_\nu \sim 10^{-19} - 10^{-20} \mu_B$ ) [232]. This makes the NMM a great place to look for new physics. The  
 1482 current best terrestrial limit of  $\mu_\nu < 3.2 \times 10^{-11} \mu_B$  at 90% CL comes from the GEMMA experiment at  
 1483 the Kalinin Nuclear Power Plant in Russia [233]. Many models for new physics allow for a NMM just below  
 1484 the current limit. The NMM can be related to the Dirac neutrino mass scale by naturalness arguments such  
 1485 that the mass scale is proportional to the product of  $\mu_\nu$  and the energy scale of new physics, which implies  
 1486 that  $|\mu_\nu| \leq 10^{-14} \mu_B$  for Dirac neutrinos [234]. NMM for Majorana neutrinos suffer from no such constraint.  
 1487 Therefore a discovery of NMM of as much as a few orders of magnitude below the current limit would imply  
 1488 that neutrinos are Majorana particles.

1489 Laboratory searches for NMM are based on neutrino-electron elastic scattering, in the scattering rate is  
 1490 studied as a function of electron recoil energy ( $T$ ). Below the maximum recoil energy, the weak differential  
 1491 cross section ( $d\sigma/dT$ ) is essentially flat, while for the electromagnetic cross section is inversely proportional  
 1492 to  $T$  [235]. The reactor experiments, which are responsible for the best terrestrial limits, are unable to detect  
 1493 the elastic scattering rate over background, but can nevertheless set limits based on the non-observation of  
 1494 an increasing rate at low  $T$ . The reactor experiments are clearly limited by the background environment  
 1495 present at the surface and by constraints on detector size imposed by the limited space close to a reactor  
 1496 and the need for massive shielding. On the other hand, experiments based on radioactive neutrinos sources,  
 1497 such as the  $^{51}\text{Cr}$  source discussed in the context of sterile searches, do not suffer from these limitations.  
 1498 Sources can be paired with proposed or existing detectors in deep underground laboratories with cavities  
 1499 large enough for kton-scale detectors and their gamma-ray shielding. In particular, dark-matter detectors,  
 1500 such as LUX [236] and CoGeNT [237], which are designed to be sensitive to nuclear recoils with electron  
 1501 equivalent energies of a few keV, would be excellent for such NMM searches. Additionally, it may be possible  
 1502 to use a single  $^{51}\text{Cr}$  source simultaneously for sterile neutrino and NMM searches.

1503 Astrophysical processes also provide very stringent bounds to neutrino electromagnetic properties [238].  
 1504 Estimates of neutrino magnetic moment bounds from the cooling of red giant stars, while somewhat de-  
 1505 pendent on astrophysical uncertainties, are one order of magnitude more stringent than the best laboratory  
 1506 bounds described above. Very recently, studies of the effects of Majorana neutrino transition magnetic  
 1507 moments in the oscillation of supernova neutrinos reveal that moments as small as  $10^{-24} \mu_B$  may leave  
 1508 a potentially observable imprint on the energy spectrum of neutrinos and antineutrinos from supernovae  
 1509 [239],[240]. Supernova neutrino explosions may prove to be the only phenomenon sensitive, in principle, to  
 1510 neutrino magnetic moments induced by standard model interactions, as long as the neutrinos are Majorana  
 1511 fermions.

## 1.10 Neutrinos in Cosmology and Astrophysics

Neutrinos come from astrophysical sources as close as the Earth and Sun, to as far away as distant galaxies, and even remnants from the Big Bang. They range in kinetic energy from less than one meV to greater than one PeV, and can be used to study properties of the astrophysical sources they come from, the nature of neutrinos themselves, and cosmology.

### 1.10.1 Ultra-low-energy neutrinos

The Concordance Cosmological Model predicts the existence of a relic neutrino background, currently somewhat colder than the cosmic microwave background,  $T_\nu = 1.95$  K. While relic neutrinos have never been directly observed, their presence is corroborated by several cosmological observables that are sensitive to the amount of radiation in the universe at different epochs. For example, precision measurements of the cosmic microwave background, and measurements of the relic abundances of light elements, independently require relativistic degrees of freedom other than photons, that are compatible with the three known neutrino species of the Standard Model of particle physics [241, 242]. Interestingly, a number of recent measurements – although well consistent with the Standard Model – seem to slightly favor a larger amount of radiation, compatible with four light neutrinos. This suggests a connection with the fact that a number of anomalies at neutrino experiments also favor the existence of a fourth “sterile” light neutrino (see Sec. 1.9). While any conclusion is premature, the question of a possible excess of cosmic radiation will be clarified by future, more precise, measurements of this quantity.

The cosmological relic neutrinos constitute a component of the dark matter, and their properties determine the way they contribute, with the rest of the dark matter, to the formation of large scale structures such as galactic halos. In particular, their mass has a strong impact on structure formation. This is because, being so light, neutrinos are relativistic at the time of decoupling and their presence dampens the formation of structure at small distance scales. The heavier the neutrinos, the more they influence structure formation, and the less structure is expected at small scales. Data are consistent with 100% cold dark matter and therefore give an upper bound on the total mass of the three neutrino species:  $\sum m_i < 0.7$  eV, approximately (see e.g., [242]). This bound should be combined with the lower limit from oscillation experiments:  $\sum m_i > 0.05$  eV (Sec. 1.5), which sets the level of precision that next-generation cosmological probes must have to observe effects of the relic neutrino masses. At this time, prospects are encouraging for answering this question.

Deviations from the Concordance Cosmological Model or new physics beyond the Standard Model of fundamental particles can dramatically modify the relationship between cosmological observables and neutrino properties. The extraction of neutrino properties from cosmological observables is, in some sense, complementary to that from terrestrial experiments. By comparing the results from these two classes of experimental efforts, we can not only determine properties of the massive neutrinos, including exotic ones, but also hope to test and, perhaps, move beyond the Concordance Cosmological Model.

The “holy grail” of neutrino astrophysics/cosmology is the direct detection of the relic neutrino background. This is extremely cold ( $1.95$  K =  $1.7 \times 10^{-5}$  eV) and today, at least two of the neutrino species are nonrelativistic. Several ideas have been pursued, and a clear path towards successfully measuring relic neutrinos has yet to emerge. Recently, the idea, first discussed in [243], of detecting relic neutrinos through threshold-less inverse-beta decay – e.g.,  $\nu_e + {}^3\text{H} \rightarrow {}^3\text{He} + e^-$  – has received some attention [244]. In a nutshell, the  $\beta$ -rays produced by the relic neutrino capture have energies above the end point of the  $\beta$ -rays produced by the ordinary nuclear decay. The expected number of interactions turns out to be accessible for intense

1553 enough nuclear samples, coupled with technology for very high resolution energy measurements. Specific  
 1554 experimental setups have been proposed recently (e.g. PTOLEMY [142], also see Sec. 1.7.2).

## 1555 1.10.2 Low-energy neutrinos

1556 Sources of low energy, MeV range, astrophysical neutrinos include the Earth, the Sun, and core-collapse  
 1557 supernovae. Since neutrinos only interact weakly they are unique messengers from these sources allowing  
 1558 us to probe deep into the astrophysical body. The following three distinct detector types proposed in the  
 1559 near future would be sensitive to low-energy neutrino physics: liquid scintillator detectors, water Cherenkov  
 1560 detectors, and liquid argon time projection chambers. Each detector type has particular advantages. Espe-  
 1561 cially in the case of supernova neutrinos, a combination of all types would allow for a better determination  
 1562 of all the potential science. Many of these low-energy signals are sensitive to backgrounds. One background  
 1563 that is poorly understood is muon-induced neutrons. A dedicated program to measure neutron production  
 1564 and transportation within various materials would have a large impact on multiple neutrino and dark-matter  
 1565 experiments both currently running and proposed [245].

### 1566 1.10.2.1 Physics and Astrophysics with Low-Energy Neutrinos

1567 **Solar neutrinos** Despite the tremendous success of previous solar-neutrino experiments there are still  
 1568 many unanswered questions, *e.g.* such as what is the total luminosity in neutrinos [31]? what is the  
 1569 metallicity of the Sun’s core [246]? The answers to these questions could change our understanding of the  
 1570 formation of the Solar System and the evolution of the Sun. Precise measurements of *pep* or *pp* neutrinos are  
 1571 required to answer the first question, and precise measurements of CNO neutrinos could answer the second  
 1572 question. Solar neutrinos, however, are also ideal probes for studying neutrino oscillation properties. The  
 1573 importance of previous solar neutrino experiments for understanding neutrino properties has been described  
 1574 in Sec. 1.5. New experiments, particularly at the energy of the *pep* neutrinos, would be very sensitive  
 1575 to nonstandard physics. An observation of a day-versus-night difference in the solar neutrino rate would  
 1576 conclusively demonstrate the so-called MSW effect [29, 32].

1577 **Geoneutrinos** Closer to home, the Earth is also a potent source of low-energy antineutrinos produced  
 1578 in the decay of uranium, thorium and potassium. Precise measurements of the flux of these neutrinos  
 1579 would allow for the determination of the amount of heat-producing elements in the earth (see, for example,  
 1580 [247]), which is currently only estimated through indirect means. Knowing the amount of heat-producing  
 1581 elements is important for our understanding of convection within the earth, which is ultimately responsible  
 1582 for earthquakes and volcanoes. The most recent measurements from KamLAND [248] and Borexino [249]  
 1583 are reaching the precision where they can start to constrain earth models. However, more detectors would  
 1584 be required as these detectors are not sensitive to the neutrino direction and are therefore sensitive to local  
 1585 variations. Ultimately we are interested in knowing the amount of heat producing elements in the earth’s  
 1586 mantle, and hence a detector located on the ocean floor away from neutrinos produced in continental crust  
 1587 would be ideal.

1588 **Supernova neutrinos** Supernovae are thought to play a key role in the history of the universe and in  
 1589 shaping our world. For example, modern simulations of galaxy formation cannot reproduce the structure of  
 1590 the galactic disk without taking the supernova feedback into account. Shock waves from ancient supernovae  
 1591 triggered further rounds of star formation and dispersed heavy elements, enabling the formation of stars

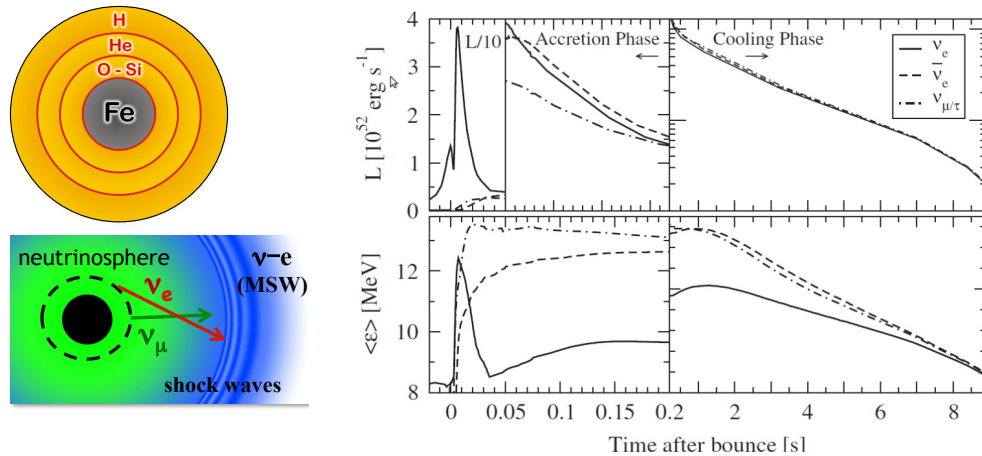


**Figure 1-22.** Supernova explosions create an extreme environment with rich physics including matter-enhanced oscillations, collective neutrino effects, and shock phenomena (left). Neutrino fluxes from supernovae encode imprints of the explosion (right). High-statistics measurements of the time distribution as well as the energy spectrum of supernova neutrino fluxes may allow the determination of the mass hierarchy. A variety of detection channels with different thresholds and sensitivities will be required for identifying the oscillation effects and distinguishing supernova models and astrophysical effects. The effect of the mass hierarchy on the diffuse supernova neutrino background appears to be too small to be distinguishable from astrophysical effects. Figures from [261, 262].

1592 like our Sun. Approximately 99% of the energy released in the explosion of a core-collapse supernova is  
 1593 emitted in the form of neutrinos. The mechanism for supernova explosion is still not understood. Supernova  
 1594 neutrinos record the information about the physical processes in the center of the explosion during the first  
 1595 several seconds, as the collapse happens. Extracting the neutrino luminosities, energy spectra, and cooling  
 1596 timescale would also allow us to study the equation of state of the nuclear/quark matter in the extreme  
 1597 conditions at the core of the collapse. Supernovae provide an incredibly rich source for the understanding of  
 1598 neutrino interactions and oscillations. As neutrinos stream out of the collapse core, their number densities  
 1599 are so large that their flavor states become coupled due to the mutual coherent scattering. This “self-  
 1600 MSW” phenomenon results in non-linear, many-body flavor evolution and has been under active exploration  
 1601 for the last five years, as supercomputers caught up with the physics demands of the problem (see, for  
 1602 example [250, 251, 252, 253, 254, 255, 256, 257, 258].) While the full picture is yet to be established, it  
 1603 is already clear that the spectra of neutrinos reaching Earth will have spectacular nonthermal features.  
 1604 Neutrino flavor evolution is also affected by the moving front shock and by stochastic density fluctuations  
 1605 behind it, which may also imprint unique signatures on the signal. All of these features will give new large  
 1606 detectors a chance to observe neutrino oscillations in qualitatively new regimes, inaccessible on Earth, and  
 1607 will very likely yield information on the neutrino mass hierarchy (see Sec. 1.5.1.1). Last but not least,  
 1608 the future data will allow us to place significant constraints on many extensions of particle physics beyond  
 1609 the Standard Model. This includes scenarios with weakly interacting particles, such as axions, Majorons,  
 1610 Kaluza-Klein gravitons, and others (see, for example [259, 260]). These new particles could be produced in  
 1611 the extreme conditions in the core of the star and could modify how it evolves and cools.

1612 Compared to the 1987A event, when only two dozen neutrinos were observed, future detectors may register  
 1613 tens – or even hundreds – of thousands of neutrino interactions from a core-collapse supernova. The burst  
 1614 will consist of neutrinos of all flavors with energies in the few tens of MeV range [263]. Because of their weak  
 1615 interactions, the neutrinos are able to escape on a timescale of a few tens of seconds after core collapse (the

1616 promptness enabling a supernova early warning for astronomers). An initial sharp “neutronization burst” of  
 1617  $\nu_e$  (representing about 1% of the total signal) is expected at the outset, from  $p + e^- \rightarrow n + \nu_e$ . Subsequent  
 1618 neutrino flux comes from NC  $\nu\bar{\nu}$  pair production. Electron neutrinos have the most interactions with the  
 1619 proto-neutron star core;  $\bar{\nu}_e$  have fewer, because neutrons dominate in the core;  $\nu_\mu$  and  $\nu_\tau$  have yet fewer,  
 1620 since NC interactions dominate for these. The fewer the interactions, the deeper inside the proto-neutron  
 1621 star the neutrinos decouple and the deeper, the hotter. So one expects generally a flavor-energy hierarchy,  
 1622  $\langle E_{\nu_{\mu,\tau}} \rangle > \langle E_{\bar{\nu}_e} \rangle > \langle E_{\nu_e} \rangle$ . From the point of view of maximizing physics harvest from a burst observation,  
 1623 flavor sensitivity – not only interaction rate but the ability to tag different interaction channels– is critical.

1624 While a single supernova in our galaxy could be expected to produce a large signal in a next-generation  
 1625 neutrino detector, such events are relatively rare (1-3 per century). However, it could also be possible to  
 1626 measure the flux of neutrinos from all the supernovae in cosmic history. The flux of these “diffuse supernova  
 1627 neutrino background” (DSNB) depends on the historical rate of core collapse, average neutrino production,  
 1628 cosmological redshift effects and neutrino oscillation effects [264, 265].

### 1629 1.10.2.2 Low-energy neutrino detectors

1630 **Liquid scintillator detectors** Depending on the depth, radiogenic purity, and location, large liquid  
 1631 scintillator detectors could be sensitive to geoneutrinos;  $pep$ ,  $pp$ , CNO,  $^8\text{B}$  solar neutrinos; and supernova  
 1632 neutrinos. The majority of the liquid scintillator experiments consist of large scintillator volumes surrounded  
 1633 by light detectors. The Borexino [34] ( $\sim 300$  tons) and KamLAND [266] ( $\sim 1,000$  tons) experiments continue  
 1634 to operate. The SNO+ experiment [35] ( $\sim 900$  tons) is currently under construction at SNOLAB, in Sudbury,  
 1635 Canada, and the Daya Bay II experiment ( $\sim 20,000$  tons) [40] is currently approved in China. The Hanohano  
 1636 experiment [267] ( $\sim 20,000$  tons) to be located on the ocean floor, and the LENA experiment [95] ( $\sim 50,000$   
 1637 tons) to be located in Europe have been proposed.

1638 The Borexino Collaboration recently announced the first positive measurement of  $pep$  neutrinos [268], along  
 1639 with a nontrivial upper bound on neutrinos from the CNO cycle, which are yet to be observed. Because of  
 1640 its greater depth, the SNO+ experiment could make a precise measurement of the  $pep$  neutrinos [35]. Unlike  
 1641 the other experiments, the LENS experiment [269] currently being planned consists of a segmented detector  
 1642 doped with In, which would allow precise measurement of the entire solar neutrino energy spectrum.

1643 Geoneutrinos were first observed in liquid scintillator detectors [270, 271] and all planned scintillator ex-  
 1644 periments would be sensitive to geoneutrinos, although the location of the Daya Bay II experiment next to  
 1645 nuclear power plants would make such a measurement very difficult. The Hanohano experiment located on  
 1646 the ocean floor would be the ideal geoneutrino experiment.

1647 All of the scintillator detectors would be sensitive to supernova neutrinos, primarily  $\bar{\nu}_e$  through neutron  
 1648 inverse beta decay, but also  $\nu_x$  neutrinos through proton scattering provided their thresholds are low  
 1649 enough [272]. The Hanohano and LENA detectors would also allow a measurement of the DSNB.

1650 **Water Cherenkov detectors** Depending on the depth and radiogenic purity, large water-Cherenkov  
 1651 detectors could be sensitive to  $^8\text{B}$  solar neutrinos and supernova neutrinos. The Super-K [273] ( $\sim 50,000$   
 1652 tons, still operating) and SNO [33] experiments ( $\sim 1,000$  tons, completed operation) have measured  $^8\text{B}$  solar  
 1653 neutrinos flux to better than 5% and measured neutrino oscillations with a precision of better than 5%. A  
 1654 measurement of the day versus night asymmetry would require increased statistics. The proposed Hyper-K  
 1655 detector [274] ( $\sim 990,000$  tons) would allow for a measurement of the day versus night asymmetry with a  
 1656 significance better than  $4\sigma$ .

1657 The tremendous size of the Hyper-K detector would result in  $\sim 250,000$  interactions from a core collapse  
 1658 supernova at the galactic center, and  $\sim 25$  interactions from a core collapse supernova at Andromeda. The  
 1659 large number of events in a galactic supernova would allow for very sensitive study of the time evolution of  
 1660 the neutrino signal. Although the IceCube detector could not detect individual events from a core collapse  
 1661 supernova, the large volume of ice visible the photomultiplier tubes would result in a detectable change in  
 1662 the photomultiplier hit rates, allowing for a study of the time evolution of a supernova [275].

1663 The addition of Gd to the Super-K [275] or Hyper-K detectors would allow for the study of DSNB within  
 1664 the range of most predictions for the total flux.

1665 **Liquid argon time projection chambers** A liquid argon time projection chamber located underground  
 1666 could provide invaluable information about a galactic core-collapse supernova. Unlike other detectors, which  
 1667 are primarily sensitive to  $\bar{\nu}_e$ , the principle signal would be due only to electron neutrino interactions, for which  
 1668 unique physics and astrophysics signatures are expected [276, 277]. For a supernova at 10 kpc approximately  
 1669 1000 events would be expected per 10 kton of liquid argon [278]. It will be critical to site LBNE underground  
 1670 in order to take advantage of the exciting and unique physics a core-collapse supernova will bring.

**Table 1-6.** Summary of low-energy astrophysics detectors. \*\*indicates significant potential, and \* indicates some potential but may depend on configuration.

Detector Type	Experiment	Location	Size (kton)	Status	Solar	Geo	Supernova
Liquid scintillator	Borexino	Italy	0.3	Operating	**	**	*
Liquid scintillator	KamLAND	Japan	1.0	Operating	**	**	*
Liquid scintillator	SNO+	Canada	1.0	Construction	**	**	*
Liquid scintillator	RENO-50	South Korea	10	Design/R&D	*	*	**
Liquid scintillator	JUNO (DB II)	China	20	Design/R&D	*	*	**
Liquid scintillator	Hanohano	TBD (USA)	20	Design/R&D	*	**	**
Liquid scintillator	LENA	TBD (Europe)	50	Design/R&D	*	**	**
Liquid scintillator	LENS	USA	0.12	Design/R&D	**		*
Water Cherenkov	Super-K	Japan	50	Operating	**		**
Water Cherenkov	IceCube	South Pole	2000	Operating			**
Water Cherenkov	Hyper-K	Japan	990	Design/R&D	**		**
Liquid argon	LBNE	USA	35	Design/R&D	*		**

### 1671 1.10.3 Neutrinos of GeV to PeV Energies

1672 One of the most tantalizing questions in astronomy and astrophysics, namely the origin and the evolution of  
 1673 the cosmic accelerators that produce the observed spectrum of cosmic rays, which extends to astonishingly  
 1674 high energies, may be best addressed through the observation of neutrinos. Because neutrinos only interact  
 1675 via the weak force, neutrinos travel from their source undeflected by magnetic fields and unimpeded by  
 1676 interactions with the cosmic microwave background, unlike photons and charged particles. Due to the low  
 1677 fluxes expected, the construction of high energy neutrino telescopes requires the instrumentation of large

1678 natural reservoirs, a concept demonstrated by AMANDA, Baikal and ANTARES. With the completion of  
1679 the IceCube Neutrino Telescope [279] in the South Polar icecap in 2010, the era of kilometer scale neutrino  
1680 telescopes has dawned, and plans for a complementary telescope in the Mediterranean are under develop-  
1681 ment. Already, IceCube has demonstrated astrophysical sensitivity by placing severe constraints on favored  
1682 mechanisms for gamma-ray bursts [280], and cascade events exceeding 1 PeV have been observed [281], which  
1683 may be a first glimpse of either a new source, or new physics.

1684 As with previous generations of neutrino telescopes, these instruments are expected to provide insight into the  
1685 nature of the messengers themselves. The background for the astrophysical fluxes sought include atmospheric  
1686 neutrinos, which are collected by IceCube at a rate of about 100,000 per year in the 0.1 to 100 TeV range.  
1687 Atmospheric neutrinos provide a probe of neutrino physics and interactions at energies that have been  
1688 previously unexplored. At TeV energies, the sensitivity of IceCube data to sterile neutrinos in the eV mass  
1689 range potentially exceeds that of any other experiment and is only limited by systematic errors. With the  
1690 addition of IceCube's low-energy infill array, Deep Core [282], which extended its energy sensitivity down  
1691 to 10 GeV, conventional neutrino oscillations have been observed at the 1 sigma level, and it is hoped  
1692 that such instruments could provide competitive precision measurements of neutrino oscillation parameters.  
1693 The copious atmospheric neutrino flux may someday also provide a glimpse into our Earth via neutrino  
1694 radiography.

1695 These instruments may also shed light on one of the most puzzling questions facing particle physics and  
1696 cosmology: the nature of the dark matter. Dark matter annihilations in the Sun and the galactic center  
1697 could be indirectly detected in neutrino telescopes, covering a region of parameter space that is inaccessible  
1698 at the LHC, and masses inaccessible to direct detection experiments. Neutrino telescopes have also been  
1699 active in the search for other exotica, such as magnetic monopoles.

#### 1700 1.10.4 Neutrinos at Energies Over 1 PeV

1701 At ultra high energies, neutrinos could be detected in dense, radio frequency (RF) transparent media via the  
1702 Askaryan effect [283, 284]. The abundant cold ice covering the geographic South Pole, with its exceptional  
1703 RF clarity, has been host to several pioneering efforts to develop this approach, including RICE [285] and  
1704 ANITA [286]. Currently, two discovery scale instruments are in the prototyping phase: the Askaryan Radio  
1705 Array (ARA) [287], which is envision to instrument a 100 square kilometer area near the South Pole with  
1706 200m deep antenna clusters, and ARIANNA [288], which would be installed on the surface of the Ross Ice  
1707 Shelf. Efforts are underway to characterize the ice in Greenland, to determine its suitability as a site for a  
1708 future cosmogenic neutrino telescope.

1709 The fact that cosmic rays have been observed at energies in excess of  $10^{20}$  eV makes the search for neutrinos  
1710 at these energies particularly tantalizing. These energies are above the threshold for pion photoproduction  
1711 on the cosmic microwave background, which would seem to guarantee a flux of ultra high energy neutrinos.  
1712 However, the neutrino flux expectations are sensitive to the composition of the ultra-high-energy (UHE)  
1713 cosmic rays, making the spectrum of UHE cosmic rays a sensitive probe of the heavy ion content. In  
1714 addition, if a sufficient sample of UHE neutrinos were amassed, it would be possible to measure the neutrino  
1715 cross section at high energies from the zenith angle spectrum.

## 1.11 Neutrinos and Society

The allure and relevance of neutrino science and technology extends well beyond the fundamental research community. The neutrino signal itself may be useful for monitoring reactors in the context of international nuclear nonproliferation, and for Earth tomography. The essential building blocks of neutrino science - detectors and accelerators - have important spin-off applications for medicine and in industry. Finally, ever since neutrinos were first postulated and discovered, their unusual, ghostlike properties and non-intuitive behavior have fascinated the general public. The success of our field depends in no small part on our ability to effectively convey both the mystery and utility of neutrino science to the public, Congress, policy-makers and funding agencies. Below we discuss the direct and spin-off applications, and the rich opportunities for outreach and education offered by fundamental and applied antineutrino science.

### 1.11.1 Applied Antineutrino Physics

Direct application of neutrinos to other domains falls into two categories. In geology, they may enable study of Earth's composition on largest scales, and in nonproliferation, they offer the prospect of improved monitoring or discovery of operating nuclear reactors. Since the signal in both cases arises from antineutrinos only, it is appropriate to refer to Applied Antineutrino Physics.

As described in Sec. 1.10, geological applications have been explored in numerous papers, and evidence for a geo-antineutrino signal has been presented by the KamLAND and Borexino collaborations.

Concerning nonproliferation, the main likely user of antineutrino-based reactor monitoring is the International Atomic Energy Agency (IAEA). IAEA is responsible for monitoring the international fuel cycle, to detect attempts to divert fissile materials and production technologies to nuclear weapons programs. The international monitoring regime administered by the IAEA is referred to as the Safeguards regime [289]. Antineutrino detectors may play a role in this regime, which focuses on timely detection of illicit removal of fissile material from known and declared reactors and other fuel cycle facilities. They may also be useful in future expanded regimes, such as the proposed Fissile Material Cutoff Treaty [290], which will seek to verify the non-existence of an undeclared fissile material production capability in a country or geographical region. In a recent report, the IAEA encouraged continued research into antineutrino-detection based applications for safeguards and other cooperative monitoring of nuclear reactors [291]. In addition, the US National Nuclear Security Administration has included a demonstration of remote reactor monitoring (1 km and beyond) as an element of its 2011 Strategic Plan [292].

Nonproliferation applications are enabled by three features of reactor antineutrinos. First, reactors emit a copious flux of  $\sim 0\text{--}10$  MeV electron antineutrinos resulting from beta decay of neutron-rich fission fragments. Second, the antineutrino inverse beta cross section is high enough to allow detectors of tractable (cubic meter) sizes to be deployed at tens-of-meter standoff from a reactor. (Much larger but still achievable sizes are required for remote monitoring, scaling roughly as the inverse square of distance, with a subdominant effect due to neutrino oscillations.) Third, the detected antineutrino flux and energy spectrum both correlate with the core-wide content of fission fragments, and through this correlation to the inventories of the main fissile isotopes that are used in weapons.

Concerning applications for existing or future reactor safeguards, cubic-meter-scale antineutrino detectors now make it possible to monitor the operational status, power levels, and fissile content of nuclear power reactors in near-real-time with stand-off distances of roughly 100 meters from the reactor core. This capability has been demonstrated at civil power reactors in Russia and the United States, using antineutrino detectors

1757 designed specifically for reactor monitoring and safeguards [293, 294]. This near-field monitoring capability  
1758 may be of use within the International Atomic Energy Agency’s (IAEA) Safeguards Regime, and other  
1759 cooperative monitoring regimes.

1760 With respect to future missions related to remote discovery or exclusion of reactors, current kiloton-scale  
1761 antineutrino detectors, exemplified by the KamLAND and Borexino liquid-scintillator detectors, can allow  
1762 monitoring, discovery or exclusion of small (few MegaWatt thermal, MWt) reactors at standoff distances up  
1763 to 10 kilometers. In principle, reactor discovery and exclusion is also possible at longer ranges. However, the  
1764 required detector masses are 10-100 times greater than the state of the art, and achieving these long range  
1765 detection goals would require significant research and development. Happily, many elements of the necessary  
1766 R & D program are already being pursued in the fundamental physics community, as we discuss below.

1767 Numerous articles, reviews, and conferences are devoted to the topic of reactor monitoring with antineutrinos.  
1768 A partial reading list, including links to a series of annual Applied Antineutrino Physics conferences held  
1769 since 2004 may be found at [295].

#### 1770 **1.11.1.1 Inverse Beta Decay detectors for IAEA Near-Field Safeguards Applications, and** 1771 **for Short Baseline Neutrino Oscillation Experiments.**

1772 Near-field (10–100 meters) antineutrino monitoring of nuclear reactors is a possible near-term addition  
1773 to the existing IAEA Safeguards regime. Current IAEA reactor safeguards protocols rely heavily on  
1774 operator declarations of reactor power and fissile content, and only sparingly on quantitative measurements.  
1775 Antineutrino monitoring offers a continuous, near-real-time, and non-intrusive quantitative record of power  
1776 production and plutonium generation of reactors. This “wireless window” into reactor cores provides a  
1777 reliable, independently measured benchmark for the entire reactor fuel cycle, and serves as a means to detect  
1778 a range of suspect activities, such as repeated short shutdowns that facilitate removal of plutonium-bearing  
1779 fuel rods.

1780 As discussed in section 1.9, and in numerous Snowmass white papers [161], short-baseline neutrino oscillation  
1781 experiments are being planned by US and overseas groups. These experiments seek to deploy 1–10 ton scale  
1782 antineutrino detectors from 5–15 meters from a nuclear reactor core. The purpose of the experiments is  
1783 to search for a possible sterile neutrino signal, and to measure the reactor antineutrino energy spectrum  
1784 as precisely as possible. The physics goals greatly constrain the experimental configuration. The need for  
1785 close proximity to the reactor requires that the detector overburden is necessarily minimal, at most  $\sim 45$   
1786 meters water equivalent (mwe). The physical dimension of the core must be as small as possible, to avoid  
1787 smearing the oscillation-related spectral distortions with multiple baselines arising from different locations in  
1788 the core. To be competitive with experiments using strong single-element radioactive sources, this requires  
1789 that a relatively low power ( $\sim 20$ -50 MWt) research reactor be used for the experiment, greatly constraining  
1790 the number of possible sites.

1791 The above requirements impose stringent constraints on detector design. The minimal overburden and  
1792 proximity to the reactor both increase backgrounds compared to previous oscillation searches, and demand  
1793 background rejection capabilities beyond the current state of the art. The detector size is also constrained to  
1794 be no more than a few tons, owing to the tight space constraints in galleries near reactor cores. In spite of the  
1795 higher backgrounds and smaller size, the detector efficiency and energy resolution should remain comparable  
1796 to those achieved in previous oscillation experiments, such as RENO [296], Double Chooz [297], and Daya  
1797 Bay [298].

1798 The technology goals for reactor short-baseline experiments and for nonproliferation applications are similar  
1799 in many respects. In both cases, R & D is required to improve background rejection at shallow depths, while

1800 maintaining high efficiency and good energy resolution. To improve specificity for the two-step inverse beta  
1801 antineutrino signature, segmented designs [299] are being contemplated for both cooperative monitoring and  
1802 short-baseline detectors, as well as the use of Li-doped plastic or liquid scintillator technologies [300].

1803 A key difference between the fundamental and applied technology needs is that the detectors for nonprolif-  
1804 eration must also be simple to operate, and may have additional cost constraints compared to the single use  
1805 detectors needed for the short baseline physics experiments.

#### 1806 1.11.1.2 CENNS detection for nonproliferation and fundamental science

1807 Numerous physics motivations for the measurement of coherent elastic neutrino-nucleus scattering (CENNS)  
1808 are described in Sec. 1.8.3.2. For monitoring applications, the process holds considerable interest, since the  
1809 100-1000 fold increase in cross section compared with the next most competitive antineutrino interaction  
1810 may enable a ten-fold or more reduction in detector volume, even with shielding accounted for. This could  
1811 simplify and expand the prospects for deployment of these detectors in a range of cooperative monitoring  
1812 contexts.

1813 Moreover, it is important to recognize that CENNS closely resembles the interaction with nuclei of a leading  
1814 dark matter candidate, the Weakly Interacting Massive Particle or WIMP. Both are coherent processes which  
1815 may induce keV scale recoils in a range of detection media. The search for direct interactions of WIMPS  
1816 in detectors on Earth is the subject of a multiple collaborative efforts in the United States and worldwide.  
1817 Due to the similarity of the event signature, advances in coherent scatter detection technology will perforce  
1818 improve the prospects for dark matter detection. Indeed, at the lowest recoil energies, neutrino-nucleus  
1819 recoils is likely to prove to be a limiting background for WIMP interactions.

1820 For CENNS detection, both phonon and ionization channel approaches are being pursued. Detector thresh-  
1821 olds must be made sufficiently low, while maintaining effective background suppression, so as to allow good  
1822 collection statistics above background in tractably sized detectors. In the last few years, several groups  
1823 worldwide have made significant progress in reducing thresholds in noble liquid [301, 302], and germanium  
1824 detectors [303], with the intent of improving both coherent scatter and dark matter detectors. White papers  
1825 focused on discovery of CENNS [304], [305] have been submitted as part of the Snowmass process. For more  
1826 information on the relevant fundamental and applied science, we refer the reader to a 2012 workshop devoted  
1827 to these topics [169].

#### 1828 1.11.1.3 Long-baseline neutrino experiments, supernovae and proton decay, and remote re- 1829 actor monitoring

1830 One-hundred-kiloton to megaton-scale liquid scintillator and water detectors have been proposed as far  
1831 detectors for long-baseline accelerator-based neutrino oscillation and CP-violation experiments [81, 306].  
1832 If they can be made sensitive to few-MeV antineutrinos, such giant detectors offer an even more diverse  
1833 physics program, including sensitivity to extra-galactic supernovae, measurement of the diffuse supernova  
1834 background (see Sec. 1.10), proton decay, and in the case of liquid scintillator detectors, sensitivity to reactor  
1835 neutrino oscillations at several tens of kilometer standoff.

1836 The same types of detector could enable discovery, exclusion or monitoring of nuclear reactors at standoff  
1837 distances from one to as many as several hundred kilometers. With sufficient suppression of backgrounds, re-  
1838 mote detectors (25-500 km standoff) on the 50-kiloton to one-megaton scale would provide a 25% statistically  
1839 accurate measurement of the power of a 10-MWt reactor in several months to a year [307].

1840 Water Cherenkov detectors are one promising approach to achieving detector masses on the scale required  
1841 to meet the above physics and nonproliferation goals. While the water Cherenkov approach is currently  
1842 disfavored in the United States' LBNE planning process, it nonetheless retains considerable interest for the  
1843 global community, in particular in Japan [81].

1844 To allow sensitivity to low energy antineutrinos through the inverse beta decay process, the water would be  
1845 doped with gadolinium, so that final-state neutron can be detected by the  $\sim 4$  MeV of measurable Cherenkov  
1846 energy deposited in the gamma-ray cascade that follows capture of neutrons on gadolinium. Sensitivity to  
1847 neutrons has already been demonstrated via this method in ton-scale detectors [308], and using a kilogram  
1848 scale sealed Gd-water test cell inserted into the center of the large Super-Kamiokande water Cherenkov  
1849 detector [309]. A logical next step is to show direct sensitivity to reactor antineutrinos in much larger  
1850 detectors uniformly doped with gadolinium. A kiloton-scale demonstration of this detector type is now  
1851 being proposed by the WATCHMAN collaboration in the United States [310].

1852 Several-hundred-kilometer standoff detection of antineutrinos from high power (GWt) reactors is already  
1853 possible using liquid scintillator technology. This has been clearly established by the KamLAND detec-  
1854 tor [311], sensitive to antineutrinos from civil power reactors throughout Japan, and with a few-percent  
1855 flux contribution from reactors in South Korea, 400 kilometers away. Despite this remarkable achievement,  
1856 significant additional work is needed to make the detectors sensitive to the few hundred-fold lower power  
1857 reactors of greatest interest for nonproliferation. Scaling of pure liquid scintillator designs such as KamLAND  
1858 or Borexino is another approach to megaton class detectors. This approach is exemplified by the LENA  
1859 collaboration in Europe [306, 95].

#### 1860 1.11.1.4 Application of Neutrino-related Technologies

1861 A high degree of synergy is evident in technology developments related to neutrino physics experiments. The  
1862 size and scale of the detectors and instrumentation needed, as well as the novel accelerator specifications,  
1863 draw on the creativity of many communities to address and solve the challenging problems encountered.  
1864 The paradigm of close collaboration between Laboratory, University and Industry has been fruitful, solving  
1865 immediate needs of the neutrino community, and providing spinoff applications in quite different fields with  
1866 broad societal impact. Examples are provided in the following sections.

1867 **Detectors:** Neutrino/antineutrino detection has motivated significant work on detection technology, the  
1868 benefits of which extend well beyond the physics community. Examples include plastic and liquid scintillator  
1869 doped with neutron-capture agents, high-flashpoint scintillators with reduced toxic hazards compared to  
1870 previous generators of scintillator, and low-cost flat-panel photomultiplier tubes. Doped organic plastic  
1871 and liquid scintillator detectors are now being pursued in the United States [312], as a means to improve  
1872 sensitivity to the reactor antineutrino signal. In a similar way, companies such as Bicron Technologies and  
1873 Eljen Technologies have devoted resources to reducing the biohazards and improving the optical clarity of  
1874 their scintillation cocktails, in order to facilitate neutrino detection. These improvements clearly benefit  
1875 other customers, such as the medical and pharmaceutical communities, which use scintillator detectors for  
1876 radio-assay in nuclear medicine applications. The overall product lines of these companies have benefited con-  
1877 siderably from research that has focused on making better neutrino detectors. Another area of research with  
1878 important spinoff potential is the development of low cost, high efficiency photomultiplier tubes. Cutting-  
1879 edge research that focused on low-cost PMTs is exemplified by the Large Area Pico-second Photo-Detectors  
1880 project [313, 314]. Beyond enabling lower-cost neutrino detectors at every scale, such detectors would lower  
1881 costs and improve performance of medical imaging devices such as Positron Emission Tomography systems,  
1882 for which the photo-detector element is often a dominant cost and critical component. Emerging nuclear

1883 security applications that demand PMT-based imaging, such as three-dimensional reconstruction of the  
1884 locations and inventories of fissile material in a reprocessing or enrichment plant, also great benefit from  
1885 lower-cost PMTs.

1886 **Accelerators:** A recent PCAST report states [315] “The science of neutrino production demands creative  
1887 new solutions for intense [accelerator-based] sources. These include high power synchrotrons such as the  
1888 Main Injector, high power high energy superconducting LINACS such as the Oak Ridge Spallation Neutron  
1889 Source and the future Project-X, powerful new ways of generating intense beams such as DAE $\delta$ ALUS,  
1890 and other ideas.” The spinoffs with broad technological impact from advanced accelerator development  
1891 are numerous and spectacular: advances in engineering with superconducting materials and magnets, high-  
1892 volume cryogenics, sophisticated control systems and power converters, one could go on and on. A very direct  
1893 connection with neutrinos, however, is provided by the DAE $\delta$ ALUS project. Based on a cascade of compact  
1894 cyclotrons capable of sending multi-megawatt beams onto neutrino-producing targets, this concept pushes  
1895 the performance of cyclotrons to new levels. Development of this technology, based on accelerating  $H_2^+$  ions, is  
1896 being pursued by a broad collaboration of US and foreign laboratories, universities and industry. Khrishnan  
1897 Suthanthiran, President of TeamBest, one of whose subsidiaries markets isotope-producing cyclotrons, states,  
1898 “[The] original motivation for the device is for it to become the injector for a very high intensity neutrino  
1899 source for pure science research (DAE $\delta$ ALUS). The same concepts you have described have an immediate  
1900 medical radioisotope application.” One of the test prototypes being developed with the assistance of Best  
1901 Cyclotron Systems Inc. is a 28-MeV cyclotron designed for  $H_2^+$  injection studies, but also suitable for  
1902 acceleration of  $He^{++}$ , and directly applicable to the production of  $^{211}At$ , a powerful therapeutic agent whose  
1903 “use for [targeted  $\alpha$  particle therapy] is constrained by its limited availability.” [316]. The development  
1904 of these compact, high-power and relatively inexpensive cyclotrons is expected to have a profound impact  
1905 on many fields, ranging from neutrino physics and isotope production to ADS applications such as driving  
1906 thorium reactors or burning nuclear waste [317].

## 1907 1.11.2 Education and Outreach

### 1908 1.11.2.1 Educating Physicists about Nonproliferation

1909 In order to reach out to the public effectively, physicists themselves should be made aware of the potential  
1910 utility of neutrinos for nuclear security. The natural overlap in signal and technology between reactor  
1911 monitoring for nonproliferation and reactor oscillation experiments already helps prepare physics students  
1912 and post-docs for work on nuclear security research. In a similar way, dark matter experiments provide  
1913 a useful education in nuclear security technology, inasmuch as the keV-MeV-scale interactions of possible  
1914 dark-matter candidates are strongly analogous to the interactions induced by the neutrons and gamma-rays  
1915 emitted by quiescent nuclear material. Detectors for these latter particles are the focus of a large scale  
1916 domestic and international effort within government laboratories, academia (mostly nuclear engineering  
1917 departments) and industry, and are used in a range of nuclear screening, nonproliferation and treaty  
1918 verification applications. As revealed by the growing field of applied antineutrino physics, awareness of  
1919 these connections has grown over the last ten years in the physics community. However, relatively few  
1920 physicists - including many actively engaged in applied research - have much if any formal education in the  
1921 structure of the global nonproliferation regime, or in the history of the atomic era that led to the current state  
1922 of affairs in nuclear security. This is especially unfortunate, since at least in the United States, this history  
1923 is closely intertwined with the development of the large scale accelerator and underground experiments that  
1924 employ many of these same physicists. In the last five years or so, a few physics departments, such as

1925 UC Davis, Virginia Tech, and others have worked to develop courses that introduce physicists to both the  
1926 relevant technology and policy of nonproliferation and nuclear security. Nuclear Engineering departments  
1927 have a closer connection to the nonproliferation regime, and many, such as MIT, UC Berkeley, Penn State,  
1928 Texas A & M, and others, have developed explicit course elements targeting the connection between nuclear  
1929 security and nuclear science. Indeed, many of these nuclear engineering departments have a strong research  
1930 presence in the relevant overlapping areas of neutrino (and dark matter) science.

### 1931 1.11.2.2 Educating the General Public about Neutrino Science

1932 An aware and enthusiastic general public is the best way to ensure support and funding for basic research.  
1933 Our work is supported by tax dollars, and the level of support depends in part on convincing both Congress  
1934 and the taxpayer that their money is being spent wisely. To this end, the challenge of the neutrino community  
1935 is to make the case that investments in our field are of benefit to the nation.

1936 Each one of us should accept our responsibility for conveying this message whenever possible. Opportunities  
1937 for this are more frequent than one would imagine: addressing local Rotarians, Kiwanis or other public  
1938 service groups (who seem always to be looking for speakers); discussions in local school science classes;  
1939 organizing field trips to labs or research centers, to give a few examples.

1940 Neutrino physics offers a wealth of fascinating and counter-intuitive concepts (e.g. oscillations, high fraction  
1941 of the Sun's energy emitted as neutrinos, and extremely low cross sections enabling neutrinos to easily  
1942 penetrate the Earth). (In regards to the faster-than-light controversy, an object lesson should be learned  
1943 of carefully managing potentially contentious information, and considering the consequences of its release  
1944 prior to a thorough vetting by independent experts, lest it damage the credibility of the field. While the  
1945 controversy did bring neutrinos into the limelight for a brief time, the adage of any publicity being good  
1946 publicity emphatically does not apply to our field. It is far preferable to accurately and conservatively report  
1947 and review results, especially such extraordinary claims.) In addition, our field sports some highly photogenic  
1948 experiments (e.g. IceCube, Borexino, Super-K). A suggestion could be made that a reservoir of material be  
1949 collected, updated and made available for persons to use in outreach talks and activities: lecture outlines,  
1950 lists of talking points, graphics, etc. CERN and FNAL provided an example of this type of collection in the  
1951 material they assembled in support of their international outreach effort for hosting public-outreach lectures  
1952 on anti-matter coordinated with the release of the Angels and Demons blockbuster film.

1953 The interesting practical applications of neutrinos described earlier for reactor monitoring and non-proliferation  
1954 treaty verification, as well as programs studying geoneutrinos in relation to understanding the heat dynamics  
1955 of the interior of the Earth, provide highly relevant and compelling topics to be communicated to the public.

1956 The importance of Education and Outreach is recognized in the establishment of a whole (Snowmass) "Fron-  
1957 tier" dedicated to this topic. Our community should embrace this effort, looking for ways of coordinating  
1958 and contributing to their activities for furtherance of our mutually compatible goals.

## References

- 1959 [1] K. Kodama et al. Observation of tau neutrino interactions. *Phys. Lett.*, B504:218–224, 2001.
- 1960 [2] F. Abe et al. Observation of top quark production in  $\bar{p}p$  collisions. *Phys. Rev. Lett.*, 74:2626–2631,  
1961 1995.
- 1962 [3] S. Abachi et al. Observation of the top quark. *Phys. Rev. Lett.*, 74:2632–2637, 1995.
- 1963 [4] B.T. Cleveland, T. Daily, R. Jr. Davis, J.R. Distel, K. Lande, et al. Measurement of the solar electron  
1964 neutrino flux with the Homestake chlorine detector. *Astrophys. J.*, 496:505–526, 1998.
- 1965 [5] W. Hampel et al. GALLEX solar neutrino observations: Results for GALLEX IV. *Phys. Lett.*,  
1966 B447:127–133, 1999.
- 1967 [6] Q.R. Ahmad et al. Direct evidence for neutrino flavor transformation from neutral current interactions  
1968 in the Sudbury Neutrino Observatory. *Phys. Rev. Lett.*, 89:011301, 2002.
- 1969 [7] J.N. Abdurashitov et al. Solar neutrino flux measurements by the Soviet-American Gallium Experiment  
1970 (SAGE) for half the 22 year solar cycle. *J. Exp. Theor. Phys.*, 95:181–193, 2002.
- 1971 [8] S. Fukuda et al. Solar B-8 and hep neutrino measurements from 1258 days of Super-Kamiokande data.  
1972 *Phys. Rev. Lett.*, 86:5651–5655, 2001.
- 1973 [9] S.N. Ahmed et al. Measurement of the total active B-8 solar neutrino flux at the Sudbury Neutrino  
1974 Observatory with enhanced neutral current sensitivity. *Phys. Rev. Lett.*, 92:181301, 2004.
- 1975 [10] Y. Fukuda et al. Evidence for oscillation of atmospheric neutrinos. *Phys. Rev. Lett.*, 81:1562–1567,  
1976 1998.
- 1977 [11] Y. Ashie et al. Evidence for an oscillatory signature in atmospheric neutrino oscillation. *Phys. Rev.*  
1978 *Lett.*, 93:101801, 2004.
- 1979 [12] K. Eguchi et al. First results from KamLAND: Evidence for reactor anti- neutrino disappearance.  
1980 *Phys. Rev. Lett.*, 90:021802, 2003.
- 1981 [13] T. Araki et al. Measurement of neutrino oscillation with KamLAND: Evidence of spectral distortion.  
1982 *Phys. Rev. Lett.*, 94:081801, 2005.
- 1983 [14] M.H. Ahn et al. Indications of neutrino oscillation in a 250 km long baseline experiment. *Phys. Rev.*  
1984 *Lett.*, 90:041801, 2003.
- 1985 [15] D.G. Michael et al. Observation of muon neutrino disappearance with the MINOS detectors and the  
1986 NuMI neutrino beam. *Phys. Rev. Lett.*, 97:191801, 2006.
- 1987 [16] Andre de Gouvea, Boris Kayser, and Rabindra N. Mohapatra. Manifest CP violation from Majorana  
1988 phases. *Phys.Rev.*, D67:053004, 2003.
- 1989 [17] A. de Gouvea. Neutrinos have mass: So what? *Mod. Phys. Lett.*, A19:2799–2813, 2004.
- 1990 [18] S. Weinberg. Baryon and Lepton Nonconserving Processes. *Phys. Rev. Lett.*, 43:1566–1570, 1979.
- 1991 [19] J.L. Hewett, H. Weerts, R. Brock, J.N. Butler, B.C.K. Casey, et al. Fundamental Physics at the  
1992 Intensity Frontier. 2012.
- 1993

- 1994 [20] R.N. Mohapatra, S. Antusch, K.S. Babu, G. Barenboim, M.C. Chen, et al. Theory of neutrinos: A  
1995 White paper. *Rept. Prog. Phys.*, 70:1757–1867, 2007.
- 1996 [21] C.H. Albright and M.C. Chen. Model Predictions for Neutrino Oscillation Parameters. *Phys. Rev.*,  
1997 D74:113006, 2006.
- 1998 [22] A. Cervera, A. Donini, M.B. Gavela, J.J. Gomez Cadenas, P. Hernandez, et al. Golden measurements  
1999 at a neutrino factory. *Nucl. Phys.*, B579:17–55, 2000.
- 2000 [23] J. Burguet-Castell, M.B. Gavela, J.J. Gomez-Cadenas, P. Hernandez, and O. Mena. On the  
2001 Measurement of leptonic CP violation. *Nucl. Phys.*, B608:301–318, 2001.
- 2002 [24] V. Barger, D. Marfatia, and K. Whisnant. Breaking eight fold degeneracies in neutrino CP violation,  
2003 mixing, and mass hierarchy. *Phys. Rev.*, D65:073023, 2002.
- 2004 [25] K. Abe et al. A Measurement of atmospheric neutrino flux consistent with tau neutrino appearance.  
2005 *Phys. Rev. Lett.*, 97:171801, 2006.
- 2006 [26] N. Agafonova et al. Observation of a first  $\nu_\tau$  candidate in the OPERA experiment in the CNGS beam.  
2007 *Phys. Lett.*, B691:138–145, 2010.
- 2008 [27] K. Abe et al. Indication of Electron Neutrino Appearance from an Accelerator-produced Off-axis Muon  
2009 Neutrino Beam. *Phys. Rev. Lett.*, 107:041801, 2011.
- 2010 [28] P. Adamson et al. Improved search for muon-neutrino to electron-neutrino oscillations in MINOS.  
2011 *Phys. Rev. Lett.*, 107, 2011.
- 2012 [29] L. Wolfenstein. Neutrino Oscillations in Matter. *Phys. Rev.*, D17:2369–2374, 1978.
- 2013 [30] J.A. Formaggio and G. P. Zeller. From eV to EeV: Neutrino Cross Sections Across Energy Scales.  
2014 2012. to be published in *Rev. Mod. Phys.*
- 2015 [31] J.N. Bahcall and C. Pena-Garay. Global analyses as a road map to solar neutrino fluxes and oscillation  
2016 parameters. *JHEP*, 0311:004, 2003.
- 2017 [32] S.P. Mikheev and A.Y. Smirnov. Resonance Amplification of Oscillations in Matter and Spectroscopy  
2018 of Solar Neutrinos. *Sov. J. Nucl. Phys.*, 42:913–917, 1985.
- 2019 [33] B. Aharmim et al. Combined Analysis of all Three Phases of Solar Neutrino Data from the Sudbury  
2020 Neutrino Observatory. 2011.
- 2021 [34] G. Alimonti et al. The Borexino detector at the Laboratori Nazionali del Gran Sasso. *Nucl. Instrum.*  
2022 *Meth.*, A600:568–593, 2009.
- 2023 [35] C. Kraus and S.J.M. Peeters. The rich neutrino programme of the SNO+ experiment. *Prog. Part.*  
2024 *Nucl. Phys.*, 64:273–277, 2010.
- 2025 [36] K. Anderson, J.C. Anjos, D. Ayres, J. Beacom, I. Bediaga, et al. White paper report on Using Nuclear  
2026 Reactors to Search for a value of  $\theta_{13}$ . 2004.
- 2027 [37] H. Minakata, H. Nunokawa, W.J.C. Teves, and R. Zukanovich Funchal. Reactor measurement of  
2028  $\theta(12)$ : Principles, accuracies and physics potentials. *Phys. Rev.*, D71:013005, 2005.
- 2029 [38] S.T. Petcov and T. Schwetz. Precision measurement of solar neutrino oscillation parameters by a  
2030 long-baseline reactor neutrino experiment in Europe. *Phys. Lett.*, B642:487–494, 2006.

- 2031 [39] P. Ghoshal and S.T. Petcov. Neutrino Mass Hierarchy Determination Using Reactor Antineutrinos.  
2032 *JHEP*, 1103:058, 2011.
- 2033 [40] S. Kettell et al. Measurement of neutrino mass hierarchy with reactor neutrinos. <http://if-neutrino.fnl.gov/whitepapers/johnson-reactor.pdf>, Mar 2013.
- 2034
- 2035 [41] J.M. Conrad and M.H. Shaevitz. Multiple Cyclotron Method to Search for CP Violation in the Neutrino  
2036 Sector. *Phys. Rev. Lett.*, 104:141802, 2010.
- 2037 [42] E. Fernandez-Martinez, G. Giordano, O. Mena, and I. Mocioiu. Atmospheric neutrinos in ice and  
2038 measurement of neutrino oscillation parameters. *Phys. Rev.*, D82:093011, 2010.
- 2039 [43] M.C. Gonzalez-Garcia, M. Maltoni, and J. Salvado. Testing matter effects in propagation of  
2040 atmospheric and long-baseline neutrinos. *JHEP*, 05:075, 2011.
- 2041 [44] T. K. Gaisser and M. Honda. Flux of atmospheric neutrinos. *Ann. Rev. Nucl. Part. Sci.*, 52:153–199,  
2042 2002.
- 2043 [45] M. C. Gonzalez-Garcia, M. Maltoni, and J. Rojo. Determination of the atmospheric neutrino fluxes  
2044 from atmospheric neutrino data. *JHEP*, 10:075, 2006.
- 2045 [46] R. Abbasi et al. Measurement of the atmospheric neutrino energy spectrum from 100 GeV to 400 TeV  
2046 with IceCube. *Phys. Rev.*, D83:012001, 2011.
- 2047 [47] S. Choubey et al. Interim Design Report for the International Design Study for a Neutrino Factory.  
2048 FERMILAB-DESIGN-2011-01.
- 2049 [48] P. Zucchelli. A novel concept for a anti- $\nu_e$  /  $\nu_e$  neutrino factory: The beta beam. *Phys. Lett.*,  
2050 B532:166–172, 2002.
- 2051 [49] A. Bernstein et al. Report on the Depth Requirements for a Massive Detector at Homestake. 2009.
- 2052 [50] R. Wendell et al. Atmospheric neutrino oscillation analysis with sub-leading effects in Super-  
2053 Kamiokande I, II, and III. *Phys.Rev.*, D81:092004, 2010.
- 2054 [51] K. Abe et al. Search for Differences in Oscillation Parameters for Atmospheric Neutrinos and  
2055 Antineutrinos at Super-Kamiokande. *Phys.Rev.Lett.*, 107:241801, 2011.
- 2056 [52] M.H. Ahn et al. Measurement of Neutrino Oscillation by the K2K Experiment. *Phys.Rev.*, D74:072003,  
2057 2006.
- 2058 [53] P. Adamson et al. An improved measurement of muon antineutrino disappearance in MINOS. 2012.
- 2059 [54] K. Abe et al. First Muon-Neutrino Disappearance Study with an Off-Axis Beam. *Phys.Rev.*,  
2060 D85:031103, 2012.
- 2061 [55] S. Abe et al. Precision Measurement of Neutrino Oscillation Parameters with KamLAND.  
2062 *Phys.Rev.Lett.*, 100:221803, 2008.
- 2063 [56] Y. Abe et al. Reactor electron antineutrino disappearance in the Double Chooz experiment. *Phys.Rev.*,  
2064 D86:052008, 2012.
- 2065 [57] J.K. Ahn et al. Observation of Reactor Electron Antineutrino Disappearance in the RENO Experiment.  
2066 *Phys.Rev.Lett.*, 108:191802, 2012.
- 2067 [58] F.P. An, J.Z. Bai, A.B. Balantekin, H.R. Band, D. Beavis, et al. Observation of electron-antineutrino  
2068 disappearance at Daya Bay. 2012. 5 figures.

- 2069 [59] G.L. Fogli, E. Lisi, A. Marrone, D. Montanino, A. Palazzo, et al. Global analysis of neutrino masses,  
2070 mixings and phases: entering the era of leptonic CP violation searches. *Phys.Rev.*, D86:013012, 2012.
- 2071 [60] K.N. Abazajian et al. Light Sterile Neutrinos: A White Paper. 2012.
- 2072 [61] Tommy Ohlsson. Status of non-standard neutrino interactions. *Rep. Prog. Phys.* 76,, 044201:044201,  
2073 2013.
- 2074 [62] A. Lenz, U. Nierste, J. Charles, S. Descotes-Genon, H. Lacker, et al. Constraints on new physics in  
2075  $B - \bar{B}$  mixing in the light of recent LHCb data. *Phys.Rev.*, D86:033008, 2012.
- 2076 [63] S.F. King. Predicting neutrino parameters from SO(3) family symmetry and quark-lepton unification.  
2077 *JHEP*, 0508:105, 2005.
- 2078 [64] Guido Altarelli and Ferruccio Feruglio. Discrete Flavor Symmetries and Models of Neutrino Mixing.  
2079 *Rev.Mod.Phys.*, 82:2701–2729, 2010.
- 2080 [65] Stephen F. King and Christoph Luhn. Neutrino Mass and Mixing with Discrete Symmetry. 2013.
- 2081 [66] Andre de Gouvea and Hitoshi Murayama. Neutrino Mixing Anarchy: Alive and Kicking. 2012.
- 2082 [67] F.P. An, Q. An, J.Z. Bai, A.B. Balantekin, H.R. Band, et al. Improved measurement of electron  
2083 antineutrino disappearance at Daya Bay. *Chin.Phys.*, C37:011001, 2013.
- 2084 [68] Pilar Coloma, Andrea Donini, Enrique Fernandez-Martinez, and Pilar Hernandez. Precision on leptonic  
2085 mixing parameters at future neutrino oscillation experiments. *JHEP*, 1206:073, 2012.
- 2086 [69] R. Plunkett and for the MINOS+ collaboration J. Thomas. Minos+: Using the numi beam as a  
2087 precision tool for neutrino physics. [http://if-neutrino.fnal.gov/whitepapers/plunkett-minos+](http://if-neutrino.fnal.gov/whitepapers/plunkett-minos+.pdf)  
2088 [.pdf](http://if-neutrino.fnal.gov/whitepapers/plunkett-minos+.pdf), Mar 2013.
- 2089 [70] J. Thomas, C. Wendt, A. Habig, K. Lang, and J.K. Nelson. Cherenkov detectors in mine pits (chips).  
2090 <http://if-neutrino.fnal.gov/whitepapers/thomas-chips.pdf>, Mar 2013.
- 2091 [71] J.J. Evans, P. Guzowski, M. Kordosky, R.J. Nichol, R.A. Rameika, B. Rebel, and A. Sousa. Glade  
2092 global liquid argon detector experiment. <http://if-neutrino.fnal.gov/whitepapers/glade.pdf>,  
2093 Mar 2013.
- 2094 [72] Andre de Gouvea, James Jenkins, and Boris Kayser. Neutrino mass hierarchy, vacuum oscillations,  
2095 and vanishing  $—U(e3)—$ . *Phys.Rev.*, D71:113009, 2005.
- 2096 [73] M. Messier for the NOvA collaboration. Extending the nova physics program. [http://if-neutrino.](http://if-neutrino.fnal.gov/whitepapers/messier-nova.pdf)  
2097 [fnal.gov/whitepapers/messier-nova.pdf](http://if-neutrino.fnal.gov/whitepapers/messier-nova.pdf), Mar 2013.
- 2098 [74] J. Strait for the LBNE collaboration M. Diwan, B. Wilson. Long baseline neutrino experiment. [http:](http://indico.cern.ch/conferenceDisplay.py?confId=244831)  
2099 [//indico.cern.ch/conferenceDisplay.py?confId=244831](http://indico.cern.ch/conferenceDisplay.py?confId=244831), Apr 2013.
- 2100 [75] Shao-Feng Ge, Kaoru Hagiwara, Naotoshi Okamura, and Yoshitaro Takaesu. Determination of mass  
2101 hierarchy with medium baseline reactor neutrino experiments. *JHEP*, 1305:131, 2013.
- 2102 [76] X. Qian, A. Tan, W. Wang, J.J. Ling, R.D. McKeown, et al. Statistical Evaluation of Experimental  
2103 Determinations of Neutrino Mass Hierarchy. *Phys.Rev.*, D86:113011, 2012.
- 2104 [77] The IceCube. PINGU Sensitivity to the Neutrino Mass Hierarchy. 2013.
- 2105 [78] Walter Winter. Neutrino mass hierarchy determination with IceCube-PINGU. 2013.

- 2106 [79] Juergen Brunner. Orca - measuring the nu mass hierarchy with a sea water based neutrino telescope.  
2107 <http://indico.cern.ch/conferenceDisplay.py?confId=224351>, Feb 2013.
- 2108 [80] The DAE $\delta$ ALUS collaboration. Whitepaper on the dae $\delta$ alus experiment. <http://if-neutrino.fnal.gov/whitepapers/daedalus.pdf>, Mar 2013.
- 2110 [81] K. Abe, T. Abe, H. Aihara, Y. Fukuda, Y. Hayato, et al. Letter of Intent: The Hyper-Kamiokande  
2111 Experiment — Detector Design and Physics Potential —. 2011.
- 2112 [82] LBNE Collaboration. Opportunities for precision tests of three-neutrino mixing and beyond with lbne.  
2113 <http://if-neutrino.fnal.gov/whitepapers/lbne-lbl.pdf>, Mar 2013.
- 2114 [83] Pilar Coloma, Patrick Huber, Joachim Kopp, and Walter Winter. Systematic uncertainties in long-  
2115 baseline neutrino oscillations for large  $\theta_{13}$ . 2012.
- 2116 [84] P. Huber, M. Lindner, T. Schwetz, and W. Winter. First hint for CP violation in neutrino oscillations  
2117 from upcoming superbeam and reactor experiments. *JHEP*, 11:044, 2009.
- 2118 [85] Ryan Patterson, 2013. private communciation.
- 2119 [86] A. Stahl, C. Wiebusch, A.M. Guler, M. Kamiscioglu, R. Sever, et al. Expression of Interest for a very  
2120 long baseline neutrino oscillation experiment (LBNO). 2012.
- 2121 [87] S. Choubey et al. International Design Study for the Neutrino Factory, Interim Design Report. 2011.
- 2122 [88] T.R. Edgecock, O. Caretta, T. Davenne, C. Densham, M. Fitton, et al. The EUROnu Project.  
2123 *Phys.Rev.ST Accel.Beams*, 16:021002, 2013.
- 2124 [89] J. J. Evans. <http://if-neutrino.fnal.gov/neutrino1-pagers.pdf>.
- 2125 [90] J. Thomas. <http://if-neutrino.fnal.gov/neutrino1-pagers.pdf>.
- 2126 [91] E. Christensen. <http://if-neutrino.fnal.gov/neutrino1-pagers.pdf>.
- 2127 [92] J. Alonso, F.T. Avignone, W.A. Barletta, R. Barlow, H.T. Baumgartner, et al. Expression of Interest  
2128 for a Novel Search for CP Violation in the Neutrino Sector: DAEdALUS. 2010.
- 2129 [93] S.K. Agarwalla, P. Huber, J.M. Link, and D. Mohapatra. A new approach to anti-neutrino running in  
2130 long baseline neutrino oscillation experiments. *JHEP*, 1104:099, 2011.
- 2131 [94] J. Alonso et al. A Study of Detector Configurations for the DUSEL CP Violation Searches Combining  
2132 LBNE and DAEdALUS. 2010.
- 2133 [95] M. Wurm et al. The next-generation liquid-scintillator neutrino observatory LENA. 2011.
- 2134 [96] J. Conrad et al. Whitepaper on the isodar experiment. <http://if-neutrino.fnal.gov/whitepapers/isodar.pdf>, 2013.
- 2136 [97] The DAE $\delta$ ALUS collaboration. Whitepaper on cyclotrons as drivers for precision neutrino experiments.  
2137 <http://if-neutrino.fnal.gov/whitepapers/cyclofornuphysics.pdf>, 2013.
- 2138 [98] D. V. Forero, M. Tòrtola, and J. W. F. Valle. *Phys. Rev. D*, 86:073012, 2012.
- 2139 [99] H. V. Klapdor-Kleingrothaus, A. Dietz, H. L. Harney, and I. V. Krivosheina. Evidence for Neutrinoless  
2140 Double Beta Decay. *Mod. Phys. Lett.*, A16:2409–2420, 2001.

- 2141 [100] III Avignone, F.T., S.R. Elliott, and J. Engel. Double Beta Decay, Majorana Neutrinos, and Neutrino  
2142 *Mass. Rev. Mod. Phys.*, 80:481–516, 2008.
- 2143 [101] E. Blucher, J. R. Klein, Gabriel D. Orebi Gann, N. Tolich, and M. Yeh. Neutrinoless double  
2144 beta decay and other neutrino physics with sno+. [http://if-neutrino.fnal.gov/whitepapers/  
2145 klein-snoplus.pdf](http://if-neutrino.fnal.gov/whitepapers/klein-snoplus.pdf), Mar 2013.
- 2146 [102] K. Lang, F. Piquemal, R. Saakyan, J. Thomas, D. Waters, and S. Söldner-Rembold on behalf of the  
2147 SuperNEMO Collaboration. Supernemo in the usa. [http://if-neutrino.fnal.gov/whitepapers/  
2148 lang-supernemo.pdf](http://if-neutrino.fnal.gov/whitepapers/lang-supernemo.pdf), Mar 2013.
- 2149 [103] D. Nygren and J. J. Gómez-Cadenas on behalf of the NEXT/OSPREY Collaboration. Discovery  
2150 potential of a large high pressure xenon gas tpc for neutrinoless double beta decay experiments. [http:  
2151 //if-neutrino.fnal.gov/whitepapers/nygren-next.pdf](http://if-neutrino.fnal.gov/whitepapers/nygren-next.pdf), Mar 2013.
- 2152 [104] Lindley Winslow. Next generation liquid scintillator based detectors: Quantum dots and picosecond  
2153 timing. <http://if-neutrino.fnal.gov/whitepapers/winslow-qd.pdf>, Mar 2013.
- 2154 [105] Hiro Ejiri. Comments on neutrinoless double beta decays. [http://if-neutrino.fnal.gov/  
2155 whitepapers/ejiri-dbd.pdf](http://if-neutrino.fnal.gov/whitepapers/ejiri-dbd.pdf), Mar 2013.
- 2156 [106] Y. Kolomensky on behalf of the US-CUORE Collaboration. Exploring neutrinoless double-beta  
2157 decay in the inverted hierarchy region with bolometric detectors. [http://if-neutrino.fnal.gov/  
2158 whitepapers/cuore.pdf](http://if-neutrino.fnal.gov/whitepapers/cuore.pdf), Mar 2013.
- 2159 [107] J. F. Wilkerson and S. R. Elliott on behalf of the MAJORANA Collaboration. A search for neutrinoless  
2160 double-beta decay of germanium-76. <http://if-neutrino.fnal.gov/whitepapers/majorana.pdf>,  
2161 Mar 2013.
- 2162 [108] M. Heffner, M. Sweany, P. Sorenson, and A. Bernstein. Gaseous xenon tpc with germanium-like energy  
2163 resolution. <http://if-neutrino.fnal.gov/whitepapers/sweany-nid.pdf>, Mar 2013.
- 2164 [109] Giorgio Gratta for the EXO Collaboration. nexo. [http://if-neutrino.fnal.gov/whitepapers/  
2165 gratta-nexo.pdf](http://if-neutrino.fnal.gov/whitepapers/gratta-nexo.pdf), Mar 2013.
- 2166 [110] Dongming Mei for the CUBED Collaboration. Advanced materials for underground physics and  
2167 applications. <http://if-neutrino.fnal.gov/whitepapers/mei-cubed.pdf>, Mar 2013.
- 2168 [111] E. Aguayo et al., 2011. Presented at the American Physical Society Division of Particles and Fields  
2169 2011, Providence RI, USA, August 2011.
- 2170 [112] A. G. Schubert et al., 2011. Submitted to AIP Conference Proceedings, 19th Particles and Nuclei  
2171 International Conference (PANIC 2011), Massachusetts Institute of Technology, Cambridge, MA, USA,  
2172 July 24-29, 2011.
- 2173 [113] *J. Phys. Conf. Ser.*, 375:042010, 2012.
- 2174 [114] F. Alessandria et al., 2011. Submitted to *Astropart. Phys.*
- 2175 [115] N. Ackerman et al. Observation of Two-Neutrino Double-Beta Decay in  $^{136}\text{Xe}$  with EXO-200. *Phys.*  
2176 *Rev. Lett.*, 107:212501, 2011.
- 2177 [116] M. Auger et al. Search for Neutrinoless Double-Beta Decay in  $^{136}\text{Xe}$  with EXO-200. *Phys.Rev.Lett.*,  
2178 109:032505, 2012.

- 2179 [117] M. Danilov et al. Detection of very small neutrino masses in double-beta decay using laser tagging.  
2180 *Phys. Lett.*, B480:12–18, 2000.
- 2181 [118] A. Gando et al. *Phys. Rev. C*, 85:045dill504, 2012.
- 2182 [119] A. Gando et al., 2013.
- 2183 [120] A. Gando et al., 2013.
- 2184 [121] E. Gómez et al., 2011.
- 2185 [122] N. Yahlali et al. *Nucl. Instrum. Meth. Phys. A*, 617:520, 2010.
- 2186 [123] R. Arnold et al. *Eur. Phys. J. C*, 70:927, 2010.
- 2187 [124] M. Bongrand et al., 2011. to be published in Proceedings 22nd Rencontres de Blois, July, 2010.
- 2188 [125] S. K. Kim, 2011. Presentation at MEDEX 2011, Prague, Czech Republic.
- 2189 [126] S. J. Lee et al. *Astropart. Phys.*, 34:732, 2011.
- 2190 [127] T. Kishimoto. *Int. J. Mod. Phys. E*, 18:2129, 2009.
- 2191 [128] Yu G. Zdesenko et al. *Astropart. Phys.*, 23:249, 2005.
- 2192 [129] K. Zuber. *Phys. Lett. B*, 519:1, 2001.
- 2193 [130] N. Ishihara et al. *Nucl. Instrum. Meth. A*, 443:101, 2000.
- 2194 [131] S. Schönert et al. *Nucl. Phys. Proc. Suppl.*, 145:242, 2005.
- 2195 [132] F. A. Danevich. *Nucl. Phys. A*, 694:375, 2001.
- 2196 [133] A. Giuliani, 2010. presentation at Beyond 2010, Cape Town, South Africa, February 2010.
- 2197 [134] C. Arnaboldi et al. *Astropart. Phys.*, 34:344, 2011.
- 2198 [135] H. Ejiri. *Mod. Phys. Lett. A*, 22:1277, 2007.
- 2199 [136] M. C. Chen. *Nucl. Phys. Proc. Suppl.*, 145:65, 2005.
- 2200 [137] M. C. Chen et al. *eConf*, page C080730, 2008.
- 2201 [138] A. Osipowicz et al. 2001. arXiv:hep-ex/0109033.
- 2202 [139] R. G. H. Robertson. *J. Phys. Conf. Ser.*, 120:052028, 2008.
- 2203 [140] B. Monreal and J.A. Formaggio. Relativistic Cyclotron Radiation Detection of Tritium Decay Electrons  
2204 as a New Technique for Measuring the Neutrino Mass. *Phys. Rev.*, D80:051301, 2009.
- 2205 [141] Joachim Kopp and Alexander Merle. Ultralow  $q$  values for neutrino mass measurements. *Phys. Rev.*  
2206 *C*, 81:045501, Apr 2010.
- 2207 [142] W.R. Blanchard et al. Development of a relic neutrino detection experiment at ptolemy: Princeton  
2208 tritium observatory for light, early-universe, massive-neutrino yield. <http://if-neutrino.fnal.gov/whitepapers/ptolemy.pdf>, 2013.  
2209
- 2210 [143] J. Lesgourgues and S. Pastor. Massive neutrinos and cosmology. *Phys. Rept.*, 429:307–379, 2006.

- 2211 [144] K.N. Abazajian et al. Cosmological and Astrophysical Neutrino Mass Measurements. *Astropart. Phys.*,  
2212 35:177–184, 2011.
- 2213 [145] Y. Y.Y. Wong. Neutrino mass in cosmology: status and prospects. *Ann. Rev. Nucl. Part. Sci.*,  
2214 61:69–98, 2011.
- 2215 [146] J. Morfin. <http://if-neutrino.fnal.gov/neutrino1-pagers.pdf>.
- 2216 [147] A. Bross et al. nustorm: Neutrinos from stored muons. <http://if-neutrino.fnal.gov/whitepapers/nuSTORM.pdf>, 2013.
- 2218 [148] D. Casper. The nuance neutrino physics simulation, and the future. *Nucl. Phys. Proc. Suppl.*, 112:161–  
2219 170, 2002.
- 2220 [149] R.A. Smith and E.J. Moniz. Neutrino reactions on nuclear targets. *Nucl. Phys.*, B43:605, 1972.
- 2221 [150] A.A. Aguilar-Arevalo et al. First Measurement of the Muon Neutrino Charged Current Quasielastic  
2222 Double Differential Cross Section. *Phys. Rev.*, D81:092005, 2010.
- 2223 [151] A.A. Aguilar-Arevalo et al. First Measurement of the Muon Anti-Neutrino Double-Differential Charged  
2224 Current Quasi-Elastic Cross Section. 2013.
- 2225 [152] V. Lyubushkin et al. A Study of quasi-elastic muon neutrino and antineutrino scattering in the  
2226 NOMAD experiment. *Eur.Phys.J.*, C63:355–381, 2009.
- 2227 [153] M. Martini, M. Ericson, G. Chanfray, and J. Marteau. A Unified approach for nucleon knock-out,  
2228 coherent and incoherent pion production in neutrino interactions with nuclei. *Phys. Rev.*, C80:065501,  
2229 2009.
- 2230 [154] J. Carlson, J. Jourdan, R. Schiavilla, and I. Sick. Longitudinal and transverse quasielastic response  
2231 functions of light nuclei. *Phys. Rev.*, C65:024002, 2002.
- 2232 [155] J.T. Sobczyk. Multinucleon ejection model for Meson Exchange Current neutrino interactions. 2012.
- 2233 [156] M. Martini, M. Ericson, G. Chanfray, and J. Marteau. Neutrino and antineutrino quasielastic  
2234 interactions with nuclei. *Phys. Rev.*, C81:045502, 2010.
- 2235 [157] G.A. Fiorentini et al. Measurement of Muon Neutrino Quasi-Elastic Scattering on a Hydrocarbon  
2236 Target at  $E_\nu \sim 3.5$  GeV. 2013.
- 2237 [158] L. Fields et al. Measurement of Muon Antineutrino Quasi-Elastic Scattering on a Hydrocarbon Target  
2238 at  $E_\nu \sim 3.5$  GeV. 2013.
- 2239 [159] A.A. Aguilar-Arevalo et al. Measurement of Neutrino-Induced Charged-Current Charged Pion  
2240 Production Cross Sections on Mineral Oil at  $E_\nu \sim 1$  GeV. *Phys. Rev.*, D83:052007, 2011.
- 2241 [160] K. Abe et al. Measurement of the Inclusive NuMu Charged Current Cross Section on Carbon in the  
2242 Near Detector of the T2K Experiment. 2013.
- 2243 [161] Received whitepapers,snowmass 2013. [http://www.snowmass2013.org/tiki-index.php?page=](http://www.snowmass2013.org/tiki-index.php?page=Received+Whitepapers)  
2244 [Received+Whitepapers](http://www.snowmass2013.org/tiki-index.php?page=Received+Whitepapers), Mar 2013.
- 2245 [162] J. Paley, Z. Djurcic, D. Harris, R. Tesarek, G. Feldman, et al. SciNOvA: A Measurement of Neutrino-  
2246 Nucleus Scattering in a Narrow-Band Beam. 2010.
- 2247 [163] C. Anderson et al. First Measurements of Inclusive Muon Neutrino Charged Current Differential Cross  
2248 Sections on Argon. *Phys.Rev.Lett.*, 108:161802, 2012.

- 2249 [164] Nu-SNS Collaboration, 2005.
- 2250 [165] J. Carlson, D. Cline, Z. Djurcic, A. Friedland, G. Fuller, E. Guardincerri, W. Louis, C. Mauger,  
2251 K. Scholberg, and G. Sinnis. Measuring neutrino cross sections on argon for supernova neutrino  
2252 detection. <http://if-neutrino.fnal.gov/whitepapers/lldr-sns.pdf>, Mar 2013.
- 2253 [166] A. Bolozdynya et al. Opportunities for neutrino measurements at the spallation neutron source.  
2254 [http://if-neutrino.fnal.gov/whitepapers/sns\\_neutrinos.pdf](http://if-neutrino.fnal.gov/whitepapers/sns_neutrinos.pdf), 2013.
- 2255 [167] A. Bolozdynya, F. Cavanna, Y. Efremenko, G.T. Garvey, V. Gudkov, et al. Opportunities for Neutrino  
2256 Physics at the Spallation Neutron Source: A White Paper. 2012.
- 2257 [168] D. Cline, Z. Djurcic, K. Lee, E. Guardincerri, C. Mauger, C. McGrew, K. Rielage, G. Sinnis, M. Tzanov,  
2258 B. Svoboda, and H. Wang. Neutron running with a liquid argon tpc to study  $\nu$ -ar final state interactions  
2259 and cosmogenic backgrounds important for lbne. [http://if-neutrino.fnal.gov/whitepapers/  
2260 lldr-neutron.pdf](http://if-neutrino.fnal.gov/whitepapers/lldr-neutron.pdf), Mar 2013.
- 2261 [169] Coherent Neutrino Scattering Conference, livermore. [http://neutrinos.llnl.gov/LLNL\\_CNS.html](http://neutrinos.llnl.gov/LLNL_CNS.html),  
2262 Dec 2012.
- 2263 [170] Kate Scholberg. Prospects for measuring coherent neutrino-nucleus elastic scattering at a stopped-pion  
2264 neutrino source. *Phys.Rev.*, D73:033005, 2006.
- 2265 [171] J. Barranco, O.G. Miranda, and T.I. Rashba. Probing new physics with coherent neutrino scattering  
2266 off nuclei. *JHEP*, 0512:021, 2005.
- 2267 [172] Jocelyn Monroe and Peter Fisher. Neutrino Backgrounds to Dark Matter Searches. *Phys.Rev.*,  
2268 D76:033007, 2007.
- 2269 [173] A. Gutlein, C. Ciemiak, F. von Feilitzsch, N. Haag, M. Hofmann, et al. Solar and atmospheric  
2270 neutrinos: Background sources for the direct dark matter search. *Astropart.Phys.*, 34:90–96, 2010.
- 2271 [174] Kelly Patton, Jonathan Engel, Gail C. McLaughlin, and Nicolas Schunck. Neutrino-nucleus coherent  
2272 scattering as a probe of neutron density distributions. *Phys. Rev. C*, 86:024612, Aug 2012.
- 2273 [175] J.A. Formaggio, E. Figueroa-Feliciano, and A.J. Anderson. Sterile Neutrinos, Coherent Scattering  
2274 and Oscillometry Measurements with Low-temperature Bolometers. *Phys. Rev.*, D85:013009, 2012. 14  
2275 pages, 10 figures. Version 2: Temperature dependence on alpha fixed from earlier version.
- 2276 [176] A.J. Anderson, J.M. Conrad, E. Figueroa-Feliciano, C. Ignarra, G. Karagiorgi, et al. Measuring  
2277 Active-to-Sterile Neutrino Oscillations with Neutral Current Coherent Neutrino-Nucleus Scattering.  
2278 *Phys.Rev.*, D86:013004, 2012.
- 2279 [177] P. Barbeau et al. Searches for cenns at the spallation neutron source. [http://if-neutrino.fnal.  
2280 gov/whitepapers/sns\\_coherent.pdf](http://if-neutrino.fnal.gov/whitepapers/sns_coherent.pdf), 2013.
- 2281 [178] S. Brice et al. Measuring cenns in the low energy neutrino source at fermilab. [http://if-neutrino.  
2282 fnal.gov/whitepapers/yoo-cenns.pdf](http://if-neutrino.fnal.gov/whitepapers/yoo-cenns.pdf), 2013.
- 2283 [179] Theory white paper– to be submitted, 2013.
- 2284 [180] C. Mariani. Study of neutrino cross sections and nuclear model. [http://if-neutrino.fnal.gov/  
2285 whitepapers/mariani\\_white\\_paper.pdf](http://if-neutrino.fnal.gov/whitepapers/mariani_white_paper.pdf), 2013.
- 2286 [181] U. Mosel. Thoughts on improving event generators and theoretical calculations of neutrino-nucleus  
2287 interactions. <http://if-neutrino.fnal.gov/whitepapers/mosel.txt>, 2013.

- 2288 [182] A. Aguilar-Arevalo et al. Evidence for neutrino oscillations from the observation of anti-  
2289 neutrino(electron) appearance in a anti-neutrino(muon) beam. *Phys. Rev.*, D64:112007, 2001.
- 2290 [183] A.A. Aguilar-Arevalo et al. Improved Search for  $\bar{\nu}_\mu \rightarrow \bar{\nu}_e$  Oscillations in the MiniBooNE Experiment.  
2291 2013.
- 2292 [184] A.A. Aguilar-Arevalo et al. Unexplained Excess of Electron-Like Events From a 1-GeV Neutrino Beam.  
2293 *Phys. Rev. Lett.*, 102:101802, 2009.
- 2294 [185] G. Mention, M. Fechner, Th. Lasserre, Th.A. Mueller, D. Lhuillier, et al. The Reactor Antineutrino  
2295 Anomaly. *Phys. Rev.*, D83:073006, 2011.
- 2296 [186] C. Giunti and M. Laveder. Statistical Significance of the Gallium Anomaly. *Phys. Rev.*, C83:065504,  
2297 2011.
- 2298 [187] Joachim Kopp, Pedro A. N. Machado, Michele Maltoni, and Thomas Schwetz. Sterile Neutrino  
2299 Oscillations: The Global Picture. 2013.
- 2300 [188] K.B.M. Mahn et al. Dual baseline search for muon neutrino disappearance at  $0.5\text{eV}^2 < \Delta m^2 < 40\text{eV}^2$ .  
2301 *Phys.Rev.*, D85:032007, 2012.
- 2302 [189] P. Adamson et al. Active to sterile neutrino mixing limits from neutral-current interactions in MINOS.  
2303 *Phys.Rev.Lett.*, 107:011802, 2011.
- 2304 [190] P.A.R. Ade et al. Planck 2013 results. XVI. Cosmological parameters. 2013.
- 2305 [191] E. Komatsu et al. Seven-Year Wilkinson Microwave Anisotropy Probe (WMAP) Observations:  
2306 Cosmological Interpretation. *Astrophys.J.Suppl.*, 192:18, 2011.
- 2307 [192] R. Keisler et al. A Measurement of the Damping Tail of the Cosmic Microwave Background Power  
2308 Spectrum with the South Pole Telescope. *Astrophys.J.*, 743:28, 2011.
- 2309 [193] J. others Dunkley. The Atacama Cosmology Telescope: Cosmological Parameters from the 2008 Power  
2310 Spectra. *Astrophys.J.*, 739:52, 2011.
- 2311 [194] B. Fujikawa et al. Investigation of the reactor antineutrino anomaly with the intense  $^{144}\text{ce}$ -  
2312  $^{144}\text{pr}$  antineutrino source in a large liquid scintillator detector. [http://if-neutrino.fnal.gov/  
2313 whitepapers/maricic-celand.pdf](http://if-neutrino.fnal.gov/whitepapers/maricic-celand.pdf), 2013.
- 2314 [195] D. A. Dwyer et al. Search for sterile neutrinos with a radioactive source at daya bay. [http://  
2315 if-neutrino.fnal.gov/whitepapers/littlejohn-db.pdf](http://if-neutrino.fnal.gov/whitepapers/littlejohn-db.pdf), 2013.
- 2316 [196] M. Pallavicini. Searching for sterile neutrinos in borexino. [http://if-neutrino.fnal.gov/  
2317 whitepapers/borexino.txt](http://if-neutrino.fnal.gov/whitepapers/borexino.txt), 2013.
- 2318 [197] Z. Djurcic et al. Search for oscillations of reactor antineutrinos at very short baselines. [http://  
2319 if-neutrino.fnal.gov/whitepapers/reactorUS\\_osc.pdf](http://if-neutrino.fnal.gov/whitepapers/reactorUS_osc.pdf), Mar 2013.
- 2320 [198] V.B. Brudanin et al. Antineutrino detector for reactor monitoring and looking for sterile neutrinos.  
2321 <http://if-neutrino.fnal.gov/whitepapers/detdans.pdf>, Mar 2013.
- 2322 [199] W. Louis et al. Oscsns: A precision neutrino oscillation experiment at the sns. [http://if-neutrino.  
2323 fnal.gov/whitepapers/louis-oscSNS.pdf](http://if-neutrino.fnal.gov/whitepapers/louis-oscSNS.pdf), 2013.
- 2324 [200] R. Guenette. Lar1: Addressing the short-baseline anomalies. [http://if-neutrino.fnal.gov/  
2325 whitepapers/lar1.pdf](http://if-neutrino.fnal.gov/whitepapers/lar1.pdf), 2013.

- 2326 [201] R. Cooper. Miniboone+: A new investigation of  $\nu_e$  oscillations with improved sensitivity  
2327 in an enhanced miniboone experiment. <http://if-neutrino.fnal.gov/whitepapers/MBplus.pdf>,  
2328 2013.
- 2329 [202] G. Mills et al. The miniboone-ii proposal: A 5 sigma test of miniboone's neutrino mode excess.  
2330 <http://if-neutrino.fnal.gov/whitepapers/mills-mb2.pdf>, 2013.
- 2331 [203] M. Antonello, D. Bagliani, B. Baibussinov, H. Bilokon, F. Boffelli, et al. Search for 'anomalies' from  
2332 neutrino and anti-neutrino oscillations at  $\Delta_m^2 \sim 1 \text{ eV}^2$  with muon spectrometers and large LAr-TPC  
2333 imaging detectors. 2012.
- 2334 [204] Z. Djurcic et al. Us reactors for antineutrino experiments. [http://if-neutrino.fnal.gov/](http://if-neutrino.fnal.gov/whitepapers/reactorUS_reactors.pdf)  
2335 [whitepapers/reactorUS\\_reactors.pdf](http://if-neutrino.fnal.gov/whitepapers/reactorUS_reactors.pdf), Mar 2013.
- 2336 [205] Christian Grieb, Jonathan Link, and R.S. Raghavan. Probing active to sterile neutrino oscillations in  
2337 the LENS detector. *Phys.Rev.*, D75:093006, 2007.
- 2338 [206] C. Arpesella et al. Direct Measurement of the Be-7 Solar Neutrino Flux with 192 Days of Borexino  
2339 Data. *Phys.Rev.Lett.*, 101:091302, 2008.
- 2340 [207] K. Schreckenbach, G. Colvin, W. Gelletly, and F. Von Feilitzsch. DETERMINATION OF THE ANTI-  
2341 NEUTRINO SPECTRUM FROM U-235 THERMAL NEUTRON FISSION PRODUCTS UP TO 9.5-  
2342 MEV. *Phys.Lett.*, B160:325–330, 1985.
- 2343 [208] A.A. Hahn, K. Schreckenbach, G. Colvin, B. Krusche, W. Gelletly, et al. ANTI-NEUTRINO  
2344 SPECTRA FROM PU-241 AND PU-239 THERMAL NEUTRON FISSION PRODUCTS. *Phys.Lett.*,  
2345 B218:365–368, 1989.
- 2346 [209] Th.A. Mueller, D. Lhuillier, M. Fallot, A. Letourneau, S. Cormon, et al. Improved Predictions of  
2347 Reactor Antineutrino Spectra. *Phys.Rev.*, C83:054615, 2011.
- 2348 [210] Patrick Huber. On the determination of anti-neutrino spectra from nuclear reactors. *Phys.Rev.*,  
2349 C84:024617, 2011.
- 2350 [211] H. Kwon, F. Boehm, A.A. Hahn, H.E. Henrikson, J.L. Vuilleumier, et al. SEARCH FOR NEUTRINO  
2351 OSCILLATIONS AT A FISSION REACTOR. *Phys.Rev.*, D24:1097–1111, 1981.
- 2352 [212] Y. Declais, H. de Kerret, B. Lefievre, M. Obolensky, A. Etenko, et al. Study of reactor anti-neutrino  
2353 interaction with proton at Bugey nuclear power plant. *Phys.Lett.*, B338:383–389, 1994.
- 2354 [213] Y. Declais, J. Favier, A. Metref, H. Pessard, B. Achkar, et al. Search for neutrino oscillations at 15-  
2355 meters, 40-meters, and 95-meters from a nuclear power reactor at Bugey. *Nucl.Phys.*, B434:503–534,  
2356 1995.
- 2357 [214] G. Zacek et al. Neutrino Oscillation Experiments at the Gosgen Nuclear Power Reactor. *Phys.Rev.*,  
2358 D34:2621–2636, 1986.
- 2359 [215] A.I. Afonin, S.N. Ketov, V.I. Kopeikin, L.A. Mikaelyan, M.D. Skorokhvatov, et al. A STUDY OF  
2360 THE REACTION ANTI-ELECTRON-NEUTRINO + P  $\rightarrow$  E+ + N ON A NUCLEAR REACTOR.  
2361 *Sov.Phys.JETP*, 67:213–221, 1988.
- 2362 [216] A.A. Kuvshinnikov, L.A. Mikaelyan, S.V. Nikolaev, M.D. Skorokhvatov, and A.V. Etenko. Measuring  
2363 the anti-electron-neutrino + p  $\rightarrow$  n + e+ cross-section and beta decay axial constant in a new  
2364 experiment at Rovno NPP reactor. (In Russian). *JETP Lett.*, 54:253–257, 1991.

- 2365 [217] G.S. Vidyakin, V.N. Vyrodov, I.I. Gurevich, Yu.V. Kozlov, V.P. Martemyanov, et al. DETECTION  
2366 OF ANTI-NEUTRINOS IN THE FLUX FROM TWO REACTORS. *Sov.Phys.JETP*, 66:243–247,  
2367 1987.
- 2368 [218] G.S. Vidyakin, V.N. Vyrodov, Yu.V. Kozlov, A.V. Martemyanov, V.P. Martemyanov, et al. Limitations  
2369 on the characteristics of neutrino oscillations. *JETP Lett.*, 59:390–393, 1994.
- 2370 [219] Z.D. Greenwood, W.R. Kropp, M.A. Mandelkern, S. Nakamura, E.L. Pasierb-Love, et al. Results of a  
2371 two position reactor neutrino oscillation experiment. *Phys.Rev.*, D53:6054–6064, 1996.
- 2372 [220] S. Hans et al. Advanced reactor antineutrino detector development. [http://if-neutrino.fnal.gov/  
2373 whitepapers/pieter-detector-dev.pdf](http://if-neutrino.fnal.gov/whitepapers/pieter-detector-dev.pdf), Mar 2013.
- 2374 [221] K. Heeger. Precision measurement of the reactor flux and spectrum at daya bay. [http://if-neutrino.  
2375 fnal.gov/whitepapers/dayabay\\_reactor.pdf](http://if-neutrino.fnal.gov/whitepapers/dayabay_reactor.pdf), 2013.
- 2376 [222] D. Asner et al. Predicting reactor antineutrino emissions using new precision beta spectroscopy.  
2377 <http://if-neutrino.fnal.gov/whitepapers/reactor-beta-spectroscopy.pdf>, 2013.
- 2378 [223] E. Church et al. Liquid argon near detector for the booster neutrino beamline. [http://if-neutrino.  
2379 fnal.gov/whitepapers/LAr\\_BNB.pdf](http://if-neutrino.fnal.gov/whitepapers/LAr_BNB.pdf), 2013.
- 2380 [224] C. Athanassopoulos et al. The Liquid Scintillator Neutrino Detector and LAMPF Neutrino Source.  
2381 *Nucl. Instrum. Meth.*, A388:149–172, 1997.
- 2382 [225] P. Kyberd et al. nuSTORM - Neutrinos from STORed Muons: Letter of Intent to the Fermilab Physics  
2383 Advisory Committee. 2012.
- 2384 [226] D. Adey, S.K. Agarwalla, C.M. Ankenbrandt, R. Asfandiyarov, J.J. Back, et al. Neutrinos from Stored  
2385 Muons nuSTORM: Expression of Interest. 2013.
- 2386 [227] H. Nunokawa, O.L.G. Peres, and R. Zukanovich Funchal. Probing the LSND mass scale and four  
2387 neutrino scenarios with a neutrino telescope. *Phys.Lett.*, B562:279–290, 2003.
- 2388 [228] Sandhya Choubey. Signature of sterile species in atmospheric neutrino data at neutrino telescopes.  
2389 *JHEP*, 0712:014, 2007.
- 2390 [229] V. Barger, Y. Gao, and D. Marfatia. Is there evidence for sterile neutrinos in IceCube data? *Phys.  
2391 Rev.*, D85:011302, 2012.
- 2392 [230] M. B. Gavela, D. Hernandez, T. Ota, and W. Winter. Large gauge invariant non-standard neutrino  
2393 interactions. *Phys. Rev.*, D79:013007, 2009.
- 2394 [231] C. Biggio, M. Blennow, and E. Fernandez-Martinez. General bounds on non-standard neutrino  
2395 interactions. *JHEP*, 08:090, 2009.
- 2396 [232] B. W. Lee and R. E. Shrock. Natural Suppression of Symmetry Violation in Gauge Theories: Muon -  
2397 Lepton and Electron Lepton Number Nonconservation. *Phys. Rev.*, D16:1444, 1977.
- 2398 [233] A.G. Beda et al. GEMMA experiment: Three years of the search for the neutrino magnetic moment.  
2399 *Phys.Part.Nucl.Lett.*, 7:406–409, 2010.
- 2400 [234] Nicole F. Bell, Vincenzo Cirigliano, Michael J. Ramsey-Musolf, Petr Vogel, and Mark B. Wise. How  
2401 magnetic is the Dirac neutrino? *Phys.Rev.Lett.*, 95:151802, 2005.
- 2402 [235] P. Vogel and J. Engel. Neutrino Electromagnetic Form-Factors. *Phys.Rev.*, D39:3378, 1989.

- 2403 [236] D.S. Akerib et al. The Large Underground Xenon (LUX) Experiment. *Nucl.Instrum.Meth.*, A704:111–  
2404 126, 2013.
- 2405 [237] C.E. Aalseth et al. CoGeNT: A Search for Low-Mass Dark Matter using p-type Point Contact  
2406 Germanium Detectors. 2012.
- 2407 [238] G.G. Raffelt. Limits on neutrino electromagnetic properties: An update. *Phys.Rept.*, 320:319–327,  
2408 1999.
- 2409 [239] Andre de Gouvea and Shashank Shalgar. Effect of Transition Magnetic Moments on Collective  
2410 Supernova Neutrino Oscillations. *JCAP*, 1210:027, 2012.
- 2411 [240] Andre de Gouvea and Shashank Shalgar. Transition Magnetic Moments and Collective Neutrino  
2412 Oscillations:Three-Flavor Effects and Detectability. *JCAP*, 1304:018, 2013.
- 2413 [241] Y.I. Izotov and T.X. Thuan. The primordial abundance of 4He: evidence for non-standard big bang  
2414 nucleosynthesis. *Astrophys.J.*, 710:L67–L71, 2010.
- 2415 [242] G. Hinshaw et al. Nine-Year Wilkinson Microwave Anisotropy Probe (WMAP) Observations:  
2416 Cosmological Parameter Results. 2012.
- 2417 [243] S. Weinberg. Universal Neutrino Degeneracy. *Phys. Rev.*, 128:1457–1473, 1962.
- 2418 [244] A. G. Cocco, G. Mangano, and M. Messina. Probing low energy neutrino backgrounds with neutrino  
2419 capture on beta decaying nuclei. *JCAP*, 0706:015, 2007.
- 2420 [245] C.J. Lin et al. Accelerator-based measurement of muon-induced neutron background for underground  
2421 sciences. <http://if-neutrino.fnal.gov/whitepapers/lin.pdf>, Mar 2013.
- 2422 [246] A.M. Serenelli, W.C. Haxton, and C. Pena-Garay. Solar models with accretion. I. Application to the  
2423 solar abundance problem. *Astrophys. J.*, 743:24, 2011.
- 2424 [247] G. Fiorentini, M. Lissia, and F. Mantovani. Geo-neutrinos and Earth’s interior. *Phys. Rept.*, 453:117–  
2425 172, 2007.
- 2426 [248] A. Gando et al. Partial radiogenic heat model for Earth revealed by geoneutrino measurements. *Nature*  
2427 *Geo.*, 4:647–651, 2011.
- 2428 [249] G. Bellini et al. Measurement of geo-neutrinos from 1353 days of Borexino. 2013.
- 2429 [250] H. Duan, G. M. Fuller, and Y.-Z. Qian. Collective neutrino flavor transformation in supernovae. *Phys.*  
2430 *Rev.*, D74:123004, 2006.
- 2431 [251] G. L. Fogli, E. Lisi, A. Marrone, and A. Mirizzi. Collective neutrino flavor transitions in supernovae  
2432 and the role of trajectory averaging. *JCAP*, 0712:010, 2007.
- 2433 [252] G. G. Raffelt and A. Y. Smirnov. Self-induced spectral splits in supernova neutrino fluxes. *Phys. Rev.*,  
2434 D76:081301, 2007.
- 2435 [253] G. G. Raffelt and A. Y. Smirnov. Adiabaticity and spectral splits in collective neutrino transformations.  
2436 *Phys. Rev.*, D76:125008, 2007.
- 2437 [254] A. Esteban-Pretel, A. Mirizzi, S. Pastor, R. Tomas, G.G. Raffelt, et al. Role of dense matter in  
2438 collective supernova neutrino transformations. *Phys. Rev.*, D78:085012, 2008.
- 2439 [255] H. Duan and J. P. Kneller. Neutrino flavour transformation in supernovae. *J. Phys. G*, G36:113201,  
2440 2009.

- 2441 [256] B. Dasgupta, A. Dighe, G. G. Raffelt, and A. Y. Smirnov. Multiple Spectral Splits of Supernova  
2442 Neutrinos. 2009.
- 2443 [257] H. Duan, G. M. Fuller, and Y.-Z. Qian. Collective Neutrino Oscillations. *Ann. Rev. Nucl. Part. Sci.*,  
2444 60:569–594, 2010.
- 2445 [258] H. Duan and A. Friedland. Self-induced suppression of collective neutrino oscillations in a supernova.  
2446 *Phys. Rev. Lett.*, 106:091101, 2011.
- 2447 [259] G. G. Raffelt. Particle Physics from Stars. *Ann. Rev. Nucl. Part. Sci.*, 49:163–216, 1999.
- 2448 [260] S. Hannestad and G. Raffelt. New supernova limit on large extra dimensions. *Phys. Rev. Lett.*,  
2449 87:051301, 2001.
- 2450 [261] C. Volpe, 2013.
- 2451 [262] L. Hudepohl, B. Muller, H.-T. Janka, A. Marek, and G.G. Raffelt. Neutrino Signal of Electron-Capture  
2452 Supernovae from Core Collapse to Cooling. *Phys.Rev.Lett.*, 104:251101, 2010.
- 2453 [263] K. Scholberg. Supernova Neutrino Detection. *Ann.Rev.Nucl.Part.Sci.*, 62:81–103, 2012.
- 2454 [264] J.F. Beacom. The Diffuse Supernova Neutrino Background. *Ann. Rev. Nucl. Part. Sci.*, 60:439–462,  
2455 2010.
- 2456 [265] C. Lunardini. Diffuse supernova neutrinos at underground laboratories. 2010.
- 2457 [266] Tadao Mitsui. KamLAND results and future. *Nucl.Phys.Proc.Suppl.*, 221:193–198, 2011.
- 2458 [267] J. Maricic. Geophysics with Hawaiian anti-neutrino observatory (Hanohano). *Nucl.Phys.Proc.Suppl.*,  
2459 221:173, 2011.
- 2460 [268] G. Bellini et al. First evidence of pep solar neutrinos by direct detection in Borexino. *Phys.Rev.Lett.*,  
2461 108:051302, 2012.
- 2462 [269] R.S. Raghavan. LENS, MiniLENS: Status and outlook. *J.Phys.Conf.Ser.*, 120:052014, 2008.
- 2463 [270] T. Araki, S. Enomoto, K. Furuno, Y. Gando, K. Ichimura, et al. Experimental investigation of  
2464 geologically produced antineutrinos with KamLAND. *Nature*, 436:499–503, 2005.
- 2465 [271] G. Bellini, J. Benziger, S. Bonetti, M.B. Avanzini, B. Caccianiga, et al. Observation of Geo-Neutrinos.  
2466 *Phys. Lett.*, B687:299–304, 2010.
- 2467 [272] Basudeb Dasgupta and John.F. Beacom. Reconstruction of supernova  $\nu_\mu$ ,  $\nu_\tau$ , anti- $\nu_\mu$ , and anti- $\nu_\tau$   
2468 neutrino spectra at scintillator detectors. *Phys.Rev.*, D83:113006, 2011.
- 2469 [273] K. Abe et al. Solar neutrino results in Super-Kamiokande-III. *Phys.Rev.*, D83:052010, 2011.
- 2470 [274] Hyper-Kamiokande Working Group. Hyper-k physics opportunities: Low-energy neutrino physics and  
2471 astrophysics with hyper-k. <http://if-neutrino.fnal.gov/whitepapers/hk-1e.pdf>, Mar 2013.
- 2472 [275] Takaaki Mori. R&D project for Gd-doped water Cherenkov detector. *J.Phys.Conf.Ser.*, 408:012077,  
2473 2013.
- 2474 [276] T. Akiri et al. The 2010 Interim Report of the Long-Baseline Neutrino Experiment Collaboration  
2475 Physics Working Groups. 2011.

- 2476 [277] Sandhya Choubey, Basudeb Dasgupta, Amol Dighe, and Alessandro Mirizzi. Signatures of collective  
2477 and matter effects on supernova neutrinos at large detectors. 2010.
- 2478 [278] A. Bueno, Ines Gil Botella, and A. Rubbia. Supernova neutrino detection in a liquid argon TPC. 2003.
- 2479 [279] A. Achterberg et al. First year performance of the IceCube neutrino telescope. *Astropart. Phys.*,  
2480 26:155–173, 2006.
- 2481 [280] R. Abbasi et al. An absence of neutrinos associated with cosmic-ray acceleration in  $\gamma$ -ray bursts.  
2482 *Nature*, 484:351–353, 2012.
- 2483 [281] M.G. Aartsen et al. First observation of PeV-energy neutrinos with IceCube. 2013.
- 2484 [282] Tyce and DeYoung. Particle physics in ice with icecube deepcore. *Nuclear Instruments and Methods in  
2485 Physics Research Section A: Accelerators, Spectrometers, Detectors and Associated Equipment*, (0):–,  
2486 2011.
- 2487 [283] Kenneth Greisen. End to the cosmic ray spectrum? *Phys. Rev. Lett.*, 16:748–750, 1966.
- 2488 [284] G. T. Zatsepin and V. A. Kuzmin. Upper limit of the spectrum of cosmic rays. *JETP Lett.*, 4:78–80,  
2489 1966.
- 2490 [285] I. Kravchenko et al. RICE limits on the diffuse ultra-high energy neutrino flux. *Phys. Rev.*, D73:082002,  
2491 2006.
- 2492 [286] P. W. Gorham. The ANITA cosmogenic neutrino experiment. *Int. J. Mod. Phys.*, A21S1:158–162,  
2493 2006.
- 2494 [287] P. Allison, J. Auffenberg, R. Bard, J.J. Beatty, D.Z. Besson, et al. Design and Initial Performance  
2495 of the Askaryan Radio Array Prototype EeV Neutrino Detector at the South Pole. *Astropart. Phys.*,  
2496 35:457–477, 2012.
- 2497 [288] Stuart A. Kleinfelder. Design and performance of the autonomous data acquisition system for the  
2498 ARIANNA high energy neutrino detector. *IEEE Trans.Nucl.Sci.*, 60:612–618, 2013.
- 2499 [289] IAEA. [http://www.iaea.org/Publications/Factsheets/English/sg\\_overview.html](http://www.iaea.org/Publications/Factsheets/English/sg_overview.html).
- 2500 [290] International Panel on Fissile Materials. Draft Fissile Material Cutoff Treaty. [http://  
2501 fissilematerials.org/library/2009/02draft\\_fissile\\_material\\_cutoff\\_.html](http://fissilematerials.org/library/2009/02draft_fissile_material_cutoff_.html), 2009.
- 2502 [291] IAEA. Proceedings of the First Meeting of the Ad Hoc Working Group on Safeguards Applications  
2503 Utilizing Antineutrino Detection and Monitoring, Aug 2012. IAEA Note to File, SG-EQ-GNRL-RP-  
2504 0002.
- 2505 [292] National Nuclear Security Administration US Department of Energy. The National Nuclear  
2506 Security Administration Strategic Plan. [http://nnsa.energy.gov/sites/default/files/nnsa/  
inlinefiles/2011\\_NNSA\\_Strat\\_Plan.pdf](http://nnsa.energy.gov/sites/default/files/nnsa/<br/>2507 inlinefiles/2011_NNSA_Strat_Plan.pdf), May 2011.
- 2508 [293] Y.V. Klimov, V. I. Kopeikin, L. A. Mikaelyan, K. V. Ozerov, and V. V. Sinev. Neutrino method  
2509 remote measurement of reactor power and power output. *Atomnaya Energiya*, 76:130, 1994.
- 2510 [294] A. Bernstein, N. S. Bowden, A. Misner, and T. Palmer. Monitoring the thermal power of nuclear  
2511 reactors with a prototype cubic meter antineutrino detector. *J. Appl. Phys.*, 103:074905, 2008.
- 2512 [295] Applied antineutrino physics conferences. <http://neutrinos.llnl.gov/links.html>.

- 2513 [296] J.K. Ahn et al. RENO: An Experiment for Neutrino Oscillation Parameter  $\theta_{13}$  Using Reactor Neutrinos  
2514 at Yonggwang. 2010.
- 2515 [297] F. Ardellier et al. Double Chooz: A search for the neutrino mixing angle  $\theta_{13}$ . 2006.
- 2516 [298] X. Guo et al. A precision measurement of the neutrino mixing angle  $\theta_{13}$  using reactor  
2517 antineutrinos at Daya Bay. 2007.
- 2518 [299] V. B. Brudanin, V. G. Egorov, M. V. Shirshenko, Yu. G. Shitov, R. V. Vasilev, M. V. Danilov, E. V.  
2519 Demidova, A. S. Kobayakin, R. S. Mazyuk, E. G. Novikov, V. Yu. Rusinov, A. S. Starostin, E. I.  
2520 Tarkovsky, I. N. Tikhomirov, and V. V. Sinev. Antineutrino detector for reactor monitoring and  
2521 looking for sterile neutrinos. <http://if-neutrino.fnal.gov/whitepapers/detdans.pdf>, Mar 2013.
- 2522 [300] S. Hans, M. Yeh, E. Blucher, R. Johnson, B.R. Littlejohn, T. Allen, S. Morrell, S. Dye, J.G.  
2523 Learned, J. Maricic, S. Matsuno, A. Bernstein, N. Bowden, T. Classen, T.J. Langford, B. McDonough,  
2524 S. Usman, G. Jocher, H.P. Mumm, J.S. Nico, R.E. Williams, R. Henning, C. Bryan, D. Dean,  
2525 P. Huber, A.B. Balantekin, H.R. Band, J.C. Cherwinka, K.M. Heeger, W. Pettus, and D. Webber.  
2526 Advanced reactor antineutrino detector development. [http://if-neutrino.fnal.gov/whitepapers/  
2527 pieter-detector-dev.pdf](http://if-neutrino.fnal.gov/whitepapers/pieter-detector-dev.pdf), Mar 2013.
- 2528 [301] S. Sangiorgio, A. Bernstein, J. Coleman, M. Foxe, C. Hagmann, T. H. Joshi, I. Jovanovic, K. Kazkaz,  
2529 K. Mavrokoridis, V. Mozin, S. Pereverzev, and P. Sorensen. First demonstration of a sub-keV electron  
2530 recoil energy threshold in a liquid argon ionization chamber. <http://arxiv.org/abs/1301.4290>.
- 2531 [302] E. Santos et al. Single electron emission in two-phase xenon with application to the detection of  
2532 coherent neutrino-nucleus scattering. <http://arxiv.org/abs/1110.3056>.
- 2533 [303] D.S. Akerib et al. A low-threshold analysis of CDMS shallow-site data. *Phys.Rev.*, D82:122004, 2010.
- 2534 [304] S. Sangiorgio, A. Bernstein, J. Coleman, M. Foxe, C. Hagmann, T. H. Joshi, I. Jovanovic, K. Kazkaz,  
2535 K. Mavrokoridis, and S. Pereverzev. Observation of coherent neutrino-nucleus scattering at a nuclear  
2536 reactor. <http://if-neutrino.fnal.gov/whitepapers/coherent-scattering-reactors.pdf>.
- 2537 [305] A.I. Bolozdynya, Yu.V. Efremenko, and K. Scholberg. Perspectives to search for neutrino-  
2538 nuclear neutral current coherent scattering. [http://if-neutrino.fnal.gov/whitepapers/  
2539 efremenko-coherent.pdf](http://if-neutrino.fnal.gov/whitepapers/efremenko-coherent.pdf).
- 2540 [306] D. Autiero, J. Aysto, A. Badertscher, Leonid B. Bezrukov, J. Bouchez, et al. Large underground, liquid  
2541 based detectors for astro-particle physics in Europe: Scientific case and prospects. *JCAP*, 0711:011,  
2542 2007.
- 2543 [307] A. Bernstein et al. Nuclear security applications of antineutrino detectors: Current capabilities and  
2544 future prospects. *Science And Global Security*, 18(3):127–192, 2010.
- 2545 [308] Observation of neutrons with a Gadolinium doped water Cherenkov detector. *Nuclear Instruments  
2546 and Methods in Physics Research Section A: Accelerators, Spectrometers, Detectors and Associated  
2547 Equipment*, 607(3):616 – 619, 2009.
- 2548 [309] H. Watanabe et al. First study of neutron tagging with a water Cherenkov detector. *Astroparticle  
2549 Physics*, 31(4):320 – 328, 2009.
- 2550 [310] S. Sangiorgio, A. Bernstein, J. Coleman, M. Foxe, C. Hagmann, T. H. Joshi, I. Jovanovic, K. Kazkaz,  
2551 K. Mavrokoridis, and S. Pereverzev. Remote monitoring of reactors: The watchman project. [http://  
2552 if-neutrino.fnal.gov/whitepapers/long-range-monitoring.pdf](http://if-neutrino.fnal.gov/whitepapers/long-range-monitoring.pdf).

- 2553 [311] K. Eguchi et al. *Phys. Rev. Lett.*, 92:071301, 2004.
- 2554 [312] Natalia Zaitseva et al. Plastic scintillators with efficient neutron/gamma pulse shape discrimination.  
2555 *Nuclear Instruments and Methods in Physics Research Section A: Accelerators, Spectrometers,*  
2556 *Detectors and Associated Equipment*, 668(0):88 – 93, 2012.
- 2557 [313] Large Area Pico-second photo-Detectors Project. <http://psec.uchicago.edu/>.
- 2558 [314] Z. Djurcic, M.C. Sanchez, I. Anghel, M. Demarteau, M. Wetstein, and T. Xian. Using large-area  
2559 picosecond photosensors for neutrino experiments. [http://if-neutrino.fnal.gov/whitepapers/](http://if-neutrino.fnal.gov/whitepapers/lappd.pdf)  
2560 [lappd.pdf](http://if-neutrino.fnal.gov/whitepapers/lappd.pdf), Mar 2013.
- 2561 [315] Reference requested of Milind.
- 2562 [316] M. Zalutsky and M. Pruszyński. Astatine-211: production and availability. *Curr. Radiopharm.*, 4(3),  
2563 2011.
- 2564 [317] L. Calabretta, D. Rifuggiato, and V. Shchepounov. High Intensity Proton Beams from Cyclotrons for  
2565  $H_2^+$ . *Proc. 1999 Particle Accel Conf, NY*, pages 3288–3290, 1999.